UNDERSTANDING EARLY HEMATOPOIETIC DEVELOPMENT IN THE MOUSE EMBRYO

GOH QIU LIN MICHELE

(B.Sc. (Hons.), NTU)

A THESIS SUBMITTED

FOR THE DEGREE OF DOCTOR OF PHILOSOPHY

IN BIOLOGICAL SCIENCE

DEPARTMENT OF BIOLOGICAL SCIENCES

NATIONAL UNIVERSITY OF SINGAPORE

2014

Declaration

I hereby declare that this thesis is my original work and it has been written by me in its entirety. I have duly acknowledged all the sources of information that have been used in the thesis.

This thesis has also not been submitted for any degree in any university previously

Goh Qiu Lin Michele

9 June 2014

TABLE OF CONTENTS

Acknowledgements

This thesis would not have been possible without the help of numerous people. I would like to thank Dr. Tara Huber for her continuous mentorship and support throughout the project, and for establishing the grounds that will guide me well through future endeavors. I would also like to thank my pre-thesis advisory committee Dr. Paul Robson and Dr. Christoph Winkler, for their invaluable feedback along the way. Special thanks goes to the Genome Institute of Singapore (GIS), which made this all possible by supporting my post-graduate studies, and has provided a nurturing environment since the day I first stepped foot into it as an undergraduate on a research attachment.

I am deeply grateful to ex-postdocs Drs. Shawn Lim, Shawna Tan, Brian Tan and Aya Wada for their discussions, advice and support, and especially for making the lab a friendlier place to be in. I would also like to thank colleagues like V. Sivakamasundari, Jeremie Poschmann, Vibhor Kumar, Ng Jia Hui, Winston Chan and Yang Sun for their patience and effort in teaching me new, invaluable protocols. I would also like to thank Dr. Andrew Hutchins, whose mentorship during that first attachment made research exciting.

Above all, I would like to thank my family and close friends for their encouragement and support throughout this entire journey. To my long-suffering husband Jonathan, I dedicate this thesis.

Summary

Hematopoietic stem cells (HSCs) were first identified more than 50 years ago, but complex mechanisms involved in hematopoiesis have yet to be fully unraveled. My project aims to further understand early hematopoietic development in the mouse embryo, by studying the earliest sites of hematopoiesis: the yolk sac (YS) and para-aortic splanchnopleura (P-Sp), which develops to form the aorta-gonad-mesonephros (AGM), from which the first adult mouse- repopulating HSCs arise; as well as differentiated embryonic stem cells (ESCs) that recapitulate YS and P-Sp hematopoiesis. YS and P-Sp hematopoietic systems have different lineage potentials, yet have both shared and differentially-expressed genes. Based on the hypothesis that differentially-expressed genes are involved in determining hematopoietic fate, we compared the transcriptomes of hematopoietic populations via microarray, to identify these differentially expressed genes for further hematopoietic characterization.

Transcriptome comparison of embryo-derived YS and P-Sp hemangioblast-derived colonies revealed that despite their difference in hematopoietic potentials, both colony types do not have vastly different transcriptomes. Bex6 and several members of the placenta-related prolactin family were selected for further study, based on their differential gene expression in the 2 colony types. Functional characterization of several differentially- expressed prolactin family members revealed their involvement in *Wnt/Notch* regulation of early erythropoiesis. Prolactins were not expressed in hematopoietic-supporting E9.5 YS stromal cells, but instead in the $FSC^{low}SSC^{low}$ population, which marks probable erythrocytes; suggesting that prolactins likely mark a more mature cell type rather than progenitor or hematopoiesis-supportive

stromal cells. Meanwhile, increase in *Bex6* expression mirrored that of definitive hematopoietic marker CD45 in differentiated embryoid bodies (EBs), and *Bex6* also marked intermediate and mature hematopoietic progenitors in fetal liver. We hypothesized that *Bex6* was involved in regulating proliferation during definitive hematopoiesis, but siRNA knockdown of *Bex6* in day 6 EBs generated no significant change in hematopoietic potential. A potential reason could be functional redundancy from homologue *Bex4*, which has 67% sequence similarity.

Transcriptome analysis of the E8.5 primitive streak as it acquires hematopoietic potential identified Pcgf5, which belongs to the Polycomb group ring finger (Pcgf) family, which in turn is part of the Polycomb Repressive Complex 1 (PRC1) involved in epigenetic silencing. Knockdown of *Pcgf5* resulted in a decrease in hematopoietic potential of day 4 EBs, and also revealed its involvement in PRC1 regulation of neural genes in the hemangioblast. Using an ESC differentiation system that recapitulates both YS and P-Sp hematopoiesis, we identify that *Pcgf5* and its partner *Cbx8* are preferentially expressed in the two derived Flk1$^+$ cell populations that correspond to YS and P-Sp hematopoiesis. Chromatin immunoprecipitation followed by high-throughput sequencing (ChIP-seq) of PRC1 components identified shared targets between RING1B and PCGF5, supporting the involvement of a PCGF5-PRC1 variant in hematopoietic development. Together with BMI1-PRC1 and MEL18-PRC1, our results show that these 3 PRC1 variants act simultaneously in the same environment, and have both shared and distinct targets. We also identify that BMI1-PRC1 is involved in epigenetic silencing of 5' Hox genes, which are associated with differentiated hematopoietic cells, in the d5.5 Flk1$^+$ population. Finally, genomic annotation

of ChIP-seq peaks suggests that DNA looping is involved in recruitment of PRC1 to the target promoter, a novel discovery in mammals previously found only in *D. melanogaster*; and we identify two novel *de novo* motifs shared between PRC1 components that may serve as the mechanism for PRC1 recruitment during early hematopoietic development.

This work reveals that the different lineage potentials between YS and P-Sp hematopoiesis is controlled by only a small number of genes, and identifies PRC1 variants that regulate distinct targets during early hematopoietic development.

List of Tables

List of Figures

List of Symbols

AGM	Aorta-gonad-mesonephros
Bex4	Brain-expressed gene 4
Bex6	Brain-expressed gene 6
bHLH	beta helix-loop-helix
BL-CFC	Blast colony-forming cell
BM	Bone marrow
Bmi1	Pcgf4
Bmp4	Bone morphogenetic protein 4
Bry	Brachyury (T)
Caf1	Chromatin assembly factor 1 subunit
CD34	CD34 antigen
CD41	Integrin alpha 2b (Itga2b)
CD45	Protein tyrosine phosphatase receptor type C (Ptprc)
CDK	Cyclin dependent kinase
ChIP	Chromatin immunoprecipitation
ChIP-qPCR	ChIP followed by qPCR
ChIP-seq	ChIP followed by high throughput sequencing
cKit	Tyrosine-protein kinase Kit (CD117)
Co-IP	Co-immunoprecipitation
Csh1	Prolactin family 3, subfamily d, member 1 (Prl3d1)
E2A	Early region 2A
EB	Embryoid body
E^D	Definitive erythropoiesis
ELC	Endothelial-like colony
EMac	Erythroid-macrophage
E^P	Primitive erythropoiesis

ESC	Embryonic stem cell
Esc	Extra sex comb
Ezh2	Enhancer of Zeste homologue 2
FGF	Fibroblast growth factor
FL	Fetal liver
Flk1	Fetal liver kinase 1
H3K27me3	Histone 3 lysine 27 trimethylation
H2AK119ub	Histone 2A lysine 119 monoubiquitination
HAT	Histone acetylase
HDAC	Histone deacetylase
Hox	Homeobox
HSC	Hematopoietic stem cell
IGF2	Insulin-like growth factor 2
LIF	Leukemia inhibitory factor
Lmo2	LIM-finger protein
LT-HSC	Long-term HSC
MACs	Model-based Analysis for ChIP-seq
MEF	Mouse embryonic fibroblast cell
Mel18	Pcgf2
P-Sp	Para-aortic splanchnopleura
Pc	Polycomb
Pcgf5	Polycomb group RING finger protein 5
PCR	Polymerase chain reaction
Ph	Polyhomeotic
Plf1	Prolactin family 2, subfamily c, member 2 (Prl2c2)
Plf2	Prolactin family 2, subfamily c, member 3 (Prl2c3)
PRC	Polycomb Repressive Complex

Prl	Prolactin
Prlr	Prolactin receptor
Prl4A1	Prolactin family 4, subfamily a, member 1
PS	Primitive streak
Psc	Posterior sex combs
qPCR	Quantitative PCR/ real-time PCR
R26R	*Rosa26* locus
Ring1A/B	Ring finger protein 1A/B
Runx1	Runt-related transcription factor 1
RSAT	Regulatory Sequence Analysis Tools
SAM	Significance Analysis of Microarrays
SCF	Stem cell factor
SCID	Severe combined immunodeficient
Scl/Tal1	Stem cell leukemia/T-cell acute lymphocytic leukemia protein 1
Sox	SRY-box containing gene
ST-HSC	Short-term HSC
Suz12	Suppressor of Zeste 12
Tie2	Endothelial-specific receptor tyrosine kinase (Tek)
TGFβ	Transforming growth factor beta
TPO	Thrombopoietin
YFP	Yellow fluorescent protein
YS	Yolk sac

CHAPTER 1:

INTRODUCTION

1.1 Hematopoietic stem cells and their derived lineages

Hematopoiesis begins early in embryogenesis, and is absolutely essential for normal development. Hematopoietic lineages are also responsible for inducing and maintaining the immune response against infections and injuries. Hence, hematopoiesis is a cornerstone of animal development and health, and defects in this system can lead to various debilitating or fatal disorders.

The hematopoietic stem cell (HSC), which is identified by its ability to self-renew and give rise to all blood cell types, stands at the top of the hematopoietic hierarchy. First discovered in bone marrow (BM) by Till & McCulloch[1], HSCs are extremely rare, constituting only about 1 in 10,000 to 1 in 100,000 cells in bone marrow[2-4]. Cell-surface markers include $CD34^{lo/-}$ $Sca1^{+}$ $Thy1^{+}$ $CD38^{+}$ $Ckit^{+}$ Lin^{-} [5,6] and $CD34^{+}CD59^{+}Thy1^{+}CD38^{lo/-}Ckit^{+}Lin^{-}$ [7] to identify mouse and human HSCs respectively, but the gold standard for HSC identification remains the hematopoietic reconstitution of lethally irradiated mice. This method reveals the existence of two types of HSCs: long-term (LT-HSCs) and short-term HSCs (ST-HSC). LT-HSCs are capable of long-term self-renewal, such that secondary transplantation of HSCs into another lethally- irradiated mouse also results in hematopoietic reconstitution. However, ST-HSCs are unable to sustain self-renewal over time, and may not reconstitute all hematopoietic lineages like the HSC. Hence, they are considered immature progenitor cells instead of true stem cells.

HSCs give rise to 3 main lineages: erythroid, myeloid and lymphoid. Erythroid cells facilitate the movement and transfer of oxygen throughout circulation,

and are essential throughout life. Primitive erythroid cells are named for their initial nucleated structures that resemble those observed in non-mammalian vertebrate species, while definitive erythropoietic cells are enucleated erythroid cells. Embryos lacking erythropoietin (*Epo*) or stem cell factor (*SCF/kit-ligand*) do not survive due to severe anemia[8]. Myeloid lineages include megakaryocytes, granulocytes, monocytes and mast cells, and are recruited to elicit both innate and adaptive immune responses against pathogens or other infections. Transcription factors involved in myeloid development include PU.1 and CCAAT/enhancer binding proteins, which, when knocked out, results in myeloid defects in mice[9]. Finally, lymphoid lineages comprise of natural killer cells (NKCs), B-cells and T-cells. Upon recognizing changes in cell-surface major histocompatibility complex (MHC) class I signatures, which are cell surface markers that mediate leukocyte interactions, NKCs expose infected cells to cytotoxic granules, while T-cells produce either cytotoxic granules or cytokines to induce apoptosis in infected cells. B-cells act as antigen-presenting cells (APCs) by making antibodies against antigens. Interleukin 7 (*IL-7*) is an essential cytokine for both T- and B-cell development. Loss-of-function mutations of *IL7* receptor α (*IL-7Rα*) results in autosomal recessive severe combined immune deficiency (SCID), while gain-of-function mutations induce cytokine-independent growth of lymphoid progenitors in leukemia cell lines[10-11].

Cytokines play an important role in modulating the fate of HSCs. Upon binding to receptors on these cells, cytokines induce the activation or suppression of various cytokine signaling pathways, which are involved in cell-fate decisions ranging from self-renewal, quiescence, differentiation, apoptosis and mobilization[12]. Stem cell factor (SCF) binding to tyrosine kinase

receptor c-Kit is not essential for HSC generation, but it is involved in prevention of apoptosis[13], and induction of HSC mobilization[14]. Self-renewal of fetal liver HSCs *in vitro* is also enhanced upon addition of SCF[15]. Thrombopoietin (TPO) is involved in HSC generation and expansion during definitive hematopoeisis[16], and mice that lack TPO or its receptor Mpl have fewer repopulating HSCs[17]. Fibroblast growth factor 1 (FGF1) and FGF2 are required for supporting serum-free expansion of bone marrow HSC *in vitro*[18,19], while FGF1 stimulates *ex-vivo* HSC expansion[20]. Insulin-like growth factor 2 (IGF2) stimulates *ex-vivo* expansion of both fetal liver and bone marrow HSCs, which express the receptors for IGF2; and the addition of IGF2, SCF, TPO and FGF1 enhances the expansion of HSCs *in vitro* by up to 8 times[21]. Notch ligands Delta and Jagged support HSC expansion in culture, and Delta 1 does so in a dose-dependent manner- low amounts of Delta 1 supports human cord blood SCID-repopulating cell numbers, while high amounts induced apoptosis instead[22]. However, conditional knockouts of Notch 1 and Jagged 1 do not have any effect on HSCs *in vivo*, indicating that Notch isoforms and their ligands are functionally redundant[23]. Bone morphogenic protein 4 (BMP4), a member of the transforming growth factor (TGF)-β superfamily, supports HSC expansion *in vitro* partly by modulating Sonic hedgehog expression[24]. BMP4/Smad signaling was also found to be involved in Scl- and Runx1-mediated HSC development[25].

Hence HSCs and their derived lineages play essential roles in development, and key cytokines that regulate their generation have been elucidated.

1.2 Hematopoietic development in the mouse embryo

Mesodermal populations, including hematopoietic, cardiac, endothelial and skeletal muscle tissue, arise from the primitive streak (PS) following patterning of the PS by embryonic morphogen gradients. These morphogens include BMP4, which is a ventralizing factor required to attenuate dorsalizing signals during dorsoventral patterning[26-27]. BMP4 deficiency results in severe mesodermal defects, leading to embryonic lethality[28]. Wnt signaling is also essential for primitive streak development, and deficiency of canonical ligand *Wnt3*, Wnt co-receptors *Lrp5/6* or *β-catenin* result in the lack of primitive streak and mesoderm formation[29-31]. BMP4 first induces ventral-posterior mesoderm, and subsequently commits mesoderm towards a hematopoietic fate by activating Wnt signaling as well as the *Cdx-Hox* pathway[32].

The first mesodermal cells from the PS migrate to the extra-embryonic region to differentiate and form the hematopoietic and endothelial cells of the blood islands[33]. T-box transcription factor Brachyury (*Bry*) is expressed in all nascent mesoderm and downregulated upon differentiation[34-35], while fetal liver kinase 1 (*Flk1*), a vascular endothelial growth factor (VEGF) receptor, marks Bry^+ mesoderm commitment towards hematovascular lineages[36-38]. Lineage-tracing methods revealed the importance of Flk1, by showing that $Flk1^+$ mesoderm gives rise to both primitive and definitive hematopoiesis[39]. Knockout of *Flk1* causes embryonic lethality by E9.5 due to lack of blood or vessels[40], while *Bry* is essential for posterior mesoderm development, and $Bry^{-/-}$ mice have posterior truncation and no notochord[41].

Hematopoietic and endothelial lineages were first observed to develop in close temporal and spatial proximity in chick embryo cultures[42-43]. Both lineages were also observed to express a large number of different genes in common, including *CD34, Flk1, Tie2, Scl/Tal1* and *Gata2*[36, 38,44-50], leading to the proposal that hematopoietic and endothelial lineages arise from a common progenitor called the hemangioblast. Given its 2 lineage potentials, the hemangioblast is a critical stage at which key fate decisions are being made. The hemangioblast-containing population was found to arise from the posterior primitive streak, and can be identified by its co-expression of *Bry* and *Flk1*[51].

The hematopoietic stem cell undergoes a complex developmental journey during early embryogenesis (Fig. 1) [52]. The earliest known sites of embryonic hematopoiesis in the mouse are the yolk sac (YS) and the para-aortic splanchopleura (P-Sp). The YS blood islands, which appear from E7.5, give rise to the primitive and definite erythroid lineages as well as a restricted myeloid subset, but not HSCs. The P-Sp, which appears from E8.5 and develops later into the aorta-gonad-mesonephros (AGM) at E10.5, is an intra-embryonic site of hematopoiesis[38]. It has no primitive erythroid potential, but instead possesses definitive erythroid, myeloid and lymphoid potentials, via HSC generation. The first adult-repopulating HSCs come from the AGM, which remains as the major site of hematopoiesis for only about 2 days, until E13.5 when the fetal liver becomes established as the major site of hematopoietic replication and expansion until birth. More recently, the placenta has also been identified as a hematopoietic niche[53]. Hence, key sites of hematopoiesis during early embryonic development have been identified.

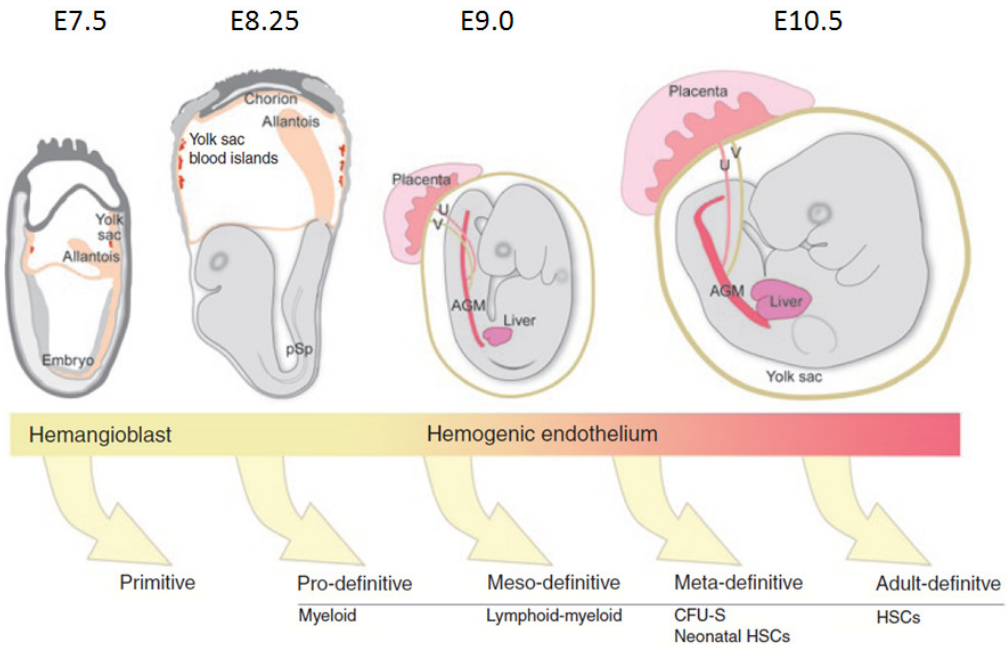

Figure 1. Timeline of hematopoietic development in the mouse embryo
Based on function, five classes of hematopoietic cells can be identified, and are subsequently generated in the mouse embryo, shown here between E7.5 and E10.5. Primitive hematopoiesis arises from the hemangioblast, while pro-, meso-, meta- and adult- definitive hematopoiesis is believed to arise from the hemogenic endothelium. Yolk sac blood islands are first observed in the E7.5 embryo. The P-Sp, which first appears at about E8.5, eventually forms the AGM by E10.5, which is the site of the first adult-repopulating HSC. The liver begins to be colonized by hematopoietic progenitors from late E9.0, and is established as a major hematopoietic organ by E13.5 (not shown). Figure adapted from Dzierzak and Speck[52].

1.2.1 Yolk sac

Consisting of a bilayer of visceral endoderm apposed to mesoderm-derived cells, the yolk sac is where hematopoiesis makes its first appearance in the form of blood islands at E6.5 of mouse embryonic development[45, 54]. This extra-embryonic structure is essential for normal development, and continues to be the primary source of red blood cells in the embryo until the establishment of AGM-derived hematopoiesis from E10.5 onwards.

The yolk sac observes several stages of hematopoiesis. During the initial wave of primitive erythropoiesis, large nucleated erythroid cells that express embryonic hemoglobins (ζ, βH1 and εy) as well as adult (α1, α2, β1 and β2) globins during cell maturation arise from the EryP-CFC, which was first identified via culture of mouse embryonic yolk sacs in semisolid media[55-56]. These progenitors emerge during early gastrulation in the yolk sac, and undergo limited expansion within the yolk sac before eventually waning by E9.0[45]. Primitive erythroid cells undergo enucleation and maturation in the bloodstream, which overlaps with the later emergence of definitive hematopoiesis[57]. Definitive erythroid progenitors (BFU-E) begin to emerge from the yolk sac at the start of somitogenesis (E8.25) [45, 58]. Prior to the onset of circulation, BFU-Es expand in the yolk sac for 48h, following which they are observed in the bloodstream from E9.5 onwards and go on to colonize and establish the liver as a major hematopoietic organ from E10.5.

The first myeloid cells in the mouse embryo appear in the E9.5 YS[59], although macrophage progenitors can be detected at early as E7.0[45]. These macrophage progenitors preferentially remain in the yolk sac even after

circulation is established; however specific microenvironments within the yolk sac have yet to be identified. Knockout of VE-cadherin (*VECad*) is embryonic lethal by E9.5 due to lack of vascular integration and subsequent blood circulation, but the yolk sac continues to retain its myeloid potential[60-61], further supporting the emergence of myeloid lineages from the yolk sac.

Whilst E10 YS cells do not contain adult-repopulating HSCs, Yoder *et al* identified that these cells contain a population that is able to reconstitute hematopoiesis in conditioned bulsulfan-treated neonates, which have depleted HSC numbers[62]. Donor-derived cells obtained from the bone marrow of primary neonatal recipients were further able to reconstitute hematopoiesis in conditioned secondary recipient adult mice, indicating that the YS is also a site of HSC generation, albeit HSCs that can only reconstitute hematopoiesis in conditioned neonatal but not adult recipients. Further study not pursued in this thesis will be needed to characterize the YS microenvironment involved in regulating YS HSC development.

1.2.2 P-Sp and AGM

At around E8.5, the para-aortic splanchnopleura (P-Sp) develops from the lateral plate mesoderm in the caudal region of the embryo. The P-Sp gradually forms the aorta-gonad-mesonephros (AGM) by E10.5, which contains the dorsal aorta, genital ridges and mesonephros. The P-Sp/ AGM is the first intra-embryonic site of definitive hematopoiesis, generating multipotent hematopoietic progenitors with B and T lymphoid as well as myeloid potential as observed from single cell *in vitro* assays[63-64]. Importantly, the first adult-repopulating HSCs are generated in the AGM via the hemogenic endothelium, which is located on the dorsal aorta.

Based on expression of endothelial marker *Tie2* and hematopoietic markers *cKit* and CD41, a transient $Tie2^{hi}cKit^{+}CD41^{-}$ endothelial population that can give rise to $CD41^{+}$ hematopoietic progenitors was generated from both cultured ESC and *in vivo*[65]. This suggests that hematopoietic progenitors arise from hemangioblasts through a hemogenic endothelial stage, providing a direct link between the two proposed mechanisms of hematopoietic development. Time-lapse imaging further supported the potential of hemogenic endothelium to generate hematopoietic cells from both ESC- and embryonic E7.5- derived mesoderm[66]. Chen *et al* identified that transcription factor *Runx1* is essential during the transition of $VEcad^{+}$ vascular endothelial cells to HSPC, but not in cells that express Runx1 target *Vav*. Lineage tracing[67] using a *VEcad-Cre* transgene and *R26R-YFP* reporter mice marked all subsequent $VECad^{+}$ progeny as YFP^{+}. 96% of $CD45^{+}$ adult blood was thus observed to be derived from cells that had expressed *VECad* at some point in time[68].

1.2.3 Fetal Liver

The fetal liver (FL) diverticulum forms by E9 and expands into a recognizable liver bud by E10, and by E13.5 the FL is established as the major fetal hematopoietic organ, providing a rich microenvironment for the massive expansion of HSCs between E12 and E16[69-71]. However the FL is not a site of *de novo* HSC generation; instead, it is colonized from E10 by existing HSCs from either the YS or AGM, via the circulatory system. Cumano & Godin postulate that the limited number of AGM HSCs and high level of hematopoietic activity even during early FL development suggest that the first HSCs that colonize the FL are of YS origin[72]. This rapid cycling of FL-derived HSCs outcompete even adult BM HSCs when transplanted in irradiated recipients, highlighting inherent differences between fetal and adult HSCs[73-74.]

The FL also contains a large population of enucleated erythrocytes that predominantly express adult β-globins, but also low levels of embryonic βH1 globins due to FL colonization by YS-derived erythromyeloid cells[75]. Together, these highlight the rich microenvironment of the fetal liver in supporting hematopoietic expansion and differentiation. Indeed, YS-derived HSCs more effectively reconstituted hematopoiesis in conditioned neonates when injected directly into the FL compared to via intravenous injection, suggesting that the FL provides an important microenvironment for YS HSC proliferation and differentiation[62]. The FL microenvironment consists of heterogenous stroma derived from mesenchymal cells. A primary human stromal cell line derived from fetal liver was shown to provide essential support of primitive HSPCs, and was more resilient in culture than BM cells[76]. In addition, FL hepatic progenitors that express SCF, which is important in hematopoiesis, as well as hepatic marker DLK, also express a range of factors involved in HSC

expansion and homing, including ANGPTL3, IGF2 and CXCL12, and have been shown to support HSC maintenance in *ex vivo* culture[77], suggesting that these are the primary stromal cells that support HSC expansion in the fetal liver.

In addition to isolating FL-derived hematopoietic-supporting stroma, identifying the key factors involved in generation and expansion of hematopoietic populations in the fetal liver could also potentially improve HSC expansion protocols. Sox17, which is a member of the Sry-related high-mobility group box (Sox) transcription factors, is known to be required for fetal HSC maintenance. Germline deficiency for *Sox17* results in complete loss of definitive HSCs, while postnatal deletion of *Sox17* results in the rapid loss of neonatal but not adult HSCs[78]. Ectopic expression of *Sox17* in adult mouse multipotent progenitors (MPPs) induced expression of fetal HSC surface markers and upregulation of fetal HSC genes in these cells, as well as conferred hematopoietic potential similar to fetal hematopoiesis, indicating that *Sox17* is a key determinant of fetal HSC identity[79]. However, *Sox17* alone does not fully convert adult hematopoietic progenitors into fetal HSCs, suggesting that other genes essential for the development of fetal HSCs remain unknown.

1.2.4 Placenta

Developing extra-embryonically from trophoblast cells, the highly vascularized placenta plays a critical role in facilitating fetal-maternal exchange during pregnancy. The placenta has also been shown to be an important hematopoietic niche, containing multipotent hematopoietic progenitors that also go on to colonize the fetal liver.

Hematopoiesis occurs in the mouse placenta from E9.0, when definitive multi-lineage progenitors are observed[80]. This is soon followed by mature HSCs from E10.5 onwards[81], which is significant as this occurs before intra-embryonic HSCs are observed, suggesting that placental HSCs are generated *in situ*. Between E11.5-12.5, placental HSCs undergo rapid expansion that surpasses that of local progenitors, suggesting that a unique HSC-supportive microenvironment exists in the placenta[70]. The concurrent accumulation of HSCs in the fetal liver during this period also suggests that the placenta is an important contributor of HSCs that seed the fetal liver.

Robin *et al* identified that the human placenta contains HSCs as early as week 6 of gestation, throughout fetal development, and at term. In addition, *CD146*$^+$/ *NG2*$^+$ placental stromal cell lines were found to support the expansion of cord blood CD34$^+$ and progenitor cells in co-culture[53], indicating the potential for placental-derived hematopoietic-supporting stroma in HSC expansion protocols. Hence, the placenta is an active hematopoietic site with potent clinical applications, both directly in HSC transplantation, as well as indirectly to expand HSCs *in vitro*.

Using a Sca1-GFP transgenic mouse that expresses the green fluorescent protein (GFP) under the regulation of HSC marker Sca1, Dzierzak *et al* identified that most Sca1-GFP-expressing cells co-express CD34, and are located within the vasculature of the placental labyrinth and the umbilical vessel[81]. Hematopoietic markers *Gata2* and *Runx1* also expressed in some endothelial cells surrounding the labyrinth vasculature, suggesting that HSCs and progenitors are localized within the labyrinth, and also that an intermediate hemogenic endothelial stage may also be involved in HSC generation in the placenta.

1.3 Hematopoietic transcription factors

Transcription factors play a key role in regulating gene expression, and this is no different in the hematopoietic system. Transcription factors have been found to be involved in a variety of roles ranging from stem cell maintenance to lineage commitment and differentiation. Hematopoietic cell fate decisions are mediated by lineage-specific transcription factors such as SCL/TAL1, LMO2, RUNX1 and GATA1/GATA. Hence, understanding key transcriptional regulators is essential towards dissecting hematopoietic development.

While differing in hematopoietic potentials, YS and P-Sp hematopoiesis share the requirement for several transcription factors, such as the T cell leukemia oncogene *Scl/Tal1* and LIM-finger protein *Lmo2*, which are essential for both extra-embryonic and intra-embryonic hematopoiesis. *Scl/Tal1* is a basic helix-loop-helix transcription factor that is considered a master gene for the establishment of primitive and definitive hematopoiesis, and is also involved in vascular and central nervous system development[82-86]. Embryos lacking SCL die at E9.5-10.5 with a complete lack of blood[87-88]. Erythroid, myeloid and lymphoid lineages are absent in differentiated *Scl/Tal1*$^{-/-}$ ESC, and lymphoid rescue of *Rag2*$^{-/-}$ mice by *Scl/Tal1* cDNA showed that *Scl/Tal1* is essential for lymphopoiesis *in vivo*[89]. The *Scl* locus contains 3 hematopoietic enhancers which drive its expression in endothelial and fetal blood progenitors (-4 kb), HSPCs and endothelial cells (+19 kb), and erythroid cells (+40 kb)[90-94], thus ensuring the timely and regulated expression of *Scl*. SCL/TAL1 function relies on its HLH domain to heterodimerize with class I bHLH such as the early region 2A (E2A) proteins, as well as its basic domain to bind the heterodimer to DNA on the E-box consensus sequence (CANNTG) for further induction of target genes[95]. Deletions and point

mutation experiments indicate that the DNA-binding domain is not required for SCL/TAL1-induced leukemogenesis in mice[96].

The *Lim domain only 2* gene (*Lmo2)* is involved in chromosomal translocations in T cell leukemia, and is required for both yolk sac hematopoiesis and adult hematopoiesis[104]. *Lmo2* expression in blood and endothelial progenitors is conserved across all vertebrate species, and mice lacking *Lmo2* are severely anemic and die at E9-10 due to a failure in YS hematopoiesis[97]. The human *LMO2* locus contains a proximal promoter that is active in several tissue types, as well as a hematopoietic-restricted distal promoter[98]. However, LMO2 binds DNA indirectly via other DNA-binding complexes involving transcription factors such as Scl/Tal1, E2A and Gata1 or Gata2[99-100].

RUNX1 plays a crucial role in definitive hematopoiesis during embryonic development. The core binding factor (CBF) transcriptional complex consisting of Runx1 (also known as acute myeloid leukemia 1 [AML1]) and non-DNA-binding protein CBFβ has high DNA affinity via the Runt domain of Runx1, which recognizes the DNA consensus sequence YGYGGTY (where Y=pyrimidine)[101-102]. *Runx1* is involved in the regulation of numerous hematopoietic-specific genes including T-cell receptor (TCR) chain genes and macrophage colony-stimulating factor (M-CSF) receptor[103-107]. Mice deficient for Runx1/CBFβ lack any definitive hematopoiesis and die by E12.5[108-109]. However, in contrast with *Scl/Tal1* and *Lmo2*, *Runx1* marks HSCs but is not essential for the primitive erythroid lineage[110-111]. Numerous chromosomal translocations involving *Runx1* generate chimeric proteins have been associated with acute myeloid leukemia (AML)[112-114], and some of these have

been targeted for therapeutic treatments with varying success. For example, anti-leukemic treatment resulted in long-term remission in about 50% of patients with AML associated with t(8;21) or inv(16), compared to 32% of patients with normal karyotype AML[115].

The GATA family consists of evolutionarily conserved proteins that bind the consensus DNA sequence (A/T)GATA(A/G) via two highly conserved zinc finger domains, hence their name[116]. GATA family members are well-characterized for their roles as lineage-restricted transcription factors. In particular, GATA1 and GATA2 expression occurs mainly in hematopoietic lineages, and are essential in the development of several hematopoietic lineages, including erythrocytes and megakaryocytes[117-120]. The dynamic changes in *GATA1* and *GATA2* is the basis of the 'GATA factor switch' during erythroid differentiation. GATA2 acts as an enhancer and binds to its own promoter, regulating its transcription. During erythroid differentiation, *GATA1* is upregulated and GATA1 replaces GATA2 at the same motifs, thus inhibiting *GATA2*[120-122]. GATA2 is also required for the proliferation and maintenance of HSPCs[123]. Mutations in either *Gata1* or *Gata2* are both embryonic lethal, with respective defects in erythroid development[117-118] and HSC proliferation and maintenance[123-124] *Gata2* is also able to rescue the embryonic lethal *Gata1* mutation, indicating that certain GATA members are partially redundant[125].

In addition, extensive cross- and autoregulatory links between transcription factors and their cofactors are believed to contribute to the complexity of the hematopoietic transcriptional regulatory network[126-127]. Genome-wide binding patterns and combinatorial interactions for key regulators of HSPCs have

identified novel interactions between a heptad of hematopoietic transcription factors (SCL, LYL1, LMO2, GATA2, RUNX1, ERG and FLI1), as well as direct protein-protein interactions between RUNX1, GATA2, SCL and ERG to stabilize complex binding to DNA[127]. These results hint the potentially immense role of cross-interactions between known transcription factors in regulating hematopoietic gene expression, and indicate that genome-wide mapping of binding events need to be employed alongside functional assays.

1.4 Epigenetic regulation of hematopoietic development

In addition to transcription factors, gene activity is also modulated by epigenetic mechanisms, which generate heritable changes in gene function that do not affect the underlying DNA sequence. These include DNA methylation, histone modifications, chromatin remodeling, and regulation by non-coding microRNA (miRNA)[128-130]. Epigenetic regulation is essential for the maintenance and differentiation of HSPCs[131-133], and understanding the mechanisms involved will benefit the diagnosis and treatment of blood and immune diseases.

A central component of epigenetic regulation is the organization of DNA into higher order structures or nucleosomes, which represent the basic repeating unit of chromatin. Each nucleosome consists of 147bp of DNA wrapped around a core of eight histones, which comprise two molecules each of H2A, H2B, H3 and H4[134]. Individual nucleosomes are joined to each other by the linker histone H1 and about 200bp DNA to form a 10nm fiber. These can be further compacted via interactions between flexible histone tails that protrude from the nucleosomal disk, to form a helical structure called the 30nm fiber. Post-translational covalent modifications of these histone tails by acetylation, methylation, phosphorylation, glycosylation, SUMOlyation or ubiquitylation act in a concerted manner to induce structural changes in the chromatin fiber, thus regulating the accessibility of gene regulatory sequences by transcriptional components[135-136].

Histone acetylation is regulated by the opposing activities of histone acetylases (HATs), which catalyse the transfer of acetyl groups from acetyl-CoA to lysine residues of target proteins, and histone de-acetylases

(HDACs), which catalyse the removal of acetyl groups. These modifications directly affect higher order chromatin structure- hyperacetylation of histones is associated with structurally 'open' chromatin and active gene transcription, while histone deacetylation is associated with heterochromatin formation and gene repression[137]. Hematopoiesis-specific transcription factor GATA1 is known to stimulate transcriptional activation by recruiting HAT-containing complexes to the β-globin locus[138], while acetylation of Scl/Tal1 by co-activators p300 and the CBP-associated factor (PCAF) is linked to increased transcriptional activation and differentiation of murine erythroleukemia (MEL) cells *in vitro*[139-140].

Small regulatory RNAs like miRNAs, small interfering RNAs (siRNAs) and Piwi-interacting RNAs (piRNAs) also regulate gene expression by binding to sequence-specific target mRNA at the 3'UTR, resulting in mRNA degradation or inhibition of translation[141-143]. MiR-125b is an important miRNA in normal HSPCs. It regulates HSC survival and promotes differentiation towards the lymphoid lineage[144]. Overexpression of miR-125b enhanced hematopoietic engraftment in humanized mice, and improved colony formation in primary mouse HSPCs[145-146]. MiR-144 and miR-451 are also involved in regulating erythropoiesis in zebrafish. MiR-144 specifically regulated the expression of embryonic α hemoglobin during primitive erythropoiesis[147], while miR-451 promotes erythroid maturation by targeting GATA2[148]. Both miR-144 and miR-451 can induce erythropoiesis by targeting GATA1 in zebrafish[149], and have recently been identified in human erythropoiesis[150-151].

DNA methylation is the addition of a methyl group at position C5 of cytosine in CpG dinucleotides. DNA methyltransferases (DNMTs) such as DNMT1,

DNMT3A and DNMT3B are required for the maintenance of DNA methylation patterns[152]. The regulation of gene expression by DNA methylation of target gene promoters is crucial for the control of several developmental processes, including X inactivation[153], genomic imprinting[154], embryonic *Hox* gene patterning[155] and in particular, hematopoiesis[133, 136, 156-157]. DNMT1 is important for the self-renewal of adult HSCs, and DNMT1-deficient HSCs tend to differentiate into myeloerythroid but not lymphoid cells[157-158]. Genome-wide DNA methylation studies identified promoter demethylation in hematopoietic-specific genes during hESC differentiation to the hematopoietic lineage[159], as well as changes in DNA methylation during the differentiation of HSPCs[160]. Specific DNA methylation profiles in HSPCs have also been found to be associated with AML, and the methylation status of the deleted in bladder cancer protein 1 (DBC1) is used as a predictor of AML with a normal karyotype[161].

Among epigenetic regulators, the repressive histone modifications by Polycomb group protein (PcG) complexes are best characterized in HSCs[162]. The canonical role of PcG is based on genetic evidence from *Drosophila melanogaster*, in which mutagenic studies first identified PcG complexes as regulators of Hox gene expression[163-164]. The two major PcG complexes are the Polycomb Repressive Complex 1 (PRC1) and PRC2. PRC1 consists of 4 proteins: Polycomb (Pc), which contains a chromodomain that binds trimethylated histone H3 lysine 27 (H3K27); Polyhomeotic (Ph), which may associate with an external sterile α-motif (SAM); RING1, the enzymatic E3 ubiquitin ligase that monoubiquitinates histone H2A lysine 119 (H2AK119); and Posterior sex combs (Psc), which forms a heterodimer with RING1 to promote H2AK119ub. PRC2 consists of 4 proteins: Enhancer of zeste (E(z)),

a H3K27 methyltransferase; Extra sex comb (Esc) and Suppressor of Zeste 12 (Su(z)12), which interact with both the target and surrounding nucleosomes to regulate PRC2 activity; and Chromatin assembly factor 1subunit (Caf1), a histone chaperone. Mammalian PRC2 consist of homologues Ezh1/2, Eed, Suz12 and Rbbp4/7[165-167].

In *D. melanogaster*, both PRC1 and PRC2 are recruited to mediate transcriptional repression of target genes. Polycomb response elements (PREs) at target genes recruit PRC1 and PRC2, possibly together with additional proteins such as Pho (a DNA-binding protein) that may enhance repression. PRC2 tri-methylates H3K27 (H3K27me3) at a target locus, preventing H3K27 acetylation and thus gene activation. The H3K27me3 mark is recognized by and subsequently recruits PRC1, which mono-ubiquitinates H2AK119 (H2AK119ub). This inhibits the progression of RNA polymerase II (Pol II) or prevents Pol II from forming the initiation complex[168-169], and together with PCGF-mediated chromatin compaction[170], the target gene is thus repressed.

Mammalian homologues of PRC1 consist of the enzymatic RING1A/B; Ph homologues PHC1, PHC2 and PHC3; 8 Pc homologues chromobox protein (CBX); and 6 Polycomb group RING finger proteins (PCGF). Mammalian PRC2 contains EZH2, EED, SUZ12 and Caf1 homologues RBBP4 and RBBP7. Despite similar functions as in *D. melanogaster*, the method of recruitment of mammalian PcG complexes is still unknown, as PRE-like homologues have yet to be verified. PCGF and CBX proteins have also been shown to have partially- overlapping targets, indicating that PcG proteins are non-redundant and can form distinct PRC1 complexes with different

targets[171-173]. Consistent with this hypothesis, overexpression of CBX7, but not CBX2, CBX 4 or CBX8, appears to inhibit a specific set of target genes, promoting self-renewal in multipotent cells but not in more differentiated progenitors[174].

While *Bmi1*-deficient mice have normal fetal liver hematopoiesis, severe postnatal pancytopenia is observed due to progressive HSC depletion as long-term self-renewal is disrupted[175]. BMI1 binds directly to the promoter of the cyclin dependent kinase (CDK) inhibitor gene $p16^{Ink4a}$ and the tumour suppressor gene $p19^{Arf}$ as part of PRC1-mediated transcriptional repression. Deletion of both $p16^{Ink4a}$ *and* $p19^{Arf}$ in *Bmi1*-deficient mice restores the self-renewal capacity of HSCs, indicating that these two genes are key Bmi1 targets in HSCs[176]. On the other hand, overexpression of *Bmi1* using conditional knock-in mice increases HSC resistance to oxidative stress, thus enhancing expansion of HSCs in *ex vivo* culture and maintaining HSC self-renewal capacity during serial transplantation[177]. Meanwhile, Ring1B restricts the proliferation of progenitors and stimulates progeny differentiation by mediating expression of cell cycle activator cyclin D2 and $p16^{Ink4a}$, and *Ring1B*-deficient mice develop a hypocellular BM containing an enlarged, hyperproliferating compartment of immature cells[178-179].

Non-canonical mechanisms of PRC1 have also recently been identified, including PRC2-independent activity and the formation of PCGF-RING1A/B complexes with RYBP, which inhibits the incorporation of other canonical PRC1 subunits like CBX and PHC[172, 180]. These results indicate that despite PcG proteins being identified close to 30 years ago, PRC1-mediated transcriptional repression remains a complex mechanism that has yet to be

fully elucidated, particularly towards the understanding of hematopoietic development.

1.5 Of mice and cells: recapitulating hematopoiesis *in vitro*

The orchestrated complexity in hematopoietic development warrants both temporal and spatial studies to elucidate the interactions involved; however, to carry out such studies only *in vivo* would be time-consuming and expensive, given the long generation time and high financial and ethical cost of using mice. Hence, *in vitro* systems that recapitulate different stages of development during *in vivo* hematopoiesis can be used to analyze how hematopoietic development occurs, particularly during early stages where critical fate decisions are likely to be made. As outlined by Keller, three criteria should be considered when using the ESC model for lineage-specific differentiation: I, the establishment of robust and reproducible protocols that generate the cell type of interest; II, the recapitulation of *in vivo* developmental programmes leading to generation of the target lineage; and III, the functional accuracy of mature cells both in culture and in appropriate animal transplants[181]. In this thesis we employ differentiation systems that recapitulate both YS and P-Sp hematopoiesis, to generate cell populations that can give rise to the respective erythroid, myeloid and lymphoid lineages.

ESCs can be grown in co-culture with mouse embryonic feeder cells[182-183], which function mainly to secrete leukemia inhibitory factor (LIF), which is essential to maintaining ESCs[184-185]. Feeder-free culture of ESCs can be maintained by the addition of recombinant LIF together with appropriate serum-containing ESC media[184]. ESCs differentiate when factors that support pluripotency are removed, and the addition of cytokines in appropriate conditions can direct differentiation towards particular lineages. ESCs can be differentiated in liquid culture to form three-dimensional embryoid bodies

(EBs), which are heterogeneous units comprising of cells from several lineages, including the hematopoietic lineage.

EBs express key hematopoietic transcription factors as they mature. For example, expression of *Runx1* and *Scl*, which are important in embryonic and definitive hematopoiesis in the YS or AGM[186-187], is induced at EB day 2.5 and subsequently peaks around day 4[188-189]. *Bry* is expressed in EBs prior to the onset of hematopoiesis, similar to its expression in the embryo[191, 56, 190]. An ESC line with GFP cDNA targeted to the *Bry* locus (GFP-*Bry*) enabled Fehling *et al* to identify 3 distinct cell populations in d3.5 EBs based on GFP-*Bry* and *Flk1* expression: pre-mesoderm (Bry^-Flk1^-), pre-hemangioblast mesoderm or primitive streak (Bry^+Flk1^-), and the hemangioblast-containing population (Bry^+Flk1^+)[78] (fig. 2).

Culture of the d3.5 Bry^+Flk1^+ population in semi-solid methylcellulose blast colony assays generates blast colonies[192], here also termed hemangioblast-derived colonies, that have both hematopoietic and endothelial potential. These colonies are not an artifact of ESC differentiation, as a similar progenitor also expressing *Bry* and *Flk1* has been found to arise in the posterior primitive streak in early mouse embryos[51]. The two lineage potentials can be further revealed by picking individual colonies using mouth pipettes and culturing them in liquid expansion assays in the presence of hematopoietic and vascular cytokines[56]. After 3-4 days of culture, two different cell types are observed: small round non- adherent cells represent the hematopoietic fraction, and culture of these cells in a methylcellulose-based hematopoietic progenitor assay generates colonies from both erythroid and myeloid lineages. Meanwhile, adherent cells represent the endothelial

fraction, and express smooth muscle actin (SMA) and vascular marker CD31. D3.5 EB-derived BL-CFCs are thus observed to recapitulate YS hematopoiesis, in that they have only primitive and definitive erythroid and limited myeloid potential, but no definitive hematopoietic potential. In particular, the hematopoietic progenitor assay reveals that the primitive erythroid lineage is a transient population that is the first to arise, soon followed by the macrophage, definitive erythroid and mast cell lineages; which recapitulates the temporal order observed in the YS[191]. Lymphoid and HSC progenitors are not observed, providing further evidence that this programme indeed recapitulates YS hematopoiesis.

Irion *et al* showed that 48h reaggregation of the d3.25 *Bry*$^{+}$*Flk1*$^{-}$ EB population in the presence of cytokines activin A, bone morphogenetic protein 4 (BMP4) and vascular endothelial growth factor (VEGF) generated a d5.25 *Flk1*$^{+}$ population that has decreased primitive erythropoiesis and increased potential for myeloid and lymphoid lineages, representing a distinct stage of hematopoiesis similar to that of P-Sp hematopoiesis[193]. While genes essential for hematopoietic development such as *Scl/Tal1* and *Runx1* were broadly expressed in both the hemangioblast-containing d3.5 *Bry*$^{+}$*Flk1*$^{+}$ population as well as the derived d5.25 *Flk1*$^{+}$ population, only the latter population expressed both fetal liver HSC marker *Sox17* as well as *Hoxb4*, which is associated with definitive hematopoietic induction, further indicating that this population recapitulates P-Sp hematopoiesis[193]. Hence both YS- and P-Sp-hematopoiesis can be recapitulated *in vitro,* thus providing powerful tools for elucidating hematopoietic development.

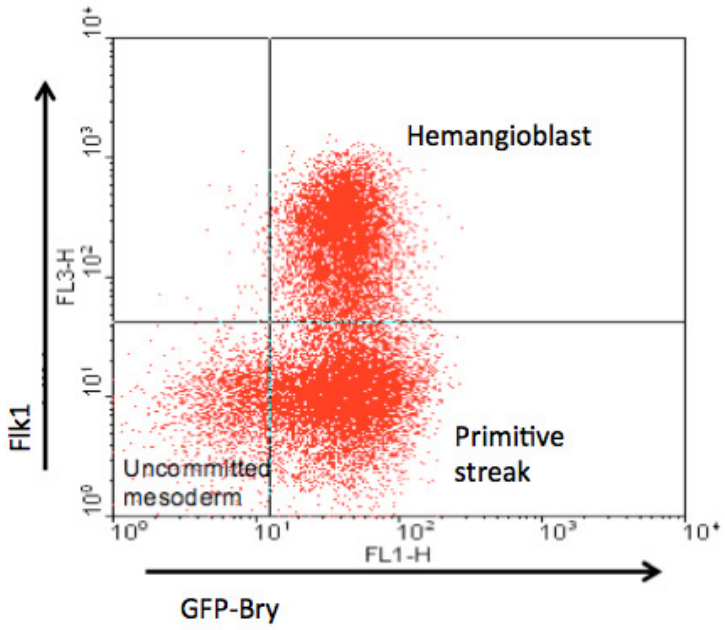

Figure 2. Distinguishing mesodermal populations in d3.5 EBs based on cell surface expression of *Flk1* and GFP-*Bry*.
FACS isolation of cell populations corresponding to uncommitted mesoderm (*Bry*$^{-}$*Flk1*$^{-}$), primitive streak (*Bry*$^{+}$*Flk1*$^{-}$) and hemangioblast-containing (*Bry*$^{+}$*Flk1*$^{+}$) populations from d3.5 EBs.

1.6 Why we need to elucidate HSC development & generation

1.6.1 HSC transplants in clinical applications

HSCs were first applied clinically for the treatment of blood cancers, i.e. leukemia and lymphoma. According to the Singapore Cancer Registry 2005-2009, lymphoma was ranked the 8th and 9th most common cancer to affect men and women respectively, with an average of 368 cases reported per year during that period[194]. At the KKH Children's Cancer Centre, leukemia makes up about 40% of pediatric cancer cases, and acute lymphoblastic leukemia (ALL) is the most common cancer in children and adolescents up to age 19[195].

Leukemia is divided into four categories, namely acute or chronic, and myeloid or lymphocytic. The acute form is characterized by a rapid increase in the number of immature hematopoietic cells, which are highly malignant and metastasize quickly to affect other organs in the body. Chronic leukemia, on the other hand, involves a slower accumulation of relatively mature blood cells due to excessive proliferation.

Myeloid lineages are affected in myeloid leukemia, while circulating lymphocyte cells are affected in lymphoid leukemia. This is in contrast to lymphoma, which originates in the lymphatic system and most commonly results in tumour mass formation in the lymph nodes or organs with lymphatic tissue e.g. the stomach or intestines. Lymphomas are divided into two categories: Hodgkin's lymphoma, which makes up about 12% of all lymphomas and is marked by the presence of the Reed-Sternberg B cell-derived cell type; and non-Hodgkin's lymphomas[196].

HSC transplant following elimination of the patient's cancerous hematopoietic cells via radiation or chemotherapy results in patient survival rate of about 60%. Data from 146,800 patients in 72 countries between 2006-2008 revealed that while a range of HSC transplant types (autologous/ allogenic bone marrow, peripheral blood/ cord blood stem cells) are now more widely available even in low- income countries, there is a widening difference in transplant rates between high- and low- income countries[197], highlighting the need to optimize HSC transplantation both clinically and economically. While the therapy has improved by leaps and bounds, HSC transplantation still faces several bottlenecks towards clinical applications.

1.6.2 Bottlenecks in HSC transplantation

Sources of HSCs

HSCs are rare, numbering only about 1 in 100,000 peripheral blood cells. While cytokines such as granulocyte-colony stimulating factor (G-CSF) can be injected to mobilize HSCs in the donor before harvest, the limited volume of blood drawn constrains the number of HSCs available for use. Bone marrow contains a higher percentage of LT-HSCs, but the procedure involved is difficult, time-consuming and painful for the donor, resulting in the search for other sources of HSCs. This includes umbilical cord blood (UCB), which is easily obtained following delivery and has become an established HSC source for patients without matched donors, as mismatched donors are permitted and UCB are more easily available than matched unrelated donor grafts[198]. UCB HSCs also appear to have a lower risk of inducing graft-versus-host disease[199]. However, UCB engraftment is delayed compared to BM or peripheral blood transplants, and the number of HSCs obtainable per UCB unit is limited, restricting the use of UCB to children and small adults. Placental HSCs are equally easy to obtain, and have the added advantage of possessing much more HSCs than in umbilical cord blood, increasing the pool of patients to include adults.

Expansion of HSCs

Attempts to optimize *ex vivo* expansion of HSCs have been ongoing for over a decade, based on $CD34^+$ HSCs obtained from *in vitro* and mouse models. Protocols in 1991 resulted in HSC survival and 10 to 20-fold expansion of progenitor cells[200-201]. More recently, an automated closed-system process involving controlled 'fed-batch" media dilution resulted in a 11-fold expansion of human HSCs in just 12 days[202]. The addition of cytokines such as SCL, FL

and TPO[203-206] to expand HSCs and inhibit apoptosis, as well as co-culture with hematopoietic-supportive stroma e.g. mesenchymal stem cells (MSCs) further improve the ability to generate sufficient numbers of HSCs for transplants[207-209]. In addition, engraftment of expanded HSCs appears to be impeded whether the expanded product was used alone or together with un-manipulated products[210-211]. Hence it remains a challenge to develop robust, rapid and efficient HSC expansion protocols for clinical transplants.

Donor Matching

Autologous transplants, in which cells for transplant are derived from the patient him/herself, avoid the risk of graft-versus-host disease but may re-introduce the patient's diseased cells into his/ her system. In addition, patients may not generate sufficient HSCs for autologous transplantation. Allogeneic transplants, which are derived from close relatives or matched donors, may induce a beneficial "graft-versus-tumor" effect that further eliminates remaining leukemic cells in the patient. However, allogeneic transplants are limited by the availability of matched donors. Up to 75% of patients lack matched family donors[212], and unrelated donors are stringently screened based on human leukocyte antigen (HLA) genes of 5 loci (A, B, C, DR and DQ). In addition, as donor matching relies heavily on the size of donor banks, racial minority groups may be less likely to find allogeneic matches.

1.7 Experimental outline and significance of work

As the sheer number of patients suffering from various debilitating hematopoietic diseases continues to rise, the demand for HSCs for transplants also increases. While vast improvements have been made in the field by identifying new and more effective sources of HSCs such as the placenta, transplantation of *in vitro* derived HSCs remain out of reach even as we continue to identify more factors that are involved in their generation, so as to optimize more robust and efficient expansion protocols.

To this goal, we focused on early hematopoietic development in the mouse embryo, where my hypotheses are:

1. Differentially expressed genes are involved in determining the distinct hematopoietic fates between YS and P-Sp hemangioblast-derived colonies.
2. Differentially expressed genes are involved in specifying mesoderm commitment towards the hematopoietic fate.
3. PRC1-mediated regulation is involved in YS and P-Sp hematopoietic development.

My experimental approaches are:

1. Transcriptome comparison of YS and P-Sp hemangioblast-derived colonies.
2. Transcriptome comparison of hematopoietic and non-hematopoietic populations derived from E8.5 primitive streak.
3. ChIP- sequencing of PRC1 components in *in vitro* populations that recapitulate YS and P-Sp hematopoiesis.

This thesis examines the developmental processes involved in early embryonic hematopoiesis, using both *in vivo* and *in vitro* derived populations. We identify that only a small number of genes differentiate the transcriptome profiles of hematopoietic- distinct YS and P-Sp hemangioblast derived colonies. We also uncover novel PCGF5 involvement in PRC1-mediated regulation, as well as a potential mechanism for PRC1 recruitment previously found only in *D. melanogaster*. We hope that future work based on the insight gained from these findings will someday improve clinical applications and benefit patients.

CHAPTER 2:

METHODS & MATERIALS

2.1 Mouse breeding and harvesting

Timed matings were carried out between *Bry*-GFP male stud mice on an ICR background, and wild-type ICR females. Vaginal plugs were counted the next morning (d0.5), and embryos were harvested following euthanasia by CO2 gas. Petra Kraus and Thomas Lufkin kindly generated chimeric *Bex6*-KO BL-6 mice from KOMP $Bex6^{tm1(KOMP)Vlgc}$ cell lines.

2.2 ESC maintenance and differentiation

The mouse ES line *Bry*-GFP[78] was used for EB differentiation. ESCs were maintained in serum-containing ESC media with the addition of LIF-containing conditioned media (1%), on mouse embryonic feeder (MEF) cells in tissue culture-treated 6-well plates. To generate EBs, ESCs were feeder-depleted by culturing on gelatin-coated plates for 3 days. ESCs were dissociated using 0.05% trypsin-EDTA, then washed and plated in 60mm low-cluster plates (Corning) at a concentration of $3.5x10^4$ cells/ml for d3.5 EBs. ESC differentiation media consists of IMDM, 2 mM glutamine, $4x10^{-4}$ M monothioglycerol (MTG) and 50 µg/ml ascorbic acid.

2.3 siRNA knockdown

siRNAs against *Bex6* were purchased from Sigma-Aldrich. D5 EBs were dissociated using 0.05% trypsin-EDTA (Sigma), then washed with 1x PBS and treated with 40 um/ml siRNA before reaggregated for 36 h.

2.4 Generating inducible shRNA cell lines

shRNA against *Pcgf5* as well as scrambled shRNA were purchased based on Sigma design. The shRNA was subcloned into the pLox-mir126-intron-GFP vector[213], and subsequently transformed together with pSalk-Cre into the AINV18 cell line[214] via electroporation followed by antibiotic selection (G418). Single colonies were picked and expanded on OP9 feeder cells, and verified by induction with 1 ng/ml Dox followed by qPCR of the intended gene knockdown.

2.5 Flow cytometry

Cells were stained by standard protocols with the following antibodies: homemade biotinylated Flk1, PECy5-conjugated streptavidin (BD Biosciences #554062), PE anti-mouse CD45 (BD #553081), PE anti-mouse Tie2 (BD 12-5987-83) and FITC anti-mouse CD41 (BD #553848) for the respective experiments. Briefly, cells were dissociated using trypsin to form a single-cell suspension. Serum was added to stop the dissociation, and cells were spun down and resuspended at 10^6 cells/ml. Cells were incubated with the antibody for 30 min on ice, and washed in between antibodies, with a final wash before passing the solution through a cell strainer. Cells were sorted on a BD FACSaria, Influx or MoFlo into 5 ml polypropylene tubes. Sorted cells were then manually counted using a hemocytometer for subsequent applications.

2.6 Hematopoietic colony growth and expansion

The serum-based blast colony assay was as previously described[78]. In brief, E7.5 embryos, E8.5 embryonic caudal regions or d3.5 EBs were dissociated to single cell suspensions using 0.5% trypsin (Gibco) and a 26G needle and syringe. Cells were then plated in 53% methylcellulose containing 10% FCS (PAA), VEGF (5 ng/ml), interleukin 6 (IL6; 5 ng/ml) and 25% D4T endothelial cell-conditioned medium. Blast colonies were counted 4 days after plating, and colonies were collected via mouth-pipet using pulled glass capillary tubes directly into cell lysis buffer for RNA extraction (Qiagen RNeasy Microkit). For Wnt perturbation assays, 300 ng/ml Dkk1 and 100 ng/ml Wnt3 were added at d0. For hematopoietic progenitor assays, cells were cultured in in 53% methylcellulose containing 15% PDS, 10% PFHM, interleukin 3 (IL3; 10 ng/ml), GM-CSF (3 ng/ml), IL-11 (5 ng/ml), EPO (10 ng/ml), IL-6 (10 ng/ml) and TPO (5 ng/ml). Primitive erythroid colonies were counted from day 4-5 while definitive erythroid and myeloid colonies were counted after 7-10 days of culture. For expansion assays, blast colonies were transferred individually via mouth pipette into a matrigel-coated well of a 96-well plate, containing 100 µl expansion media as previously described[42]. Adherent and non-adherent populations were scored at day 4 of expansion. All cytokines were purchased from R&D.

2.7 Microarray data acquisition and analysis

RNA was harvested using Qiagen RNeasy Microkit, and quantified by Nanodrop. Samples selected for microarray had RIN >6 as determined by Agilent RNA 6000 Pico Kit. RNA was labeled using Epicentre TargetAmp Nano-g Biotin-aRNA Labelling Kit for the Illumina System. Where necessary, RNA was first concentrated to the required volume using an Eppendorf Speedvac. cRNA samples were hybridized to Illumina Mouse WG-6 v2 Expression BeadChip genome-wide arrays. The arrays were scanned on an Illumina BeadArray Reader at scan factor 1. Raw data was subject to background subtraction using Illumina Beadstudio, and quantile normalization using Agilent GeneSpring software. The sample probe profile was analyzed by significance analysis of microarrays (SAM) using a two class unpaired approach and cutoff value of false discovery rate (FDR) <7%.

Microarray of YS vs P-Sp hemangioblast-derived colonies:
6 biological replicate sets of blast assays, each from culture of E7.5 or E8.5 embryos derived from 6-11 timed-mated mice, were used to harvest the respective hemangioblast-derived colonies. 30ng RNA was then used from each of the 12 samples for microarray using 2x Beadchips.

Microarray of d3.5 Bry^+/ d3.5 Bry^+Flk1^+/ d5.5 $Flk1^+$ EBs
RNA was obtained from 2 biological replicates each of the 3 cell populations. 50ng RNA was then used from each of the 6 samples for microarray using 1 Beadchip.

2.8 High-Throughput Single-Cell qPCR

RNA from individual blast colonies was obtained using Qiagen RNeasy Microkit. 10µl RNA was transcribed into cDNA using the High Capacity cDNA Reverse Transcription kit (Applied Biosystems). Inventoried TaqMan Gene Expression assays (Applied Biosystems) were pooled to a final concentration of 0.2X. cDNA was preamplified using the Taqman assay pool and Taqman PreAmp Master Mix (Applied Biosystems). These preamplified products were diluted 10-fold prior to analysis with Taqman Universal PCR Master Mix and inventoried TaqMan Gene Expression assays (Table 1), in 48.48 Dynamic Arrays on a BioMark system (Fluidigm). Ct values were calculated using the system's BioMark Real-time PCR Analysis software.

Gene	Assay ID	Gene	Assay ID
AA4.1	Mm00440239_g1	Hey1	Mm00468865_m1
ACE	Mm00802048_m1	HoxB4	Mm00657964_m1
Actb	Mm00607939_s1	Klf2	Mm00500486_g1
BMP2	Mm01340178_m1	Klf4	Mm00516104_m1
BMP4	Mm00432087_m1	Lhx2	Mm00839783_m1
Bmpr1a	Mm00477650_m1	Meis1	Mm00487664_m1
Cbfβ	Mm00491548_m1	Mib1	Mm00523008_m1
CD150	Mm00443316_m1	Mll	Mm01179233_m1
Cdx4	Mm00432451_m1	Msx2	Mm00442992_m1
c-myb	Mm00501741_m1	Notch1	Mm00435245_m1
Dll1	Mm00432841_m1	Pbx3	Mm00479413_m1
Dll4	Mm00444619_m1	Pecam	Mm00476702_m1
Eng	Mm00468256_m1	Plxdc2	Mm00470649_m1
Fli1	Mm00484410_m1	Rac1	Mm01201653_mH
Foxo1	Mm00490672_m1	Runx1	Mm01213404_m1
Gapdh	Mm99999915_g1	Sca-1	Mm00726565_s1
Gata-1	Mm01352636_m1	Smad5	Mm03053603_s1
Gata-2	Mm00492300_m1	Sox11	Mm01281943_s1
Gata-3	Mm00484683_m1	Sox4	Mm00486317_s1
Gata-6	Mm00802636_m1	Sox7	Mm00776876_m1
Hand1	Mm00433931_m1	Tie2	Mm01256904_m1
Hbb-b1	Mm01611268_g1	VE-cadherin	Mm03053719_s1
Hbb-bh1	Mm00433932_g1	Wnt3A	Mm00437337_m1
Hes1	Mm00468601_m1	Wnt5A	Mm00437347_m1

Table 1. List of Taqman Gene Expression probes used.

2.9 Quantitative reverse-transcription PCR (qPCR)

RNA was extracted using Qiagen RNeasy Microkits according to manufacturer's instructions, and then transcribed using Superscript II Reverse Transcriptase (Invitrogen). Primers were designed using PrimerBlast (NCBI) and verified against self-complementation and heterodimers using Oligocalc (Northwestern University) and OligoAnalyser (IDT). qPCR was run in triplicate using Sybr Green (Applied Biosciences) on an AB7500HT machine. Analysis of relative transcription levels was performed by the 2-ΔΔCT method with β-actin as the internal control for normalization. Standard deviation between 3 replicates was used to define error bars.

2.10 Generating cell populations tracking mesoderm commitment to hematopoietic fate

E8.5 *Bry*-GFP embryos were harvested from timed-mated mice, and PS (Bry^+Flk1^-) cells were isolated using FACS. These cells were then reaggregated in hematopoietic (15% FCS, 2 mM L-glutamine, 4.5×10^{-4} M MTG, 50 ng/ml ascorbic acid, 5 ng/ml VEGF, 1 ng/ml BMP4, StemPro-34 SFM) and non-hematopoietic (2 mM L-glutamine, 4.5×10^{-4} M MTG, 50 ng/ml ascorbic acid, 5 ng/ml VEGF, 1 ng/ml bFGF, 1 ng/ml BMP4, 2 ng/ml activin, 50 ng/ml Wnt3a) supporting conditions. Cells were cultured for 24 hours at a density of 10^3 cells/ ul in ultra low attachment 24-well plates (Costar). Cultures were maintained in a humidified chamber in a 5% CO2/air mixture at 37℃.

2.11 Western Blot

Cells were lysed in RIPA buffer (Pierce) containing protease inhibitors (Roche). 10 µg total protein for each sample was resolved on a 10% SDS-

PAGE gel and transferred to methanol-activated PVDF membranes (GE Healthcare). After washing once with TBST (20 mM Tris, 500 mM NaCl, 0.1% Tween 20, pH 7.5), the membranes were blocked with 5% milk in TBST for 1h at room temperature with mild shaking. The blots were then incubated with primary antibody at the appropriate dilution in 5% milk and TBST overnight with gentle shaking at 4℃. Blots were then washed 3x for 15 min with TBST and incubated with horseradish peroxidase-conjugated secondary antibody for 1 h at room temperature. The blots were then washed for 3x for 5 min with TBST and visualized using a chemiluminescent substrate (ECL Plus Western Blotting Substrate, Thermo Scientific Pierce). Primary antibodies used: H3K27me3 (Millipore 07-449), H2AK119ub (Cell Signaling 8240S/P), RING1B (Abcam AB3832), BMI1 (Bethyl Labs, A301-694A), PCGF5 (Abcam AB112000), MEL18 (Santa Cruz SC-10744), CBX8 (a kind gift from Adrian P. Bracken), CBX7 (Abcam AB21873), β-actin (Abcam AB8227).

2.12 Co-immunoprecipitation (Co-IP)

Cells were crosslinked with 1% paraformaldehyde in PBS for 10 min at 4ºC and quenched with 125 mM glycine. Cells were then lysed in 50 mM Tris-HCL pH 8.0, 350 mM NaCl and 0.5% NP40 (Buffer A) or 25 mM HEPES buffer pH 7.5, 150 mM NaCl and 0.5% NP40 (Buffer B) at 4ºC for 30 min, and centrifuged at 13.2 kRPM for 15 min. Supernatant was then incubated with washed antibody-conjugated Protein G Dynabeads (Invitrogen) overnight at 4ºC. Antibodies used are same as those listed for Western blot. The next day, beads were washed 4x with lysis buffer, then resuspended in SDS loading buffer and boiled at 95ºC for 6 min. Samples were then loaded onto an SDS-PAGE gel for Western blot and transfer, and subsequent probing with antibody of interest.

2.13 Chromatin Immunoprecipitation (ChIP)

Protocol was based on small-scale ChIP-seq method described in Ng *et* al[215]. Briefly, $5x10^5$ FACS-sorted EB cells were crosslinked with 1% paraformaldehyde in PBS for 10 min at room temperature and quenched with 125 mM glycine. Cells were lysed in 50 mM HEPES-KOH pH 7.5, 2 mM EDTA, 1% SDS and protease inhibitors. Cell lysate was sonicated (30 s on/ 30 s off cycle at low power) in a Diagenode Bioruptor to achieve a mean DNA fragment size of 200–400 bp. Lysate was precleared with protein G-Dynabeads (Invitrogen) for 1 h at 4℃. Supernatant was then incubated with antibody-bound Dynabeads overnight at 4 ℃. Antibodies used are same as those listed for Western blot. The next day, Dynabeads were washed with 50 mM HEPES-KOH pH 7.5, 2 mM EDTA and 0.1% SDS, then incubated with elution buffer (50 mM Tris-HCl pH 7.5, 10 mM EDTA, 1% SDS, proteinase K) at 68 ℃ for DNA elution. Pronase and SDS-elution buffer was then added to chromatin solution and incubated at 42℃ for 2h and 68℃ for 6 h for protein digestion and crosslink reversal. ChIP DNA was then purified by phenol-chloroform extraction and ethanol precipitation, and DNA pellet was resuspended in MilliQ water.

2.14 *ChIP-qPCR*

ChIP DNA was obtained as above, and qPCR was run in triplicate using Sybr Green (Applied Biosystems) on an AB7900HT machine (Applied Biosystems). Quantitative PCR primer sequences were obtained from Luca Mazzarella and Masafumi Muratani, and are as listed in Table 2. Analysis of relative transcription levels was performed by the 2-ΔΔCT method with β-actin as the internal control for normalization.

Gene	Forward	Reverse
Gapdh	CCCCAGATCCAGAAAGGTCACAC	GGCCAGGATGTAAAGGTCATTAAGAGG
Oct4	GTGAGCCGTCTTTCCACCAGG	GGGTGAGAAGGCGAAGTCTGAA
Sox2	CCATCCACCCTTATGTATCCAAG	CGAAGGAAGTGGGTAAACAGCAC
Rex1	TTTGCGGGAATCCAGCAGT	CGTCCCATCGCCACTCTAGAC
Math1	CCCTCACTCAGGTCGCCTG	CGTGCGAGGAGCCAATCA
Nkx2.2	CGAACCCTGCCACTGCTAGA	AGAGGAATAGGCTTGGACATGC
Nkx2.9	CCACTTTGGTCTAATCAGACAATCG	TGCTACTCGGAGGGCTTTGAA
Sox1	ACAAGAGGAGGCAGCGAACC	TCGCAGGTGGAAAGTTTCTCC
Bry	TCACCCAGGAGGCTGGAGAGTTT	CACAACTTAGCAACCTTGCCGTAG
Flk1	GGAAACCGGGAAACCCAAAC	GGAAACACAGCTTACTCTCTTGGG
Ikaros	CCAGTTTCAGGGACTCGGCT	TCGGGGAACACGGGACAC
Myf5	GGAGATCCGTGCGTTAAGAATCC	CGGTAGCAAGACATTAAAGTTCCGTA
Negative	TGTTGGGTTCTTGCCACGAT	CCAAAACTTGTGCCAATGCA

Table 2. List of ChIP-qPCR primers used.

2.15 ChIP-Sequencing

ChIP DNA was amplified using Sigma GenomePlex Single Cell Whole Genome Amplification Kit (WGA4), followed by preparation for Solexa sequencing using NEBNext ChIP-Seq Library Prep for Illumina (NEB E6200) and NEBNext Multiplex Oligos for Illumina (Index Primers Set 1) (NEB E7335). Briefly, 10 ng of ChIP DNA was subject to end repair followed by dA-tailing and adaptor ligation, and then PCR-amplified using Phusion High Fidelity DNA polymerase. 200-300 bp library fragments were then isolated using AMPure XP beads (Beckman Coulter). Quality and concentration of the purified library was verified using Agilent DNA 1000 LabChip on an Agilent Bioanalyser, and ChIP-sequencing was performed on an Illumina Solexa. Antibodies used: H3K27me3 (Abcam AB6002), H2AK119ub (Cell Signaling Technology D27C4). Remaining antibodies used are the same as that for Western blot and co-IP.

2.16 ChIP bioinformatics analysis

Peaks were mapped using DFilter[216] (peak p-value cutoff 10^{-5}, bin size 100bp) and targets with peak overlap of >1 kb were identified with GALAXY MACs software. HOMER software was used for genomic annotation of the binding sites, and Ingenuity Pathway Analysis (IPA) was used to identify related networks from the target list. Regulatory Sequence Analysis Tools (RSAT) oligo-analysis was used to generate *de novo* motifs (6-8bp lengths), and STAMP software was used to annotate identified motifs against TRANSFAC and JASPAR databases, following trimming of motif edges with information content <0.4.

CHAPTER 3:

TRANSCRIPTOME ANALYSIS OF YOLK SAC VERSUS P-SP HEMANGIOBLAST-DERIVED COLONIES

3.1 INTRODUCTION

"Begin at the beginning, and go on till you come to the end: then stop."

-Lewis Carroll, *Alice's Adventures in Wonderland*

Hematopoietic stem cells remain an enigma, their complete mechanism of development and specific cell-surface identity still being explored even 50 years after first being identified by Till & McCulloch[1]. To further elucidate the developmental steps leading to HSC generation, I focused on the earliest hematopoietic sites in the mouse embryo, where the initial clues to hematopoietic fate decisions may lie: the E7.5 yolk sac, and the E8.5 P-Sp. Separated by both developmental space and time, these 2 sites possess distinct hematopoietic potentials- the yolk sac with erythroid and myeloid potential, and the P-Sp with the additional lymphoid potential, presumably arising from the HSC. These potentials are evident from *in vitro* culture assays such as the blast colony and hematopoietic progenitor assays, which reveal the lineage potentials of embryo hemangioblast-derived colonies.

While differing in hematopoietic potentials, YS and P-Sp hematopoiesis share the requirement for a number of genes. For example, both the T cell leukemia oncogene *Scl/Tal1* and LIM-finger protein *Lmo2* are essential for both extra-embryonic and intra-embryonic hematopoiesis. In contrast, core-binding factor *Runx1* marks HSCs but is not essential for the primitive erythroid lineage[105-106]. Hence, we hypothesize that differences in gene expression of key factors are involved in determining hematopoietic fate.

Using gene expression microarray to profile the transcriptomes of YS and P-Sp hemangioblast-derived colonies, we identified genes that are differentially

expressed in the 2 populations. Selected genes were then further studied to identify their role in hematopoietic development.

3.2 RESULTS

3.2.1 Microfluidic gene expression profiling of single embryo hemangioblast-derived colonies

Based on the hypothesis that differentially expressed genes are involved in determining hematopoietic fate in YS and P-Sp hemangioblast-derived colonies, we performed single-colony gene expression profiling on 17 hemangioblast-derived colonies each from blast assay culture of E7.5 and E8.5 mouse embryos. A selected panel of genes including hematopoietic, mesodermal and endothelial genes was queried to see if gene expression changes were associated with any particular lineages. Microfluidic qPCR followed by hierarchical clustering of results revealed that YS and P-Sp hemangioblast-derived colonies did not cluster into distinct groups (fig. 3). However, there appears to be a small subgroup of YS hemangioblast-derived colonies that express Bmp2, which is associated with the pre-hemangioblast stage[191], and Sox7 and VE-cadherin, which are involved in development of the hemogenic endothelium[221], suggesting that there may be some heterogeneity across individual colonies within groups.

Key hematopoietic genes *Runx1, Gata2, Pecam, Mll* and *Klf2* are highly expressed across all colonies, indicating that they are broadly required for hematopoiesis. On the other hand, *Sox4* is broadly downregulated across the colonies, as per its association with pluripotency. The expression of remaining genes did not strongly associate with either colony type, suggesting that gene expression changes of these genes are not critical in specifying hematopoietic potential at this point. Hence, based on expression profiles of selected genes, YS and P-Sp hemangioblast-derived colonies

appear to be largely similar despite their differences in hematopoietic potential.

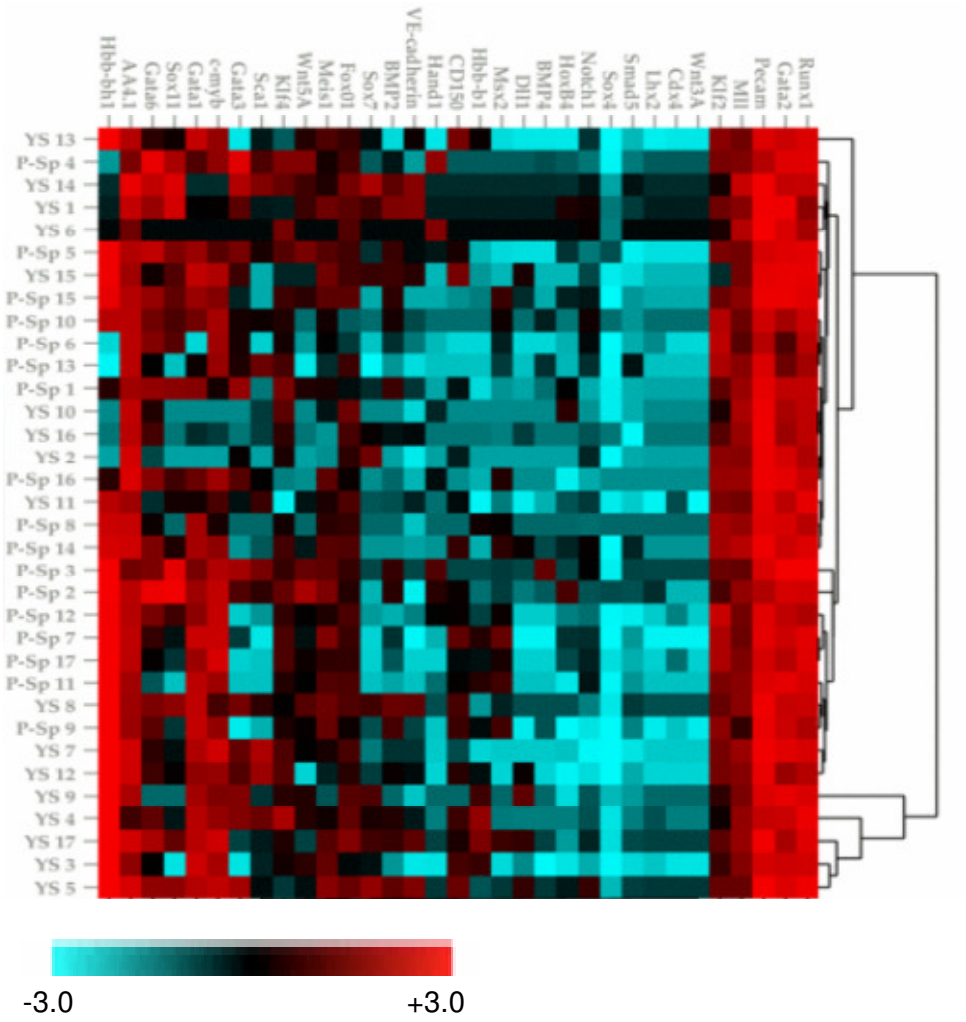

Figure 3. YS and P-Sp hemangioblast-derived colonies have similar gene expression profiles.
Heat map followed by hierarchical clustering of individual YS and P-Sp hemangioblast-derived colonies based on gene expression of selected genes. 3 blast assay replicates, each involving culture of E7.5 or E8.5 embryos from 2-4 timed-mated mice, were used to generate the respective hemangioblast-derived colonies. 17 colonies of each were then individually picked for microfluidic qPCR. X-axis: genes tested; Y-axis: (YS) YS hemangioblast-derived colony, (P-Sp) P-Sp hemangioblast-derived colony; Numerals refer to colony number. Red indicates increase in expression, green indicates decrease in expression.

3.2.2 Optimization of small-scale DNA microarray protocol

To further study our hypothesis that differentially expressed genes are involved in determining hematopoietic fate, we sought to perform microarray transcriptome analysis of YS and P-Sp hemangioblast-derived colonies. Microarrays can query a greater number of genes than those previously used in qPCR, due to the physical constraints of using the microfluidic qPCR chip; thus providing a more detailed snapshot of the colonies' gene expression profile. However, embryo hemangioblast-derived colonies are rare and require the sacrifice of numerous mice; hence the amount of RNA we could feasibly collect would be smaller than the amount required in standard DNA microarray protocols. Hence, we first needed to optimize a small-scale DNA microarray protocol and determine if we could derive sufficient numbers of embryo hemangioblast-derived colonies for microarray. To do so, we opted to use *in vitro*-derived hemangioblast-derived colonies for initial studies, which are easier to derive in much greater quantities.

Sorted d3.5 $Bry^{+}Flk1^{+}$ EBs were cultured in blast assays to generate ESC hemangioblast-derived colonies. Analysis of RNA concentration of pools of 20-400 colonies identified that a single hemangioblast-derived colony contained 1-5 ng RNA (fig. 4), indicating that we would require 6-30 colonies to obtain 30 ng RNA, and 80-400 colonies to obtain 400 ng RNA, which represent the lower and upper limits of the TargetAmp amplification kit used for microarray sample preparation. Comparison of microarray data using 30 ng and 400ng ESC hemangioblast-derived colony RNA from a single sample of d3.5 $Bry^{+}Flk1^{+}$ EB showed high correlation between both sets of results, indicating that 30ng RNA is sufficient to obtain robust microarray data (fig. 5).

Hence, we would only require 6-30 colonies for each replicate to perform the microarray. As these numbers can be feasibly obtained from embryo cultures, we proceeded to perform microarray analysis of embryo hemangioblast-derived colonies.

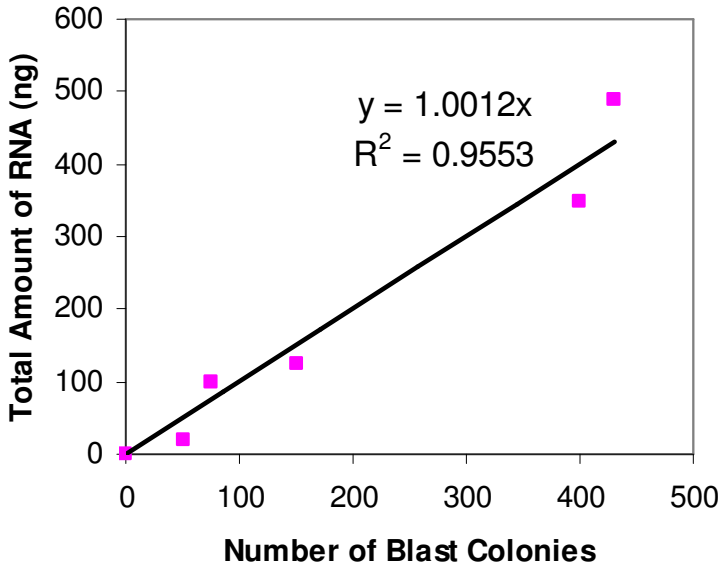

Figure 4. Calculating amount of RNA per hemangioblast-derived colony. Linear regression was applied to a graph of RNA quantities to derive the approximate RNA quantity of a single colony. 3 replicates of d3.5 $Bry^{+}Flk1^{+}$ cells were cultured in blast assay to generate ESC hemangioblast-derived colonies. Pools of 20-400 colonies were harvested for RNA, and quantified using Nanodrop.

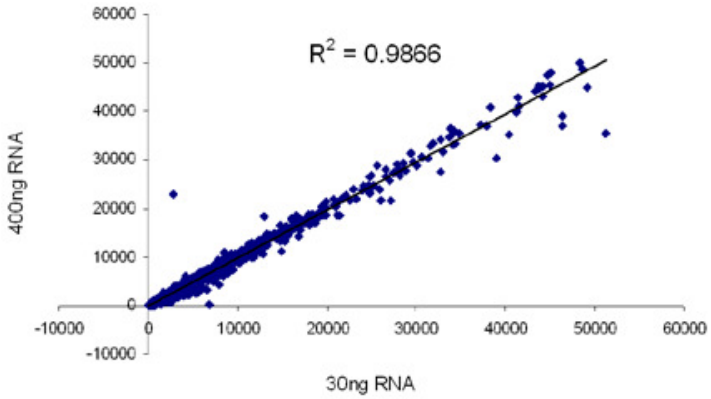

Figure 5. Small-scale DNA microarray generates robust data. Correlation plot comparing microarray results obtained using 30 ng and 400 ng RNA from ESC hemangioblast-derived colonies. R^2 value of best-fit line shown. 4 replicates of d3.5 $Bry^{+}Flk1^{+}$ cells were cultured in blast assay to generate ESC hemangioblast-derived colonies. Pools of colonies were harvested for RNA, and quantified using Nanodrop. 3 replicates each of 30 ng and 400 ng RNA were used for the microarray.

3.2.3 YS and P-Sp hemangioblast-derived colonies have similar transcriptomes

Microarray comparison of YS and P-Sp hemangioblast-derived colonies, obtained from culture of E7.5 and E8.5 embryos respectively, revealed largely similar transcriptome profiles (17699 genes unchanged) with a relatively small subset of genes being differentially expressed (fig. 6). Of these, 107 were more highly expressed in YS hemangioblast-derived colonies compared to P-Sp hemangioblast-derived colonies, and three vice versa.

Three groups of genes that were higher expressed in YS compared to P-Sp hemangioblast-derived colonies were identified: hematopoiesis-related, endothelial-related, and prolactin family genes (Table 3). The high expression of hematopoietic and endothelial genes in YS hemangioblast-derived colonies validate our microarray results, as the major function of the YS programme is to generate a large number of erythroid cells in association with primitive erythropoiesis. In addition, YS hemangioblast-derived colonies were observed to have greater endothelial expansion, as compared to P-Sp hemangioblast-derived colonies (unpublished data).

Unexpectedly, a number of prolactin family members were also highly expressed in YS hemangioblast-derived colonies (Table 4). Prolactins are most commonly studied in lactation and placenta development, which occurs at a later stage of embryogenesis. The placenta is an important site for embryonic hematopoiesis in both mice and humans[80], hence the strong presence of prolactin family members in YS hemangioblast-derived colonies are both novel and of interest in the study of embryonic hematopoiesis. Amongst the 23 mouse homologues that share 5 conserved exons[222],

members of the prolactin family are known to improve human CD34$^+$ HPC development and enhance erythropoiesis *in vitro*[223]. *Plf2* was previously found to enhance *ex vivo* expansion of HSCs[224], while validated antibodies, including a homemade antibody from the Linzer lab verified in other publications[225], exists for PLF1, thus ensuring available reagents for further study. During gene expression profiling of maturing hemangioblast-derived colonies, *Csh1* expression pattern was similar to that of *Plf2*, while *Prl4a1* had an opposite expression pattern, thus piquing our interest in these 2 members (fig. 12B, further analysis in section 3.2.6). Hence, we selected a total of four prolactin family members (*Plf1, Plf2, Csh1* and *Prl4a1*) to study their potential role in hematopoietic development.

The 3 genes more highly expressed in P-Sp hemangioblast-derived colonies compared to YS hemangioblast-derived colonies are an uncharacterized Riken, protease cathepsin G (*Ctsg*), and Brain-expressed gene 6 (*Bex6*). Due to the lack of commercially-available reagents to study the novel Riken and my lab's unfamiliarity in characterizing enzymes, we decided to focus on *Bex6* for further study. Little is known about the function of this gene, which was originally discovered in a study of ventral mesencephalic dopamine neurons[226], and its expression uncovered here in early hematopoietic development is further studied later in this thesis (chapters 3.2.7-8).

Hence from our microarray comparison, we identified that despite their differences in hematopoietic potential, YS and P-Sp hemangioblast derived colonies have vastly similar transcriptomes. Nonetheless, selected several prolactin family members and *Bex6* are selected for subsequent characterization of their roles in early hematopoietic development.

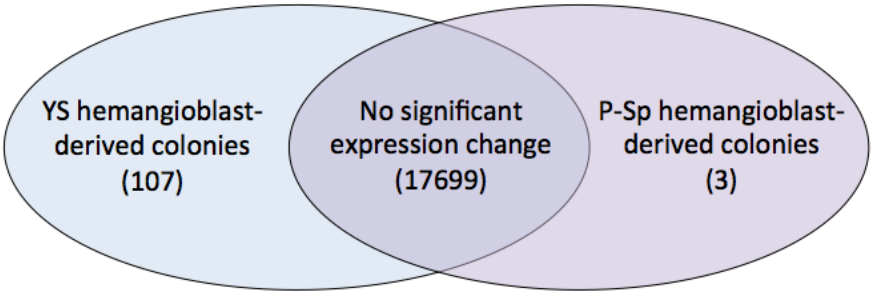

Figure 6. YS and P-Sp hemangioblast-derived colonies have similar transcriptome profiles.
Venn diagram of SAM identified-differentially expressed genes in YS and P-Sp hemangioblast-derived colonies. FDR <6%, fold change >1.2

Hematopoietic genes	*CD55, Epas1, Eraf, F8, Hbb-a1 Hbb-y, Tspan33*
Endothelial genes	*Admr, Krt1-14, Krt1-18, Krt2-8, Tfpi*
Prolactin family genes	*Plf1, Plf2, Plf3, Plf4, Csh1, Plib, Plig, Prl4a1, Prlpm*

Table 3. Selected groups of genes more highly expressed in YS vs P-Sp hemangioblast-derived colonies.

	Average microarray signal	
	YS hemangioblast-derived colony	P-Sp hemangioblast-derived colony
Prl2c2 (Plf1)	5072.03	7.04
Prl2c3 (Plf2)	4760.93	4.84
Prl2c4 (Plf3)	3934.60	1.78
Prl2c5 (Plf4)	12.00	-8.74
Prl3d1 (Csh1)	240.7	-1.4
Prl3d2 (Plib)	502.27	-1.54
Prl3d3 (Plig)	3453.58	5.42
Prl4a1 (Prlpa)	6949.60	1.04
Prl2a1 (Prlpm)	2207.67	-5.18

Table 4. Average microarray signal of prolactin family members in YS and P-Sp hemangioblast-derived colonies.

3.2.4 PLF1-responsive hemangioblast-derived colonies have increased primitive erythroid potential

As embryo hemangioblast-derived colonies are rare and require the sacrifice of numerous mice, we performed initial functional characterization of prolactins in an *in vitro* system. However, despite their similarity in hematopoietic potential, ES hemangioblast-derived colonies do not express the high levels of prolactins observed in YS hemangioblast-derived colonies (fig. 7). This raised the question of whether *in vitro*-derived colonies are responsive to prolactins. To test this, we selected 50-500 ng/ml PLF1, as PLF1 lysate was commercially available, for addition into blast colony assay culture of d3.5 $Bry^{+}Flk1^{+}$ cells to observe if this induced any changes in hematopoietic potential. This resulted in a decrease in the number of hemangioblast-derived colonies generated, even at the lowest dose (50 ng/ml) (fig. 8A).

As colonies still remain in the culture even with doses of 500 ng/ml PLF1, I was interested to find out whether these colonies were normal or had been affected in any way. Gene expression analysis of these PLF1-treated blast colonies identified upregulated expression of hematopoietic genes Gata1 and CD41 compared to control colonies (fig. 8B). We hypothesize that the addition of PLF1 lysate resulted in the inhibition of PLF1-sensitive colonies, which do not develop in the presence of PLF1, resulting in the generation of only PLF1-responsive colonies. To see if the hematopoietic potential of the remaining PLF1-responsive colonies was affected, treated and control blast colonies were expanded in liquid culture containing hematopoietic cytokines. Both treated and control expansions had similar levels of adherent cells representing the non-hematopoietic endothelial population. However, the

expansion of non-adherent round cells representing the hematopoietic fraction varied, with low, medium and high levels categorized as (+), (++) and (+++) respectively. The number of colonies in each category was tabulated and compared between control and treated colonies. Treated colonies appear to have greater hematopoietic expansion compared to control, as observed from treated expansions spanning both the (++) and (+++) categories but not (+). When these expansions from treated colonies are collected and subjected to qPCR for globins, they were found to express higher levels of primitive erythroid markers *Hbb-y* and *Hbb-bh1* (fig. 8C-E).

Further hematopoietic progenitor assay culture of the non-adherent cells revealed that PLF1-responsive colonies generated greater primitive erythroid cells but fewer macrophage (Mac) and erythroid-macrophage (Emac) cells (fig. 8F), suggesting that PLF1-responsive colonies may preferentially expand the primitive erythropoietic lineage more rapidly, or at the expense of myeloid expansion. Mayani *et al*[227] and Yang *et al*[228] respectively identified that cytokine induction and osteoblastic miR17 were able to specifically expand the erythroid lineage during culture of cord blood-derived HSPCs. However, neither paper conclusively identified if this was a preferential effect over remaining lineages. Hence, the preferential expansion of primitive erythroid over the myeloid lineage appears to be novel, and will require future work to see if PLF1 has a similar effect on other hematopoietic populations to verify this effect.

Autoregulation by rat prolactin (PRL) has been shown in the hypothalamus, pituitary and in somatoloactotroph cells[229-230], in which PRL inhibited transcription and translation in a cell- and promoter-specific manner. The

prolactin receptor (PRLR) is a transmembrane protein comprising extracellular, transmembrane and intracellular domains, and prolactin binding to PRLR can activate signaling cascades including the JAK-STAT pathway, which induces DNA transcription and activity in the cell[231-232]. Hence, we were interested to find out whether the addition of PLF1 affects the transcription of the prolactins studied. Interestingly, addition of up to 100 ng/ml PLF1 increases the expression of prolactin family members, but addition of 500 ng/ml PLF1 does not further enhance this response (fig. 9). These results suggest that PLF1 is able to auto-regulate gene expression of prolactin family members, enhancing transcription only to a certain extent, following which the effect becomes inhibitory.

Hence, the addition of PLF1 appears to select for a subset of PLF1-responsive hemangioblast-derived colonies that enhances erythropoiesis at the expense of myeloid lineages, whilst inhibiting the development of PLF1-sensitive colonies. This raises the question of the role of PLF1 in the YS, given the above results. The E7.5 YS is the earliest site of embryonic hematopoiesis, tasked to generate the initial wave of primitive erythropoiesis that, though transient, is essential for normal embryonic development[233]. This pool of primitive erythroid progenitors is poised to enter the embryonic bloodstream once circulation is initiated around E8.25[234]. PLF1 may function during this period to ensure great expansion of primitive erythropoiesis as required by the embryo. Regulation of its effects by the local microenvironment is also likely, so as to maintain the proper balance between promoting primitive erythropoiesis as well as myeloid lineages, which are also generated by the YS during the same period. It remains to be seen whether similar effects are observed with other prolactin family members.

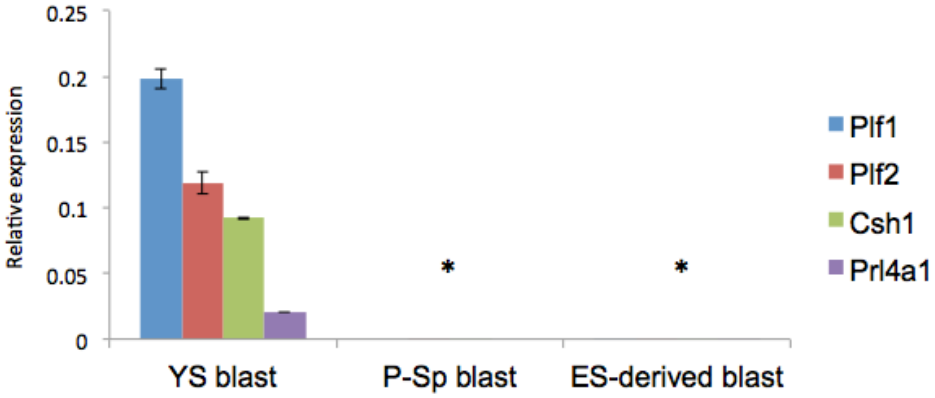

Figure 7. Prolactins are more highly expressed in embryo-derived compared to ESC-derived blast colonies.
QPCR of prolactin family members in ESC vs embryo hemangioblast-derived colonies. (*) indicates non-zero low expression. Expression relative to β-actin.

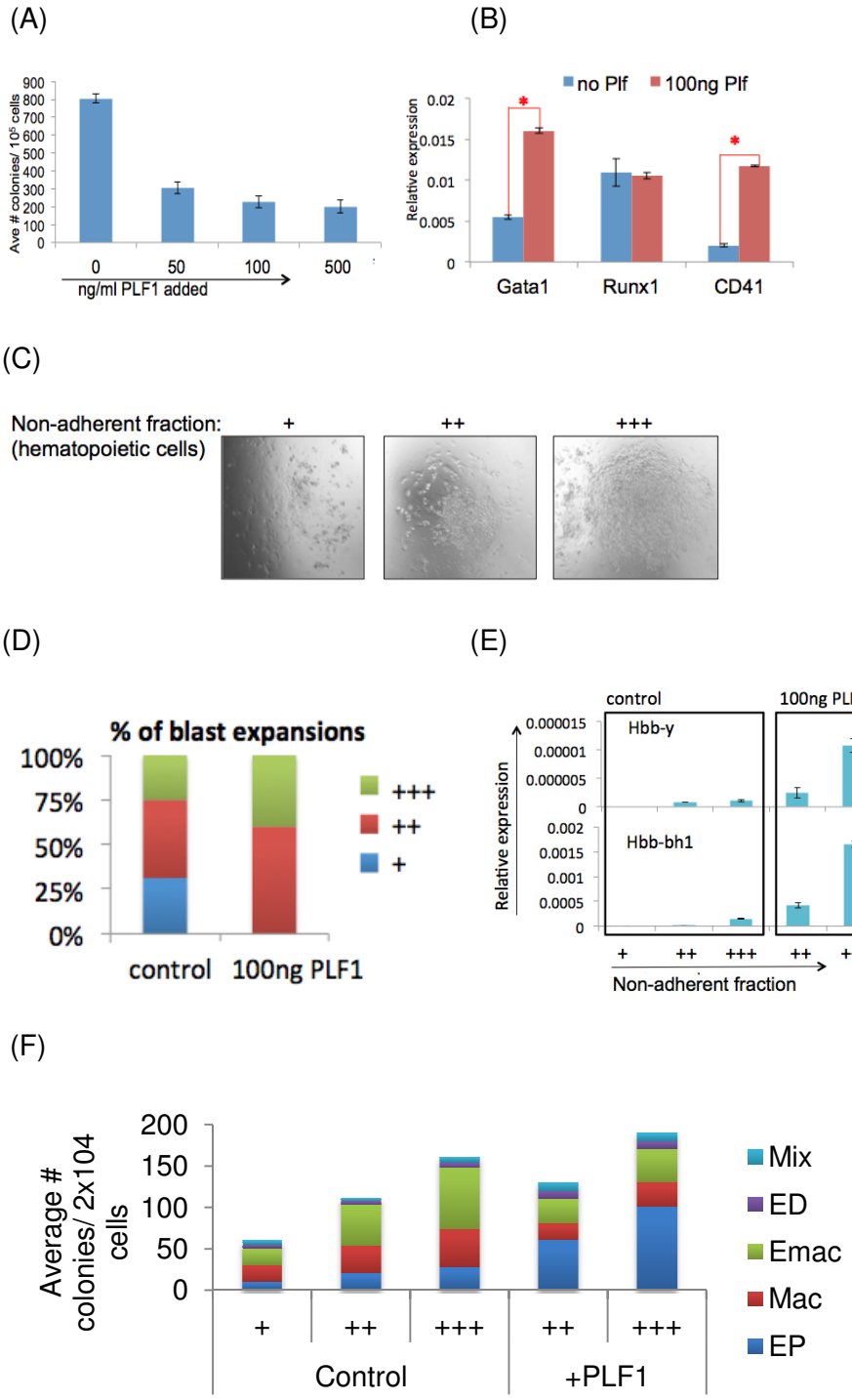

Figure 8. PLF1-responsive colonies have greater primitive erythroid potential at the expense of myeloid lineages.
(A) Number of hemangioblast-derived colonies obtained with addition of PLF1. (B) QPCR of hematopoietic markers upon addition of PLF1, expression relative to *β-actin*. (C) Non-adherent cell categories +, ++ and +++ following expansion of ESC hemangioblast-derived colonies. (D) Percentage of colony expansions belonging to non-adherent cell categories. (E) QPCR of primitive erythroid markers *Hbb-y* and *Hbb-bh1* in non-adherent fraction of colony expansions. (F) Hematopoietic progenitor assay of non-adherent fractions of colony expansions.

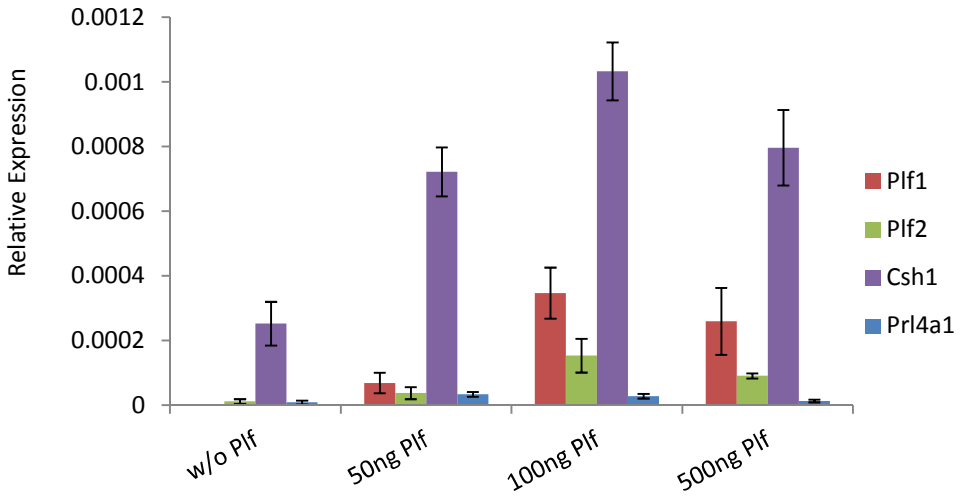

Figure 9. PLF1 auto-regulates gene expression of prolactin family members.
QPCR of prolactin family members in day 4 ESC hemangioblast-derived colonies upon addition of PLF1 at day 0. Expression relative to *β-actin.*

3.2.5 Prolactins are not associated with E9.5 YS hematopoietic-supportive stroma

Blast colony assays generate 2 types of colonies, the aforementioned hemangioblast-derived colonies, as well as morphologically different colonies here termed as endothelial-like colonies (ELCs) (fig. 10A, B). ELCs consist of only a round core, while hemangioblast-derived colonies have a similar core surrounded by small round cells. Previous studies have shown that the outer loose cells represent the hematopoietic component of the blast colonies, whereas the inner core contains the progenitors with endothelial and vascular potential. In an expansion assay, ELCs give rise to only the adherent endothelial fraction, but not the non-adherent hematopoietic fraction obtained when hemangioblast-derived colonies are expanded.

Hematopoietic and endothelial lineages develop in close spatial and temporal proximity emerging from the hemangioblast; hence we wanted to study if prolactins contributed to the endothelial potential of hemangioblasts. The prolactins studied are particularly highly expressed in E7.5 embryo-derived ELCs, even more so than in the YS hemangioblast-derived colonies they were originally identified in (fig. 10C). The negligible expression of prolactins in both E8.5 ELCs and hemangioblast-derived colonies further supports the specific involvement of prolactins in YS hematopoiesis. We were interested to find out if prolactins are involved in hematopoietic-supportive endothelial stroma, which could explain their expression in both hemangioblast-derived colonies and ELCs, albeit higher expression in ELCs due to the homogeneity of cells found there. Prolactins are highly expressed in E9.5 YS. However, when E9.5 YS was isolated and sorted based on CD41, Tie2 and Flk1

markers, they were not found to be highly expressed in hematopoietic-supporting $CD41^{-}Tie2^{-}Flk1^{+}$ endothelial cells[235], or in fact in any of the sorted populations (fig. 11A). Further analysis of the E9.5 YS revealed an unexpected association of prolactins' expression in the $FSC^{low}SSC^{low}$ population (fig. 11B). Given their small particle size and lack of cellular granularity, this population likely consists of mature enucleated erythrocytes. Indeed, this population expresses adult hemoglobin *Hbb-b1*, but not embryonic hemoglobins *Hbb-γ* or *Hbb-bh1* (fig. 11C, D)

Hence, we identified that whilst the selected prolactins are highly expressed in E7.5 ELCs, they are not associated with E9.5 YS-derived hematopoietic-supportive stromal cells, but instead with mature definitive erythroid lineages.

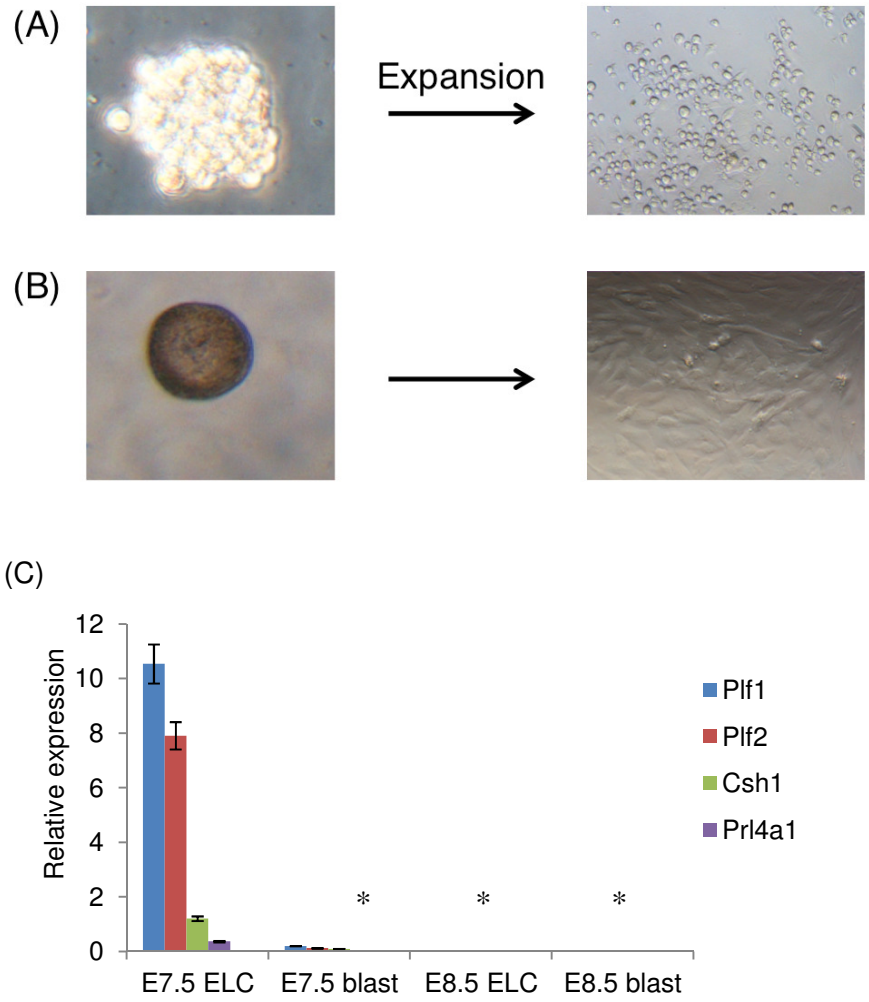

Figure 10. Selected prolactins are highly expressed in ELCs.
Differential morphology of day 4 (A) hemangioblast-derived colony and (B) ELC and expansions of. (C) QPCR of prolactins in embryo-derived colonies. Colonies were picked at day 4 of blast assay culture of E7.5 or E8.5 embryos, and further expanded in liquid expansion assay for 4 days. ELC: endothelial-like colony; blast: hemangioblast-derived colony. E: embryonic dpc. (*) refers to low, non-zero expression. Expression relative to *β-actin.*

(A)

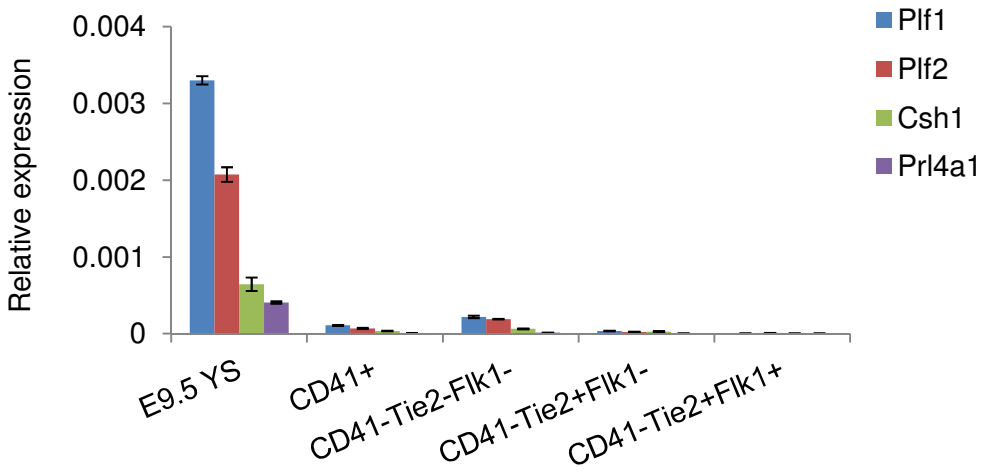
Relative expression
0.004
0.003
0.002
0.001
0
Plf1
Plf2
Csh1
Prl4a1
E9.5 YS
CD41+
CD41-Tie2-Flk1-
CD41-Tie2+Flk1-
CD41-Tie2+Flk1+

(B)

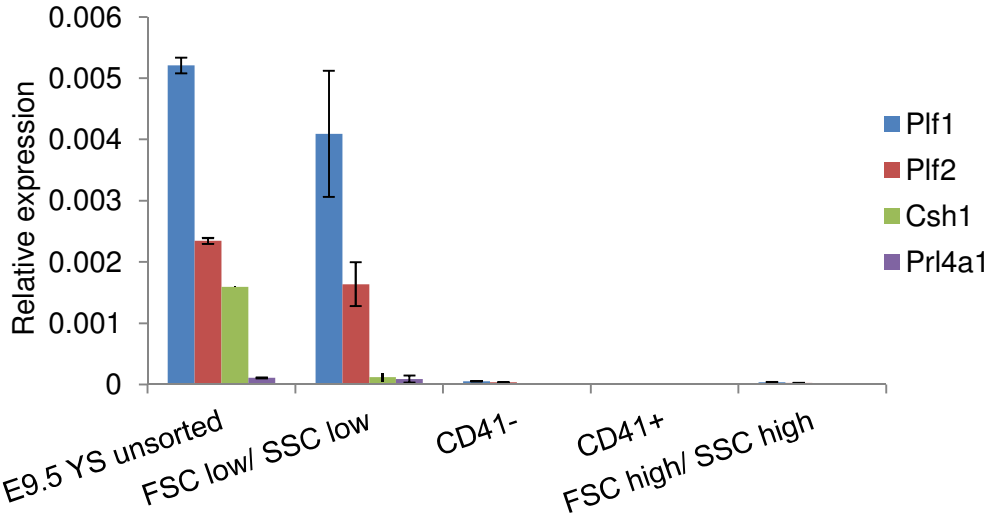
Relative expression
0.006
0.005
0.004
0.003
0.002
0.001
0
Plf1
Plf2
Csh1
Prl4a1
E9.5 YS unsorted
FSC low/ SSC low
CD41-
CD41+
FSC high/ SSC high

(C)

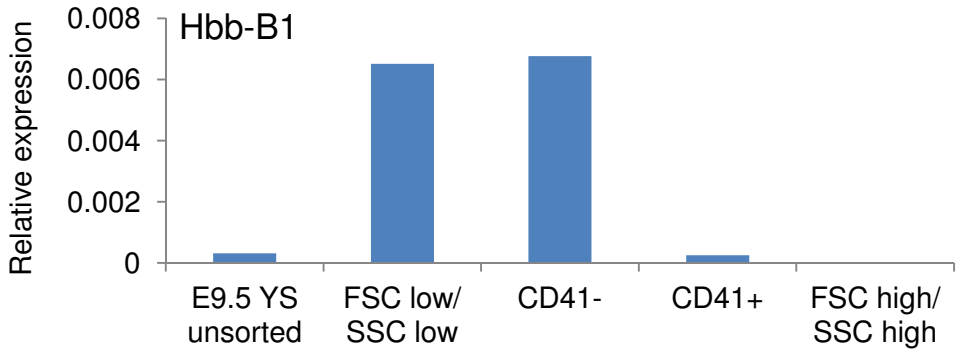
Relative expression
0.008
0.006
0.004
0.002
0
Hbb-B1
E9.5 YS unsorted
FSC low/ SSC low
CD41-
CD41+
FSC high/ SSC high

(D)

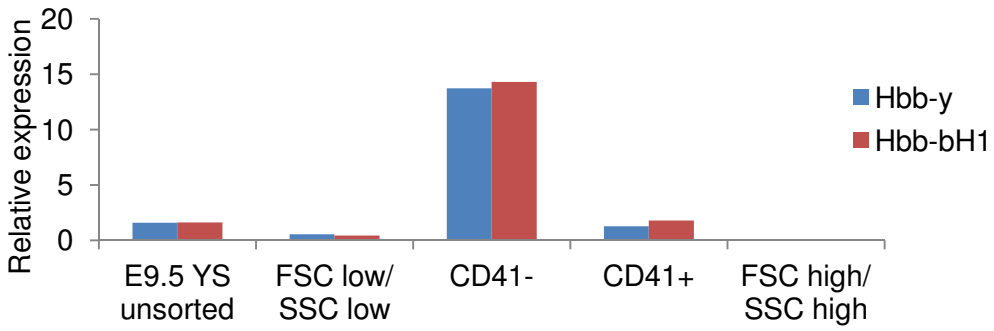

Figure 11. Prolactins are not associated with hematopoietic-supportive stroma derived from E9.5 YS.
QPCR of (A, B) prolactin family members, (C) adult hemoglobin *Hbb-b1* and (D) embryonic hemoglobins *Hbb-γ* and *Hbb-bh1* in sorted E9.5 YS populations. Expression relative to *β-actin*.

3.2.6 Prolactins are involved in Wnt/ Notch regulation of early erythropoiesis.

The impact on primitive erythroid development observed in section 3.2.4 is particularly intriguing, due to the fact that primitive erythropoiesis is a characteristic feature of YS but not P-Sp hematopoiesis. Wnt and Notch signaling pathways regulate the establishment of primitive and definitive erythropoiesis early in ESC hemangioblast-derived colony development, which recapitulates YS hematopoiesis[236]. Within 24 h of hemangioblast-derived colony development, active Wnt signaling together with Numb-mediated inhibition of Notch induces primitive erythropoiesis. This inhibition of Notch signaling is later lifted, leading to the inhibition of primitive erythropoiesis by activating Wnt pathway inhibitors such as *Sfrp1, Sfrp2* and *Sfrp5*[237]. The expression of *Axin2*, a downstream target of Wnt signaling, decreases rapidly in developing hemangioblast-derived colonies, as the expression of Notch ligand *Jag1* increases (fig. 12A). This results in primitive erythropoiesis eventually giving way to definitive erythropoiesis by 48h of hemangioblast-derived colony development[236]. Hence, we were interested to find out whether PLF1 interacts with Wnt/ Notch regulation of early erythropoiesis.

As erythropoiesis is established and regulated early on in hemangioblast-derived colony development, we sought to identify the gene expression profiles of studied prolactins from day 0-4 colonies. QPCR of developing hemangioblast-derived colonies showed that several prolactin family members are dynamically expressed as the colony matures (fig. 12B). Expression levels change around 48 h of blast colony development, which marks the transition from primitive to definitive erythropoiesis in the colony.

Prl4a1 is upregulated only during the window associated with primitive erythropoiesis and downregulated thereafter, while *Plf2* and *Csh1* are upregulated during the period of definitive erythropoiesis. *Plf1* expression does not appear to be associated with either lineage. These results suggest that whilst prolactins are closely related and may be involved in erythropoiesis, their function may not be redundant, and individual members may be directed towards different targets and lineages.

To study the effect of PLF1 on Wnt signaling in ESC hemangioblast-derived colonies, 100 ng/ml PLF1 was added to blast colony assay culture of d3.5 EBs. This resulted in significant upregulation of *Axin2* and a concurrent decrease in Wnt antagonists *Sfrp1* and *Nlk* at day 1 of colony development, which is the period during which primitive erythropoiesis is induced. We next analyzed Wnt pathway expression at day 4 of colony development, which was the developmental stage at which colonies were picked for microarray analysis, and by which time primitive erythropoiesis has given way to definitive erythropoiesis. *Sfrp1* and *Nlk* were significantly upregulated by day 4 as expected, resulting in decrease in *Axin2* expression (fig. 13). This suggests that PLF1 enhances the signaling through the Wnt pathway during the early window (day 1) but does not alter the overall pattern of Wnt activity, which decreases with colony maturation.

To identify whether prolactins were similarly affected by perturbations in Wnt/ Notch signaling in YS hemangioblast-derived colonies, Wnt3 was added to blast assay culture of E7.5 YS. Unexpectedly, this caused downregulated expression across all 4 studied prolactins in day1 hemangioblast-derived colonies. On the other hand, addition of Wnt antagonist Dkk1, which inhibits

primitive erythroid development[236], downregulated *Plf1* and *Plf2* but upregulated *Csh1* and *Prl4a1* gene expression in day 4 hemangioblast-derived colonies (fig. 14). This indicates that whilst prolactins may be involved in early erythroid development, their close homology yet differential response to Wnt antagonism makes it challenging to identify the key member(s) involved and their exact function.

Hence we identify that PLF-1 can modulate Wnt signaling in early hemangioblast-derived colonies. Given that Wnt signaling is an important regulator of early erythropoiesis and that earlier data show that addition of PLF1 to blast assays can enhance the number of derived erythroid colonies (fig. 8F), together these results indicate that PLF1, and potentially its related homologues, is involved in early erythropoiesis. However, individual prolactins appear to have discrete roles based on expression pattern, suggesting that a dynamic balance of prolactin activity is involved.

(A)

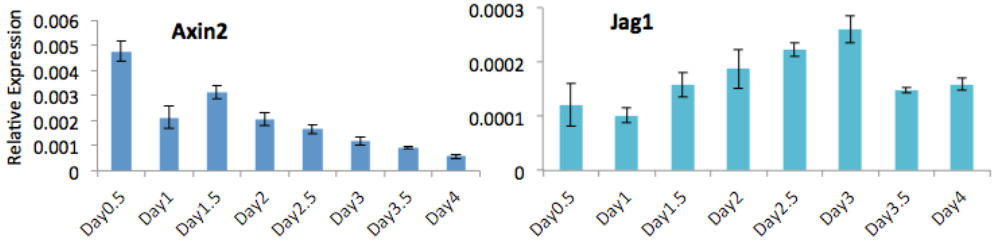

(B)

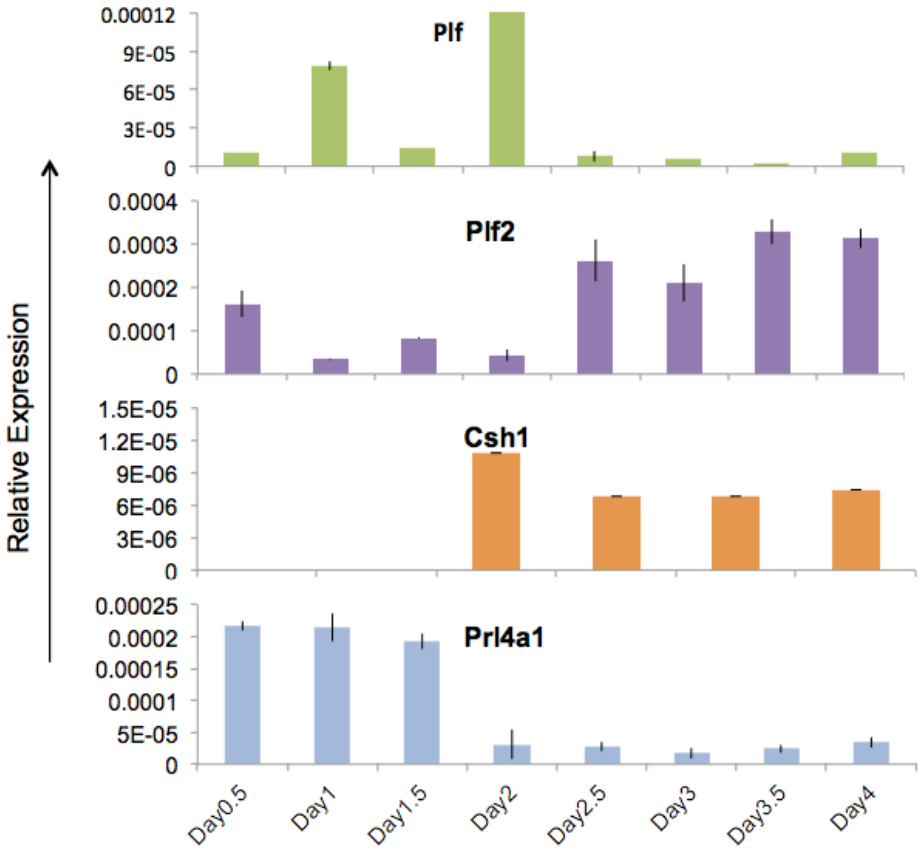

Figure 12. Prolactins have dynamic expression in maturing hemangioblast-derived colonies.
QPCR of (A) *Axin2* and *Jag1* and (B) prolactin family members in ESC hemangioblast-derived colony development. EB: embryoid body; day: day of blast colony formation. Expression relative to *β-actin*.

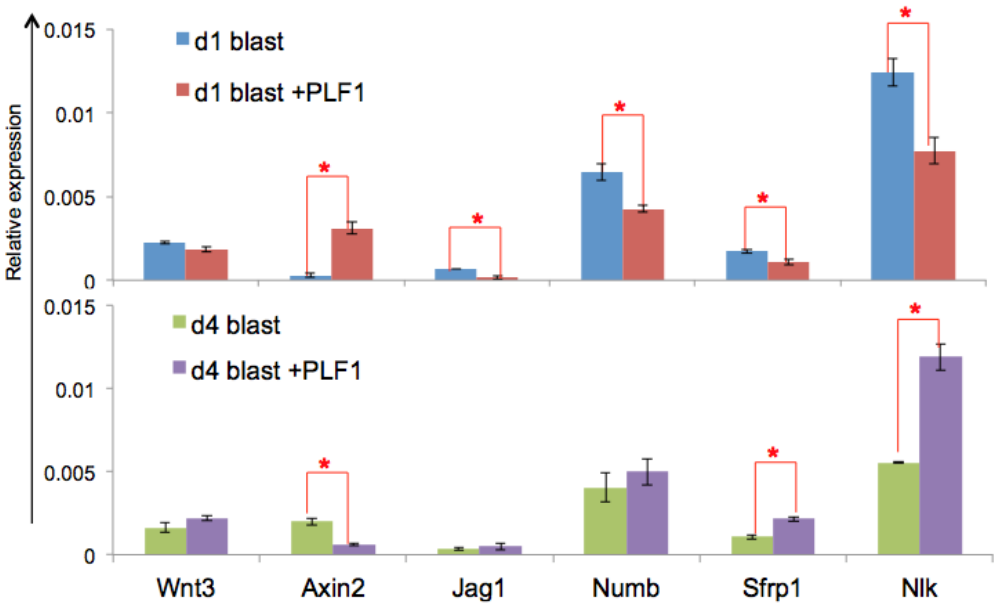

Figure 13. Effect of PLF1 on day1 and day3 hemangioblast-derived colonies.
QPCR expression profiles of Wnt/ Notch signaling factors in (top) day 1 and (bottom) day 4 hemangioblast-derived colonies, following addition of 100 ng/ml PLF1 to hematopoietic assay culture. Expression relative to *β-actin*.

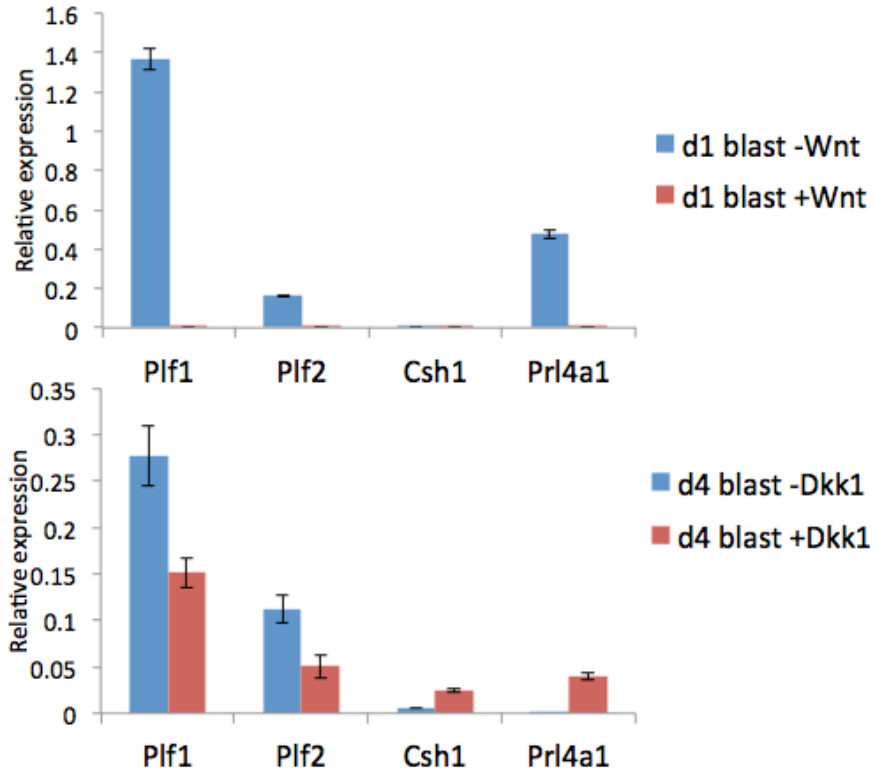

Figure 14. Perturbation of Wnt/Notch signaling in YS hemangioblast-derived colonies.
QPCR of prolactins in E7.5 YS hemangioblast-derived colonies at (top) day 1, upon addition of Wnt, and (bottom) day 4, upon addition of Dkk1. Expression relative to *β-actin.*

3.2.7 *Bex6* marks hematopoietic progenitor populations *in vivo*

One of only 3 genes identified from microarray analysis to be more highly expressed in P-Sp versus YS hemangioblast-derived colonies, *Bex6* is highly upregulated in a HPC line overexpressing *HoxB4*, which enhances HSC self-renewal and expansion[238]. Genome-wide ChIP-sequencing analysis of 10 hematopoietic transcription factors indicate that 6 of these transcription factors, including *Runx1* and *Scl*, have binding sites in the *Bex6* locus[239], suggesting a potential role of *Bex6* in hematopoiesis.

QPCR of hematopoietic sites in early embryos indicate that *Bex6* is highly expressed in fetal liver from E10.5 onwards (fig. 15A). Section in-situ results using E13.5 embryos indicate similarly (fig. 15B). The fetal liver is the major embryonic site of definitive hematopoietic expansion from about E11-12 onwards[240]. Expression of CD41 in the mouse embryo marks the initiation of definitive hematopoiesis. In addition, CD41 and CD45 can be used to track the developmental stage of hematopoietic progenitors (HPC)[241] (fig. 16A). Early HPCs express only CD41. As HPC development progresses, CD45 is also expressed, while CD41 gradually decreases. Finally, mature HPCs express only CD45. QPCR of embryonic fetal livers sorted on CD41 and CD45 showed that *Bex6* is specifically expressed on $CD45^+$ E10.5 and E13.5 fetal liver populations (figure 16B), indicating that *Bex6* marks later definitive hematopoietic lineages.

(A)

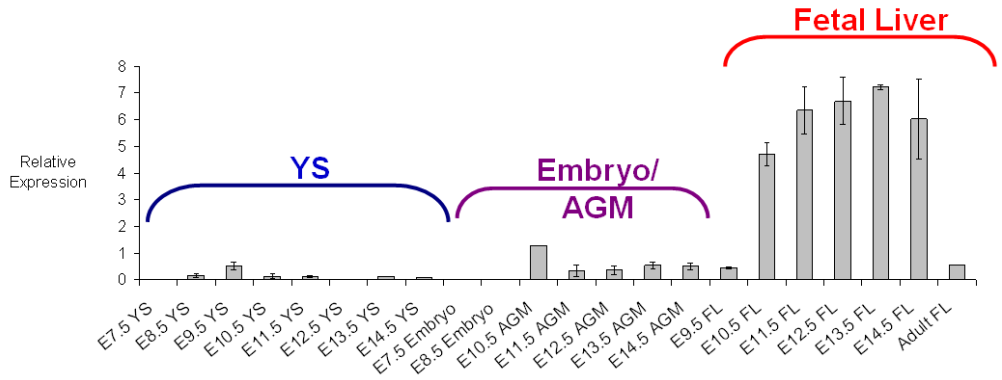

(B)

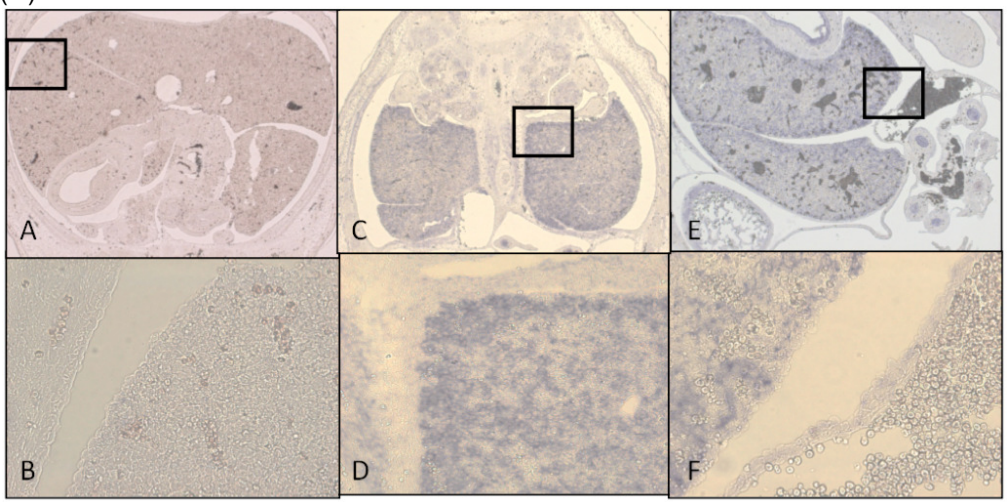

Figure 15. Bex6 is highly expressed in fetal liver tissue.
(A) QPCR of *Bex6* expression in E7.5-E14.5 embryonic tissues and adult fetal liver. Data relative to *β-actin* expression. (B) Section *in situ* hybridization of E13.5 mouse fetal liver. (A, B) Negative control (no probe added). (C, D) Bex6 probe using coronal section. (E, F) Bex6 probe using sagittal sections. Insets indicate site of subsequent picture, e.g. B=inset of A.

(A)

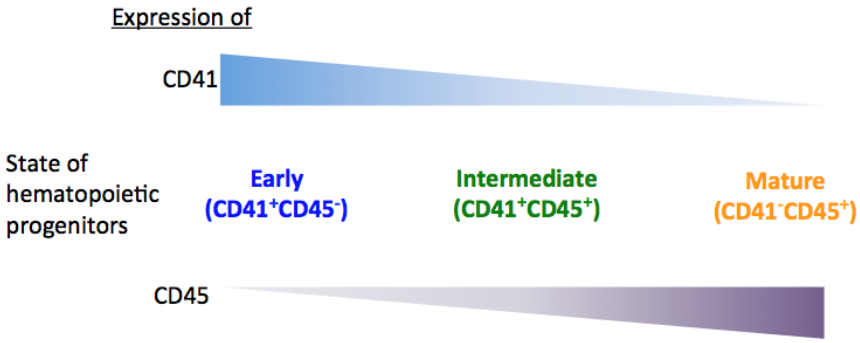

(B)

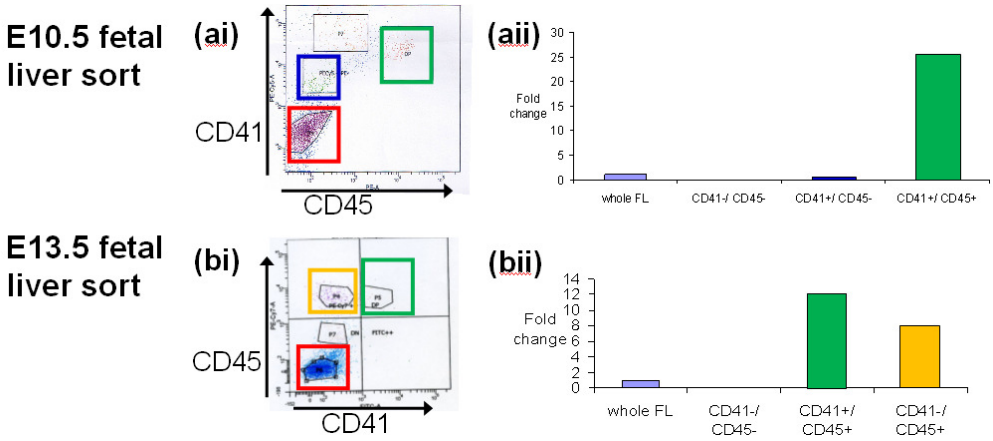

Figure 16. *Bex6* is associated with intermediate and mature hematopoietic progenitors.
(A) Defining state of hematopoietic progenitors by CD41 and CD45 expression. (B)FACS (i) and qPCR (ii) of *Bex6* expression from E10.5 (a) and E13.5 (b) fetal liver sorted on CD41 and CD45. QPCR expression relative to *Bex6* expression in whole fetal liver.

3.2.8 *Bex6* knockdown does not affect hematopoietic potential in vitro

Bex6 is expressed in EBs only from day 6 onwards (fig. 17), which is when hematopoietic progenitors are first observed from EBs[191]. siRNA knockdown of *Bex6* decreased expression of *Bex6* by 70-80%, along with CD45 expression; however hematopoietic markers *Runx1*, *Scl* and CD41 increased with siRNA #1 knockdown of *Bex6* (fig. 18A). In addition, knockdown of *Bex6* was not associated with significant change in hematopoietic precursors observed from methylcellulose assays (fig. 18B), suggesting that the transient effect of siRNA was insufficiently sustained to affect hematopoietic assay numbers, which are usually counted after more than 6 days.

Bex6$^{tm1(KOMP)Vlcg}$ cell line, which has a targeted deletion at the *Bex6* locus, was purchased from Velocigene for generation of knockout mice. 4 chimeric males (20%-80% by coat colour) were generated from 2 separate clones (fig. 19); however none displayed germline transmission as observed by lack of offspring with homozygous mutation even after more than 6 litters. The lack of knockout mice prevented us from obtaining valuable functional observations of *Bex6* and verifying the effect of *Bex6* knockout in hematopoietic development.

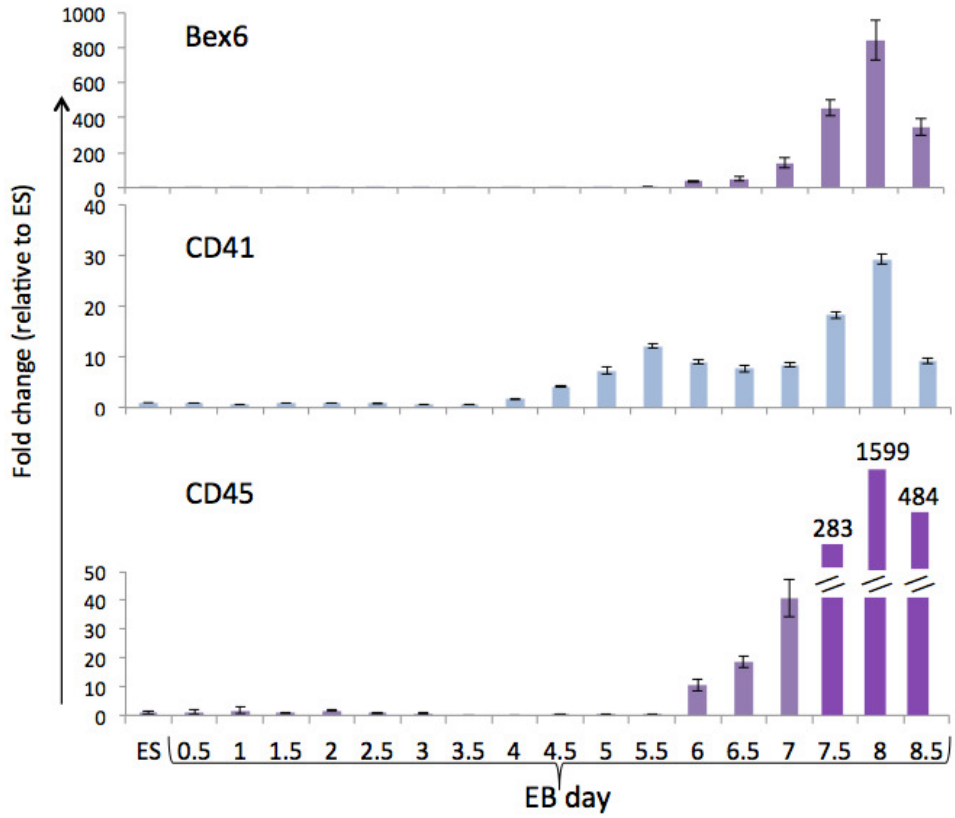

Figure 17. *Bex6* is associated with onset of hematopoietic potential in developing EBs.
QPCR analysis of *Bex6*, CD41 and CD45 along EB development. ES: EB d0. Expression relative to gene expression in ES.

(A)

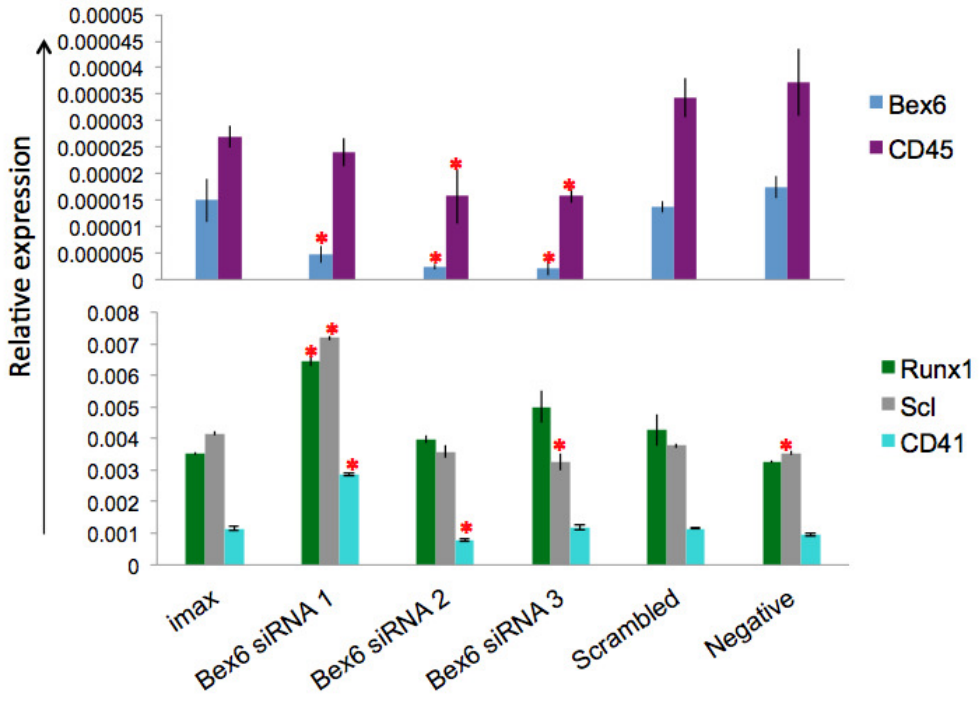

(B)

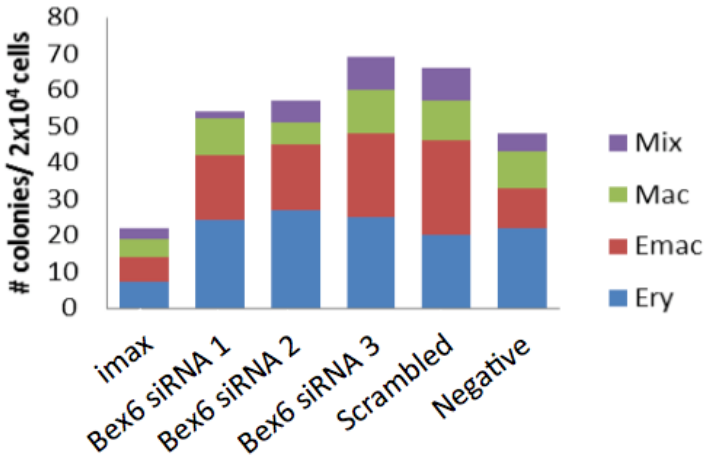

Figure 18. siRNA knockdown of *Bex6* does not generate significant results.
(A) QPCR analysis of *Bex6* and hematopoietic markers 36 h after *Bex6* knockdown in day 5 EBs. Controls: no siRNA (Imax), scrambled siRNA (Scrambled), no siRNA/ transfection reagent (Negative). B1, B2, B3: 3 different *Bex6*-targeting siRNAs. Expression relative to *β-actin*, asterisks indicate significant ($p<0.05$) change in expression compared to Imax control. (B) Average hematopoietic colony numbers obtained from hematopoietic progenitor assays 6 days after *Bex6* knockdown.

(A)

Knockout ES line	Date of microinjection	Date of birth	#chimeras/ chimeric ε
Bex6-KO#AB5	12.08.2011	31.08.2011	1 male (35%) 1 female (15%)
Bex6-KO#AF1			3 males (20/ 65/ 80%)

(B)

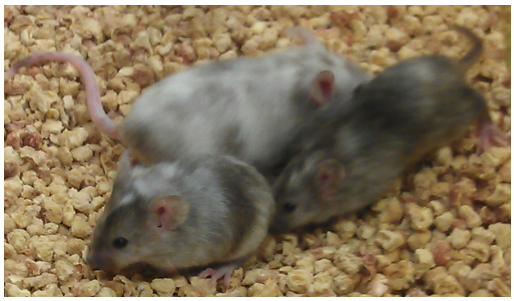

Figure 19. Unsuccessful generation of Bex6-KO mice.
(A) List of *Bex6*-KO chimeras generated using 2 different cell lines obtained from KOMP. Chimeric ε refers to estimated contribution of transgenic cell line by observation of coat colour. (B) Examples of *Bex6*-KO chimeras generated.

3.3 SUMMARY AND DISCUSSION

In summary, we performed a small-scale DNA microarray comparison of YS and P-Sp hemangioblast-derived colonies, which identified that despite their difference in hematopoietic potential, the two colony types have vastly similar transcriptomes. Prolactins were more highly expressed in the YS hemangioblast-derived colonies, even more so than in ESC-derived colonies that recapitulate YS hematopoiesis *in vitro*. PLF1-responsive hemangioblast-derived colonies have greater EP potential at the expense of myeloid, and PLF1 appears to modulate the Wnt/ Notch regulation of early erythroid development. They are also highly expressed in ELCs that have only endothelial but not hematopoietic potential, but are not associated with hematopoiesis-supportive E9.5 YS stroma. Meanwhile, *Bex6* expression is upregulated in P-Sp hemangioblast-derived colonies. Characterization of its expression in fetal liver links it to a more mature hematopoietic cell type, but knockdown of *Bex6* did not result in perturbation of hematopoietic potential as assessed by *in vitro* hematopoietic assays.

By selecting day 4 hemangioblast-derived colonies from the two embryonic stages, we hypothesized that a comparison of colonies with different hematopoietic potentials would reveal genes upregulated in the P-Sp hemangioblast-derived colonies, reflecting the induction of lymphoid and HSPC lineages. However, the small number of differentially- expressed genes identified by the microarray comparison suggests that only a brief, transient window, during which key fate decisions are being made, exists; which was missed in our approach in harvesting day 4 colonies which display the disparate lineages. Cheng *et al*[236] showed that even by 12 h of

hemangioblast-derived colony development, dynamic interactions between *Wnt* and *Notch* signaling pathways actively regulate primitive erythropoiesis. Hence on hindsight, perhaps an earlier harvest could identify changes in key transcription factors responsible for hematopoietic fate decisions. Indeed, microfluidic qPCR revealed heterogeneous gene expression profiles across individual YS hemangioblast-derived colonies (fig. 3), suggesting that a subset of these colonies may have a slightly different developmental profile compared to the majority of colonies harvested. Advancements in single-cell analysis platforms such as Fluidigm now enables the tracking of more gene expression changes in more samples with greater accuracy. This means that we could potentially perform more extensive transcriptome profiling of hemangioblast-derived colonies as they develop from day 0, allowing for clearer and more detailed insights into the fate decisions made during hematopoietic development.

The identification of PLF1-responsive and PLF1-sensitive colonies reflects the importance of cytokines in hemangioblast-derived colony development. Several cytokines have been well characterized for their use in culture to induce or enhance particular hematopoietic fates. Whilst both VEGF and bFGF are important for hemangioblast development from EBs, Faloon *et al*[242] identified that bFGF is not essential for the formation of hemangioblast-derived colonies. Culture of $Flk1^{+}$ cells with bFGF instead of VEGF resulted in a decrease in number of hemangioblast-derived colonies, while the addition of both VEGF and bFGF resulted in a slight, albeit non-significant decrease in colony number. Here, our results suggest that PLF1 may be another factor that can affect hematopoietic specification and development. The distinctions between colony responses to PLF1 also support the possibility of

heterogeneity within groups of hemangioblast-derived colonies, which may be due to slightly different developmental rates or biologically distinct populations. Further study of such heterogeneity will be useful in elucidating hematopoietic development.

The prolactin receptor (Prlr) is expressed in a large number of tissues including the liver and kidney[243-244], and consists of an extracellular domain for ligand binding, a single transmembrane region, and an intracellular domain that activates signal cascades upon dimerization of the receptor, including the DNA transcription-inducing JAK-STAT pathway. Knockout of Prlr results in numerous deficiencies, including infertility in female mice and decreased bone formation[245], but no effect on hematopoiesis has yet been reported. However, alternative gene splicing is known to generate long and short isoforms of PRLR[246-247], which appear to have different signaling pathways and expression patterns, and can additionally be activated by human growth hormone (GH) and placental lactogen[248-250]. This indicates that further characterization of PRLR and its isoforms, whilst ruling out potential signal interference from GH and placental lactogen during hematopoietic development, is required to fully elucidate the role of prolactins during this period.

In vitro cultures are widely used for their relative ease of culture, potential for scaling up, reproducibility and decreased reliance on live animals, and most importantly their recapitulation of *in vivo* systems. However, the latter largely depends on the extent of knowledge we know about the system, and the optimization of protocols towards those standards. In a way, *in vitro* models present a catch-22 situation, in which we can only identify dissimilar

characteristics when we encounter them. From our experiments, we identified that prolactins are greatly upregulated in YS hemangioblast-derived colonies, even more so than in ESC hemangioblast-derived colonies which recapitulate YS hematopoiesis *in vitro*. However, this should not detract from how invaluable the ESC differentiation system, which has been successfully used, characterized and validated in *in vivo* systems in numerous peer-reviewed publications; is towards elucidating hematopoietic generation and development. Rather, we have identified that while growth hormones such as prolactins can affect hematopoietic potential and development, they do not appear to be essential for normal hematopoiesis.

Previous studies have described the successful use of αPLF antibody to knock down PLF for functional studies[251-253]. We attempted to similarly knockdown PLF1 using a commercially-available αPLF1 antibody[252]; however the antibody failed to identify E13.5 placenta as a positive control in Western blot, indicating that the antibody was not able to recognize the target protein (data not shown). Efforts to obtain validated homemade α-PLF1 antibody and Plf-expressing cell lines from another lab for knockdown and overexpression studies were also unsuccessful. Hence, we were unable to perform loss-of-function studies on prolactins to determine their role in hematopoiesis. In addition, any future re-attempts to knockdown prolactins should take into consideration that perturbation of large gene families is complex and requires detailed analyses of the effects on all members so as to rule out redundancy and pinpoint the member(s) responsible for the activity in question.

siRNA knockdown of *Bex6* in day 6 EBs generated no significant change in hematopoietic potential. While this could be due to functional redundancy

from homologue *Bex4*, which has 67% sequence similarity to *Bex6*[226], characterization of Bex members have revealed distinguishing features between them. Most Bex members are located on the X chromosome, but Bex6 is located on chromosome 16, and is included in the Bex family due to sequence similarity. *Bex4* is also highly upregulated in the heart and skeletal muscle, in addition to the regular association of Bex genes with brain tissue[226]. These indicate that despite their sequence similarity, Bex4 and Bex6 may not function in the same environments, and whether Bex4 or any other Bex homologues are indeed able to function in place of Bex6 remains to be explored.

CHAPTER 4:

TRANSCRIPTOME ANALYSIS OF MESODERM DURING HEMATOPOIETIC COMMITMENT

4.1 INTRODUCTION

The path towards hematopoietic commitment of mesoderm can be recapitulated *in vitro* by tracking the expression of *Bry* and *Flk1* in d3.5 EBs: $Bry^{-}Flk1^{-}$, which marks pre-mesodermal cells; $Bry^{+}Flk1^{-}$, which marks the primitive streak, and $Bry^{+}Flk1^{+}$ cells, which marks the hemangioblast-containing population[192]. The PS population is of particular significance, as it contains cells that will soon develop into hematopoietic cells, yet do not yet have any hematopoietic potential. Hence, they are at a crucial point of fate determination. PS cells can give rise to multiple mesodermal lineages including cardiac, endothelial and hematopoietic cells[254-255]. By controlling culture conditions *ex-vivo*, PS cells may be directed towards a specific developmental program of interest.

To uncover key regulators involved in hematopoietic commitment, PS cells from E8.5 mouse embryos were isolated and differentiated towards a hematopoietic or non-hematopoietic program. Based on the hypothesis that differentially expressed factors would be involved in determining hematopoietic potential, we performed microarray transcriptome comparison of the PS and the derived hematopoietic and non-hematopoietic populations, and selected Pcgf5 for further study of its potential role in hematopoietic development.

4.2 RESULTS

4.2.1 Microarray analysis of mesodermal commitment towards hematopoietic fate

Bry$^+$ PS cells were isolated from E8.5 Bry-GFP embryos using FACS, and directed towards either a hematopoietic (H) or non-hematopoietic (NH) fate in serum-containing and serum-free conditions respectively. “H” cells, when plated on hematopoiesis-supporting OP9, can give rise to hematopoietic cells, while “NH” cells do not (fig. 20A). The hematopoietic potential of the derived “H” population rivals that of E8.5 Bry$^+$Flk1$^+$ cells with known hematopoietic potential, as observed from the similar production of myeloid and lymphoid lineages following culture on OP9 (Fig. 20B). Hence, these 3 derived populations (PS, H and NH) are observed to have different hematopoietic potentials.

Microarray transcriptome comparisons of PS, H and NH populations identified several genes that are differentially expressed in mesoderm cells directed towards the hematopoietic fate (fig. 21). In particular, we were interested in genes most highly expressed in the “H” group compared to the PS and “NH” populations, as these are most likely to be involved in hematopoietic specification. In addition, by excluding genes upregulated on commitment to the “NH” group, this sector of 322 genes was expected to narrow in on factors specific to hematopoietic development. Key hematopoietic genes *Runx1* and *Gata2*, which are required for normal hematopoietic development, were found in this sector, validating the logic behind analysis of this sector, and providing evidence that the microarray went well. As the microarray was previously performed and analyzed by ex-colleague Dr. Brian Tan, this thesis will not cover detailed analysis of the remaining microarray results.

Polycomb ring finger protein 5 (*Pcgf5*) was identified in the same analysis sector as *Runx1* and *Gata2*. *Pcgf5* is one of 6 members of the Polycomb group ring finger (*Pcgf*) family, which also includes *Bmi1* and *Mel18.* Given its unknown role in PRC1 regulation of hematopoietic development, we selected Pcgf5 for further characterization. *Pcgf5* is highly upregulated in the “H” microarray population, not only compared to the PS and “NH” populations, but also compared to other *Pcgf* homologues (fig. 22A). In addition, given that PCGF5 is known to be associated with CBX8[256-257], we studied the expression of *Cbx8* in these populations. We found that *Cbx8* is also upregulated in the "H" population (fig. 22B), providing evidence that *Pcgf5* may be involved in PRC1 regulation during hematopoietic development.

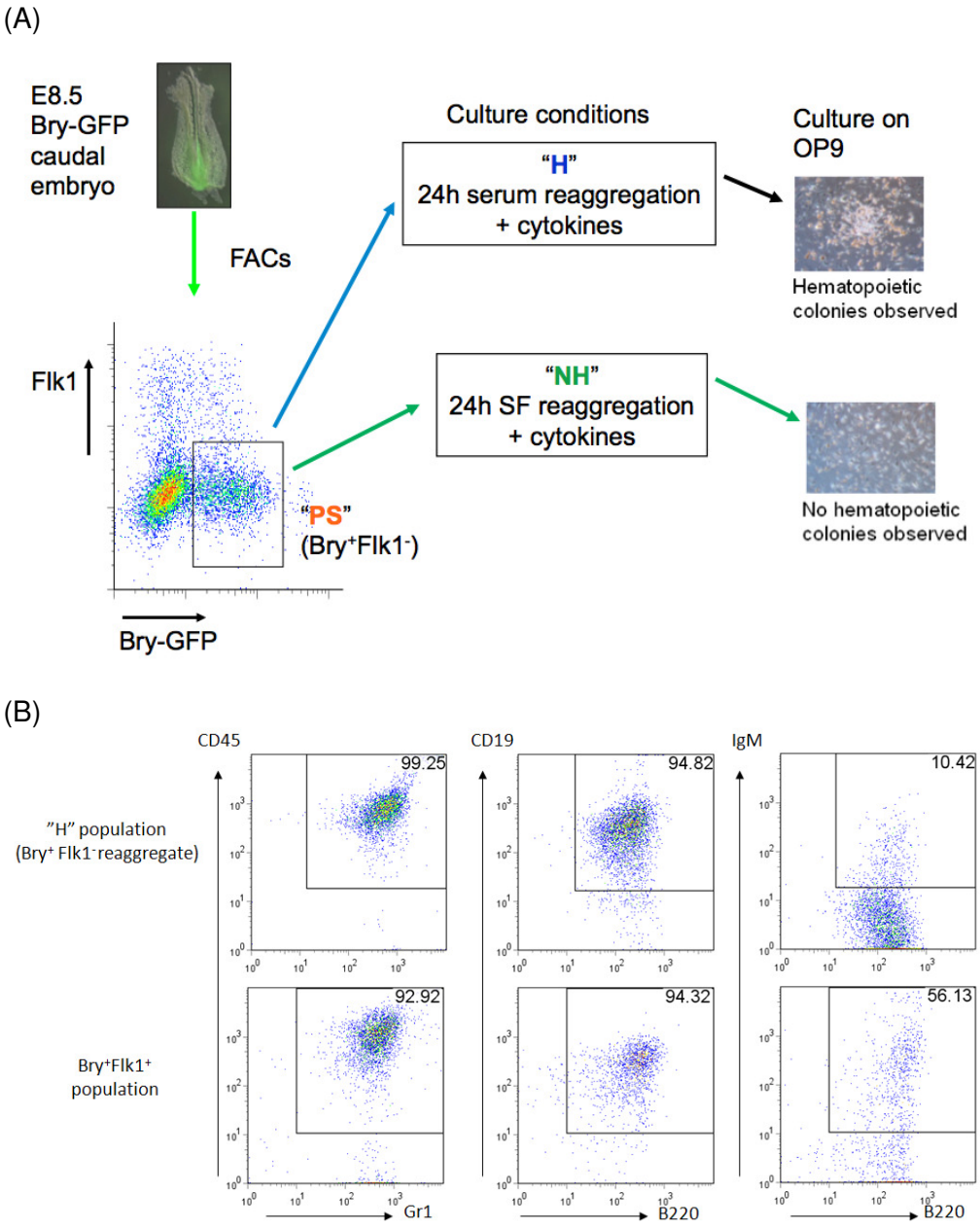

Figure 20. Hematopoietic potential of E8.5 Bry$^+$Flk1$^+$ (PS) and derived "H" and "NH" populations.

(A) Schematic showing derivation of PS, H and NH populations from E8.5 embryo, and subsequent generation of round, non-adherent hematopoietic cells from H but not NH population. (B) Myeloid and lymphoid potential of "H" population, and E8.5 Bry$^+$Flk1$^+$ hemangioblast-containing population. FACS plots of myeloid (CD45$^+$Gr1$^+$) and lymphoid (CD19$^+$B220$^+$ and IgM$^+$B220$^+$) populations obtained after 3-week culture of "H" (top row) and E8.5 Bry$^+$Flk1$^+$ (bottom row) populations on OP9.

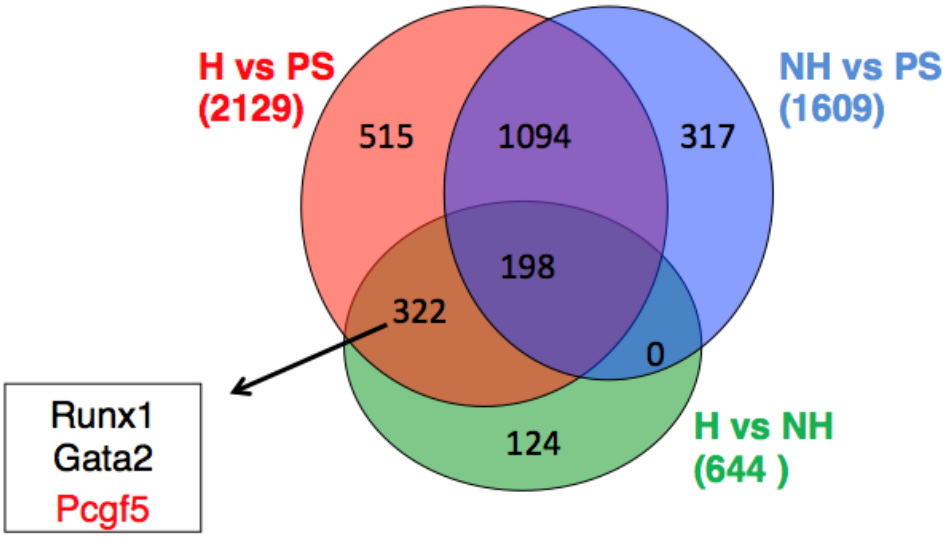

Figure 21. Microarray analysis of genes upregulated during mesoderm commitment to hematopoiesis.
Significance analysis of microarrays (SAM) was used to analyse the microarray results, using fold change >2 and false discovery rate (FDR) <0.05. Numbers of genes upregulated in the respective comparisons are shown in the Venn diagram.

(A)

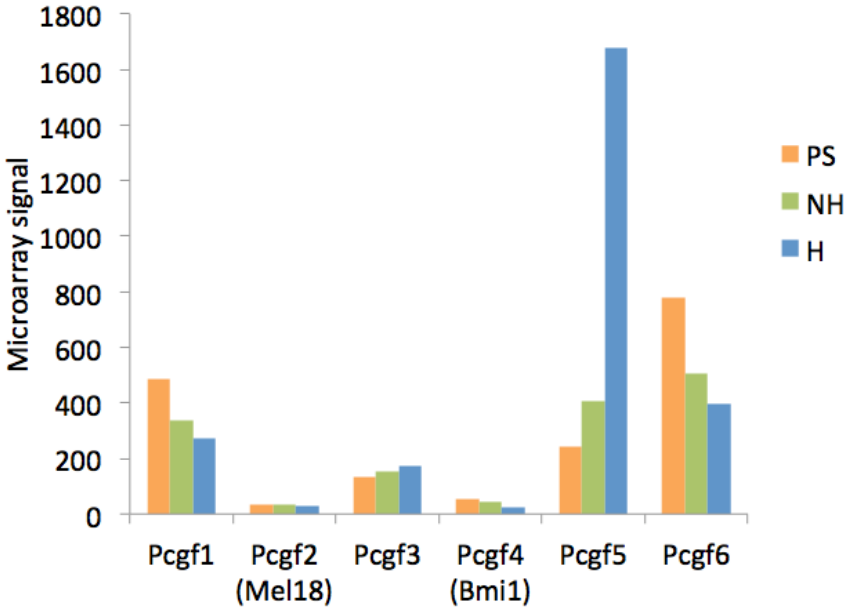

(B)

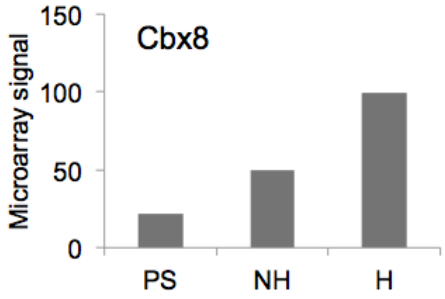

Figure 22. *Pcgf5* and partner *Cbx8* are preferentially expressed in the hematopoietic "H" population.
(A) Average microarray signal of *Pcgf* homologues. (B) Average microarray signal of *Cbx8*.

4.2.2 *Pcgf5* knockdown disrupts the balance between hematopoietic and neural genes

Pcgf5 and its known partner *Cbx8* are expressed in EBs from d3.5 onwards, coinciding with the onset of hemangioblast development in EBs (fig. 23). This is in contrast to homologues *Bmi1* and *Mel18* as well as *Ring1B*, which appear to have stable or decreasing expression patterns. To study the effect of *Pcgf5* knockdown in hematopoietic development, we generated an inducible *Pcgf5*^{kd}-plox-GFP-Intron-miR cell line containing shRNA against *Pcgf5*, based on the plox-GFP-Intron-miR vector[213]. Dox- induction of shRNA against *Pcgf5* resulted in up to 50% decrease in *Pcgf5* expression in d4 EBs, but did not significantly affect expression of *Ring1B* or its homologues *Bmi1* and *Mel18*. These results indicate that the shRNA against *Pcgf5* is not non-specific, and also provide further proof that *Pcgf* homologues are non-redundant, as *Bmi1* and *Mel18* do not compensate for the loss of *Pcgf5* (fig. 24A, B).

Knockdown of *Pcgf5* in day 4 EBs resulted in a decrease in hematopoietic genes *Flk1* and Runx1, as well as upregulation of neuroectodermal genes *NeuroD* and *Sox1*, particularly using shRNA 2 (fig. 24C). These results corresponded with other data generated using lentiviral shRNA knockdown of *Pcgf5*, which also showed downregulation of endodermal genes *Foxa2*, *Gata4* and *Sox17* at d4 (fig. 25). Together, these results echo findings involving RING1B knockdown that PRC1 is required to regulate neural gene expression in bivalently-poised Bry^{+}Flk1^{+} hemangioblasts, in which lowly-expressed neural-specifying genes are marked by gene-silencing H3K27me3 as expected, but surprisingly also by the activating H3K4me3 mark despite the cell population's association with hematopoietic potential[258]. In addition,

induced day 4 Pcgf5^{kd}-plox-GFP-Intron-miR EBs displayed a decrease in hematopoietic potential as assessed by blast colony assay and hematopoietic progenitor assays (fig. 26). Hence, these results suggest that *Pcgf5* may be involved in PRC1 maintenance of the balance between hematopoietic and neuronal lineages in early hematopoietic development.

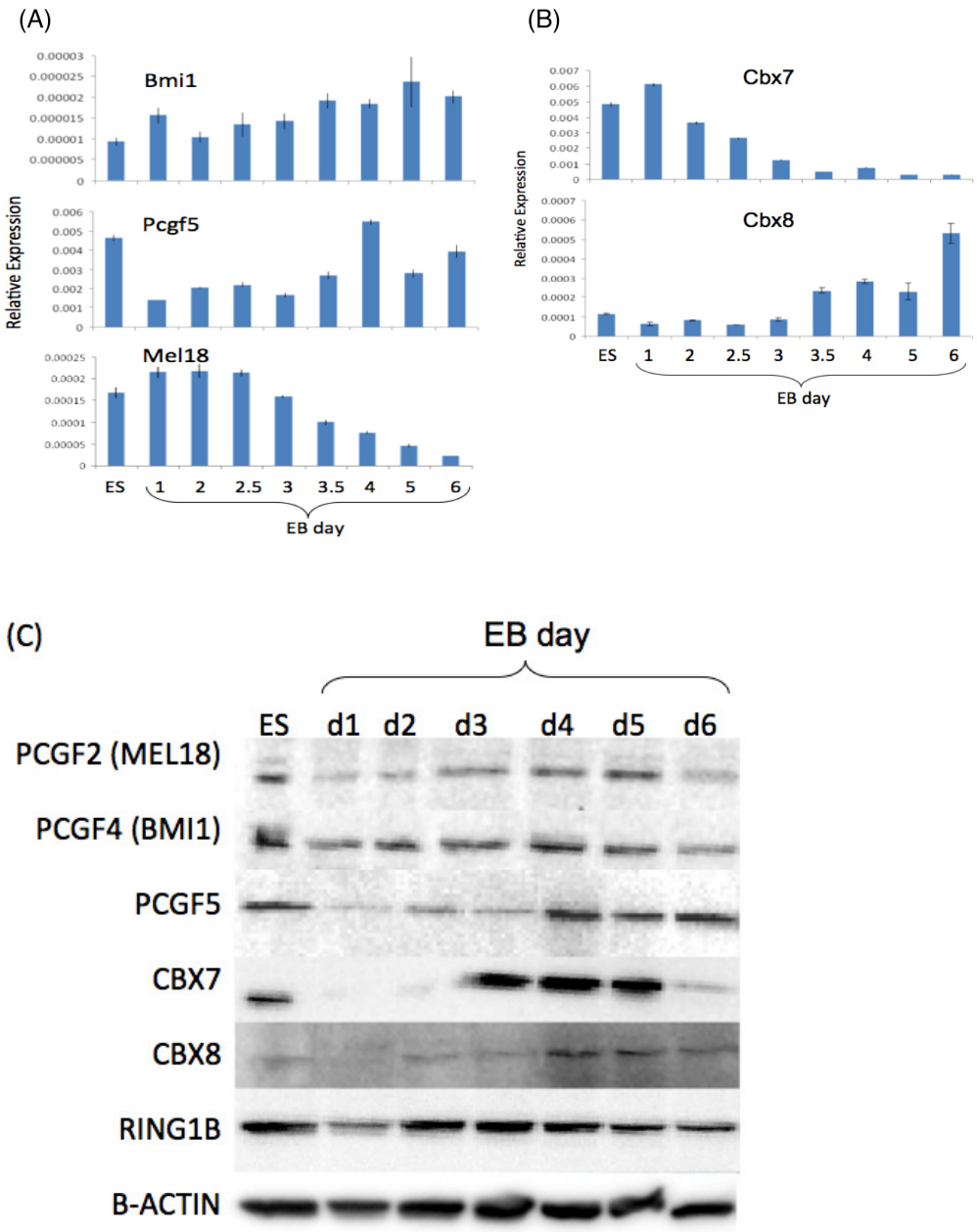

Figure 23. Dynamic expression of *Pcgf* homologues and selected *Cbx* genes during EB development.
QPCR expression profiles of (A) *Pcgf* homologues *Bmi1*, *Pcgf5* and *Mel18*, and (B) *Cbx7* and *Cbx8*. Expression relative to *β-actin*. (C) Western blot of PCGF5 protein expression in ESC and maturing EBs.

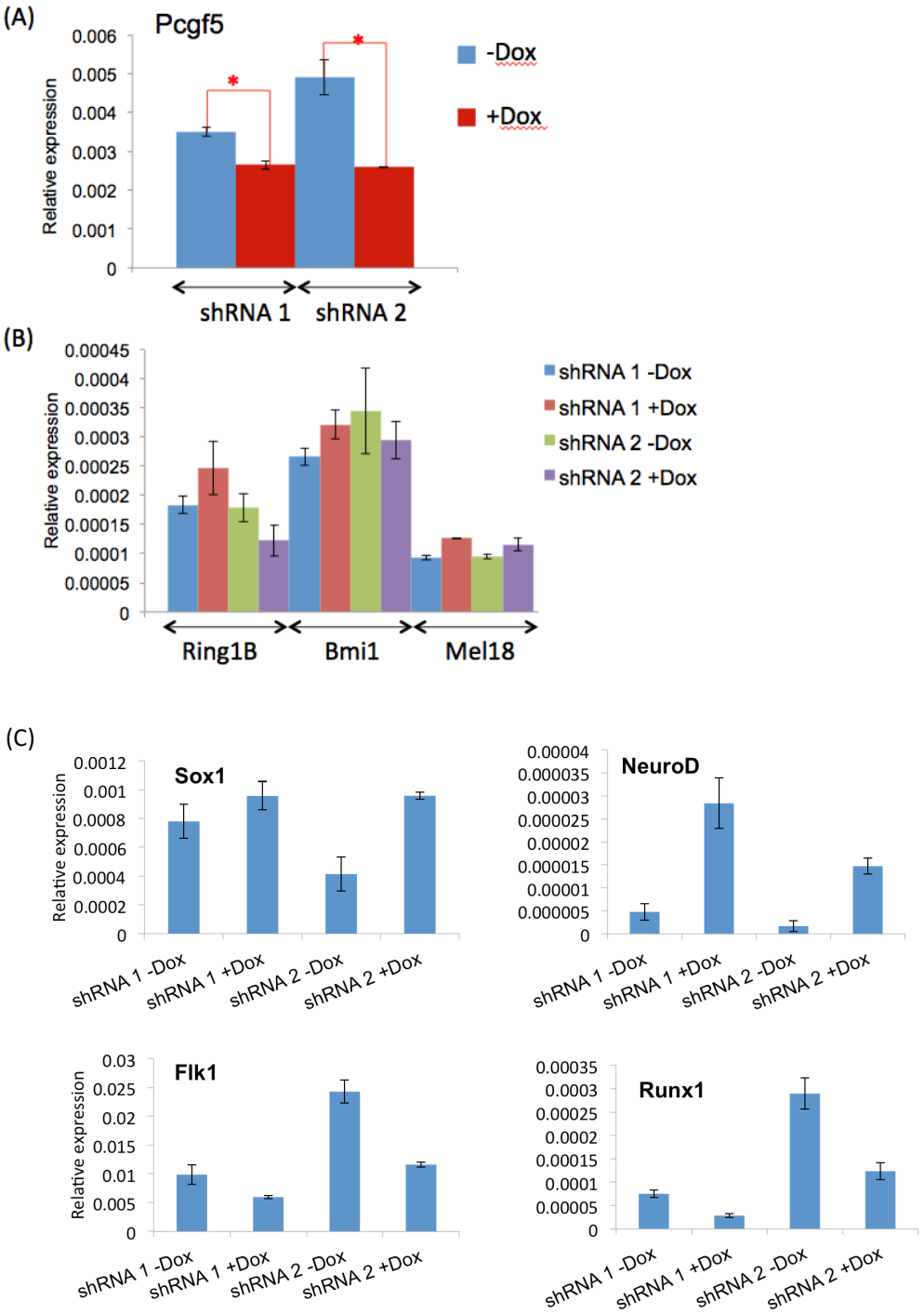

Figure 24. Knockdown of *Pcgf5* is specific and disrupts bivalently-poised day 4 EBs.
QPCR expression of (A) *Pcgf5*, (B) *Ring1B, Bmi1* and *Mel18*, and (C) neuroectodermal and hematopoietic markers in induced and uninduced Pcgf5^{kd}-plox-GFP-Intron-miR cell line. Expression relative to *β-actin*.

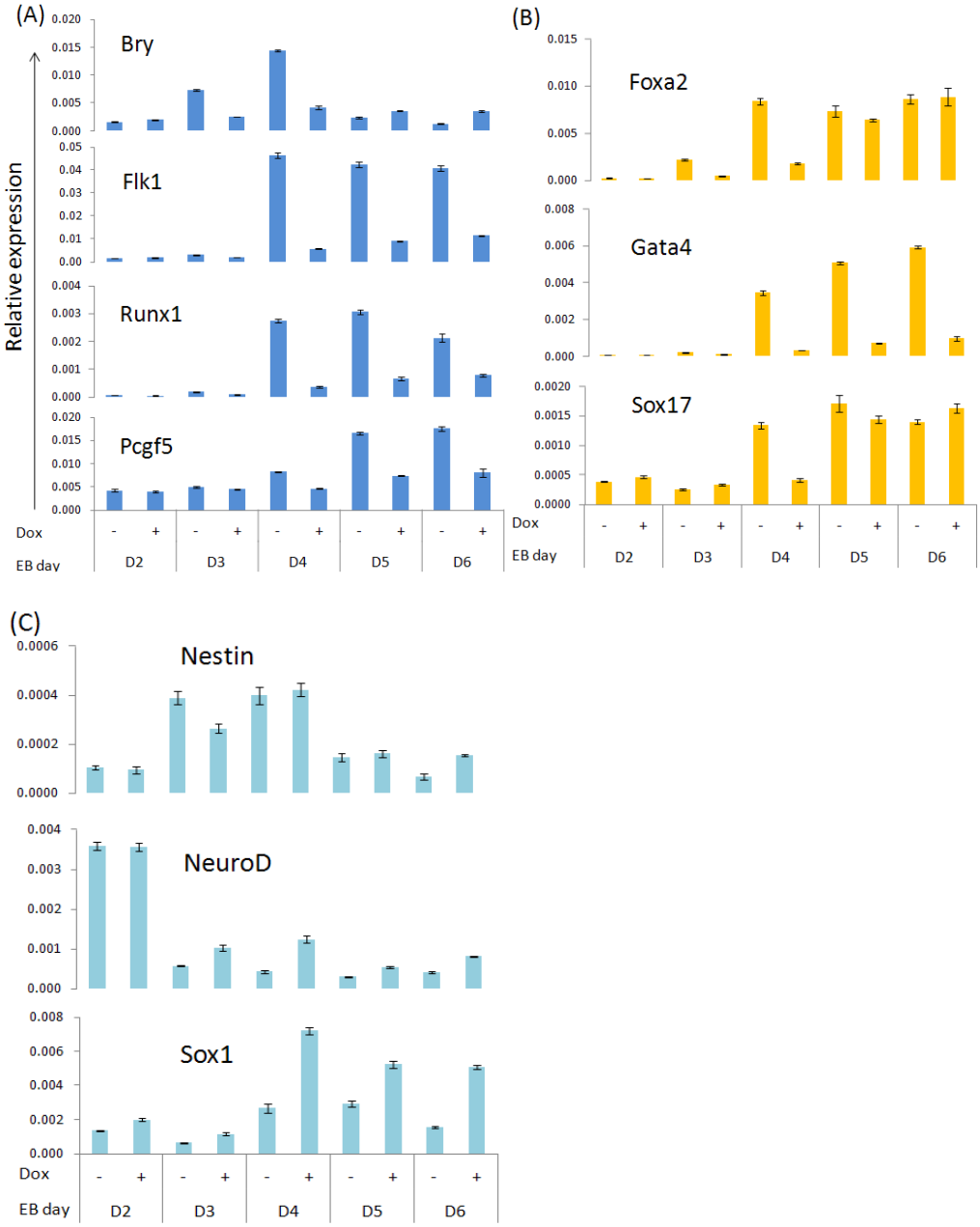

Figure 25. Lentiviral shRNA knockdown of *Pcgf5* disrupts bivalently-poised hemangioblast cells.
QPCR expression of (A) meso-hematopoietic, (B) endodermal and (C) neuroectodermal markers upon lentiviral shRNA knockdown of *Pcgf5*. Expression relative to *β-actin*. Work done by Brian Tan.

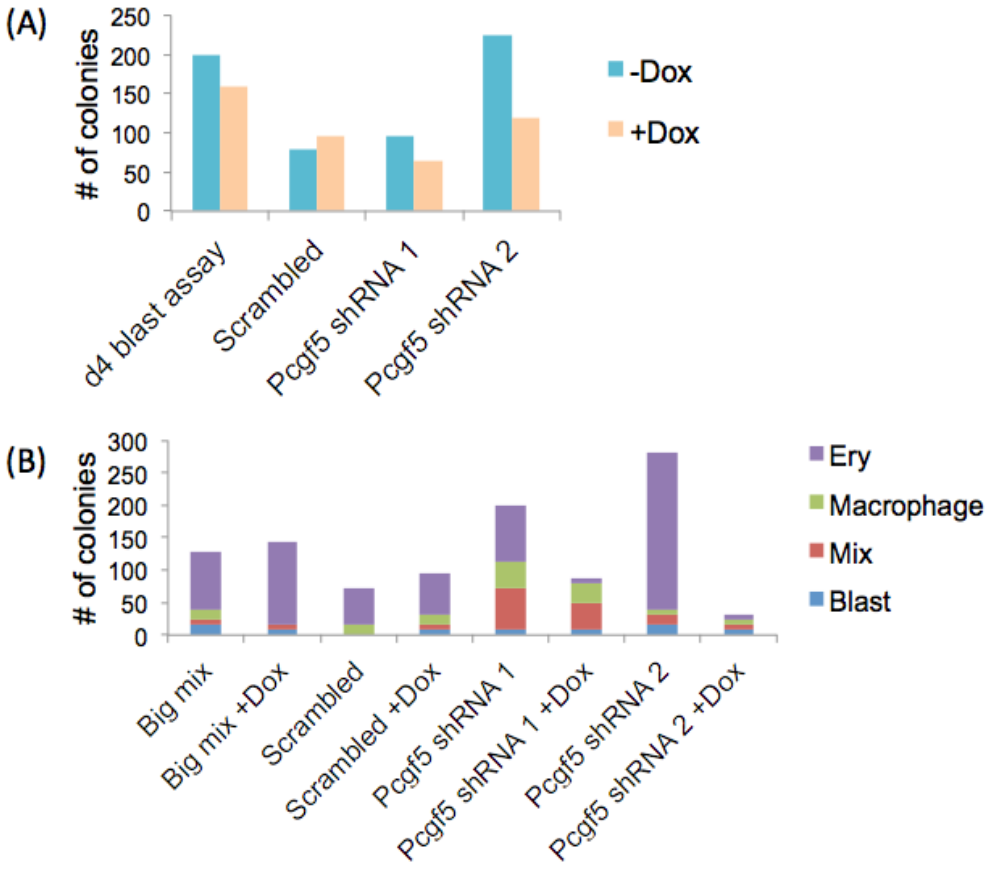

Figure 26. Knockdown of *Pcgf5* decreases hematopoietic potential. (A) Blast colony assay of day 4 hemangioblast-derived colonies and (B) hematopoietic progenitor assay of day 6 hemangioblast derived colonies in induced and uninduced Pcgf5^{kd}-plox-GFP-Intron-miR cell line. Data obtained from average results of 3 biological replicates.

4.2.3 Differential targeting of lineage-specific genes by PCGF5 across YS and P-Sp hematopoiesis-recapitulating populations

D3.5 Bry^+Flk1^+ EBs can recapitulate YS hematopoiesis in that both primitive and definitive erythroid as well as myeloid lineages can be generated. However, only d5.5 $Flk1^+$ cells formed by 48 h reaggregation of d3.5 Bry^+Flk1^- cells (fig. 27A, B) in the presence of cytokines can generate the additional lymphoid lineage, thus recapitulating P-Sp hematopoiesis[193]. Hence, these distinct temporally separated populations provide a powerful tool with which hematopoietic development can be modeled and dissected *in vitro.*

Pcgf5 is highly expressed in the reaggregated $Flk1^+$ population representing P-Sp hematopoiesis (fig. 27C), even more so than the d3.5 Bry^+Flk1^+ hemangioblast-containing population. This suggests that *Pcgf5* may be involved in regulation of early hematopoietic development, in particular that leading to generation of lymphoid cells via the HSC. Hence, we were interested to identify if PCGF5 is part of a PRC1 complex active during hematopoietic development. To do so, we first sought to identify if PCGF5 binds to RING1B. Co-immunoprecipitation (co-IP) of day 4 EBs with αRING1B antibody followed by Western blot with αCBX7 or αBMI1 identified 34 kDa and 37 kDa bands respectively. Thus, co-IP verified that RING1B was able to bind to each of these 2 known targets (fig. 28A). However, binding of RING1B to PCGF5 using the same method was not observed even after attempts to optimize the protocol (fig. 28B). The co-IP protocol is notoriously variable; over-fixation of protein complexes via formaldehyde cross-linking may result in loss of protein binding sites, while under- or lack of protein fixation may cause the target protein complex to dissociate. Thus, a lack of observed binding can potentially be a false negative result.

In order to address the question of whether PCGF5 was in a PRC1 complex from a different angle, we opted to proceed with chromatin immunoprecipitation followed by qPCR (ChIP-qPCR) to identify if there are overlapping targets in a RING1B- and PCGF5- ChIP-qPCR. Although this does not definitively prove that the two proteins form a binding complex together, the identification of shared targets via a specific 20-24bp DNA sequence indicates that the two proteins are located in close proximity, and are likely to form a complex together. Using ChIP-qPCR primers shared by Mazzarella *et al*, RING1B ChIP-qPCR of d3.5 $Bry^{+}Flk1^{+}$ EBs revealed the strong association of RING1B with ES (*Sox2, Rex1*), neural (*Nkx2.2, Sox1*), and mesodermal (*Ikaros, Myf5*) genes (fig. 29A). This is in line with published work by Mazzarella *et al*[258] showing that PRC1 is required for repression of bivalently-poised neural genes in d3.5 $Bry^{+}Flk1^{+}$ hemangioblast cells, as previously explained.

Meanwhile, ChIP-qPCR of PCGF homologues BMI1, PCGF5 and MEL18 revealed that the homologues targeted similar as well as unique ES, neural and mesodermal targets in the d3.5 $Bry^{+}Flk1^{+}$ population (fig. 29A). ES targets *Oct4* and *Rex1* were strongly targeted by all 3 homologues, while only MEL18 additionally strongly bound *Sox2*. Neural genes *Nkx2.2* and *Sox1* were strongly bound by PCGF5 and MEL18, but *Sox1* binding by BMI1 was relatively low. Finally, only MEL18 strongly associates with mesodermal targets *Flk1* and *Ikaros*. This not only reveals that RING1B and PCGF5 indeed have shared targets, supporting the possibility that they form a binding complex together; but also that PCGF homologues, potentially as part of different PRC1 variants, appear to be active at the same time but do not have

identical targets. This supports the knowledge that PCGF members occupy distinct genomic loci, as observed from exclusive or predominant binding by a single PCGF to selected promoters[259]. Together, these results suggest that several distinct PRC1 complexes may be simultaneously involved in PRC1 regulation in the hemangioblast.

ChIP-qPCR of the same targets in the reaggregated d5.5 $Flk1^+$ population showed that not only did ES, neural and mesodermal targets remain regulated by PRC1, but also that regulation of genes were dynamic in terms of which PCGF homologue dominantly targeted the lineage in that population (fig. 29B). BMI1 and MEL18 remained associated with targets from all 3 lineages, albeit less strongly and widely in the d5.5 $Flk1^+$ population compared to the d3.5 Bry^+Flk1^+ population. Most notably, PCGF5 targeted genes from all 3 lineages in the d3.5 hemangioblast population, but strongly targeted only mesodermal genes (*Flk1, Ikaros* and *Myf5*) in the reaggregated d5.5 $Flk1^+$ population, suggesting that PCGF5 provides complex regulation of mesodermal lineages as development progresses.

Hence, we show that PCGF homologues BMI1, PCGF5 and MEL18 are simultaneously active in *in vitro*-derived populations that recapitulate YS and P-Sp hematopoiesis, and that PCGF5 may be particularly involved in the regulation of developing mesoderm. Comparison of mesodermal (*Bry, Flk1*) and neural (*Sox1*) targets following *Pcgf5* knockdown (fig. 25) as well as PCGF ChIP-qPCR (fig. 29A) shows that while *Pcgf5* knockdown in d4 EBs resulted in decreased expression of *Bry* and *Flk1* but upregulation of *Sox1*; RING1B and MEL18 bind strongly to all 3 targets in d3.5 Bry^+Flk1^+ population, while PCGF5 binds strongly to *Bry* and *Sox1*, but relatively weakly

to Flk1, and finally BMI1 binds strongly only to *Bry* but relatively weakly to *Flk1* and *Sox1*. This suggests that when *Pcgf5* is downregulated, homologues BMI1 and MEL18 are unable to rescue the effect on PCGF5 target genes despite binding to the same target, further supporting the non-redundancy of PCGF homologues. In addition, PCGF5 binding to *Sox1* (fig. 29A) appears to directly inhibit expression of *Sox1*, as knockdown of *Pcgf5* results in *Sox1* upregulation (fig. 25). However, despite binding of PCGF5 to *Bry* and *Flk1* (fig. 29A), knockdown of *Pcgf5* results in downregulation of these 2 genes (fig. 25), suggesting that PCGF5 is not the only factor involved in regulating the expression of important hematopoietic genes *Bry* and *Flk1* at this stage.

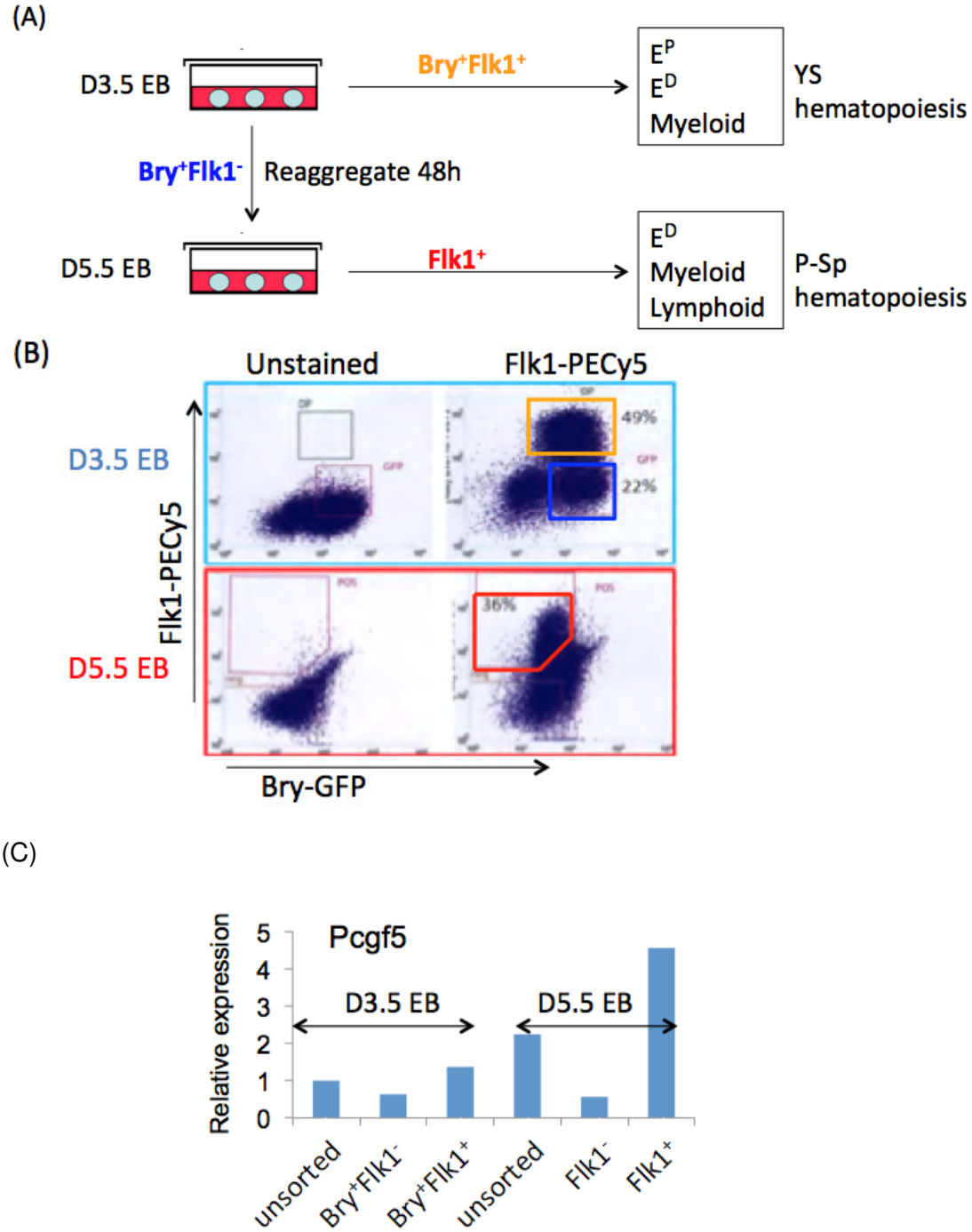

Figure 27. *Pcgf5* is highly expressed in reaggregated d5.5 Flk1$^+$ population recapitulating P-Sp hematopoiesis.
(A) Schematic of generation of *in vitro* populations that recapitulate YS and P-Sp hematopoiesis. (B) FACS plot of d3.5 and reaggregated d5.5 EBs sorted based on expression of *Bry* and *Flk1*. Percentages indicate relative to population. (C) QPCR expression of *Pcgf5* in d3.5 and reaggregated d5.5 Bry and Flk1- sorted EB populations. Expression relative to *β-actin*.

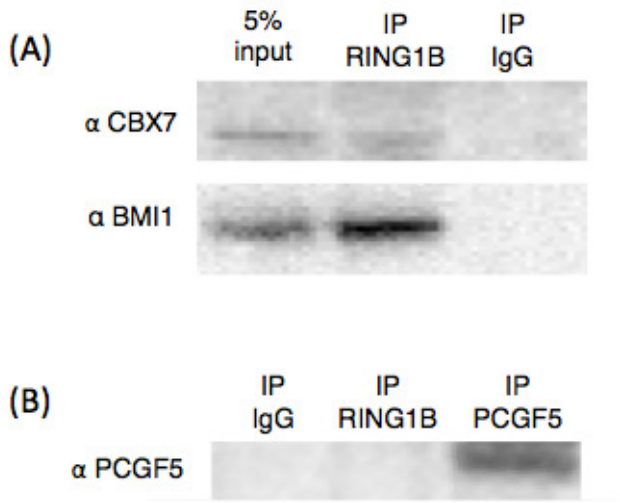

Figure 28. Co-IP does not reveal PCGF5 binding to RING1B in d4 EBs. (A) Co-IP of RING1B with CBX7 or BMI1. (B) Co-IP of RING1B (test) or PCGF5 (positive control) with PCGF5. All protein lysates obtained from day 4 EBs. IgG: negative control.

(A)

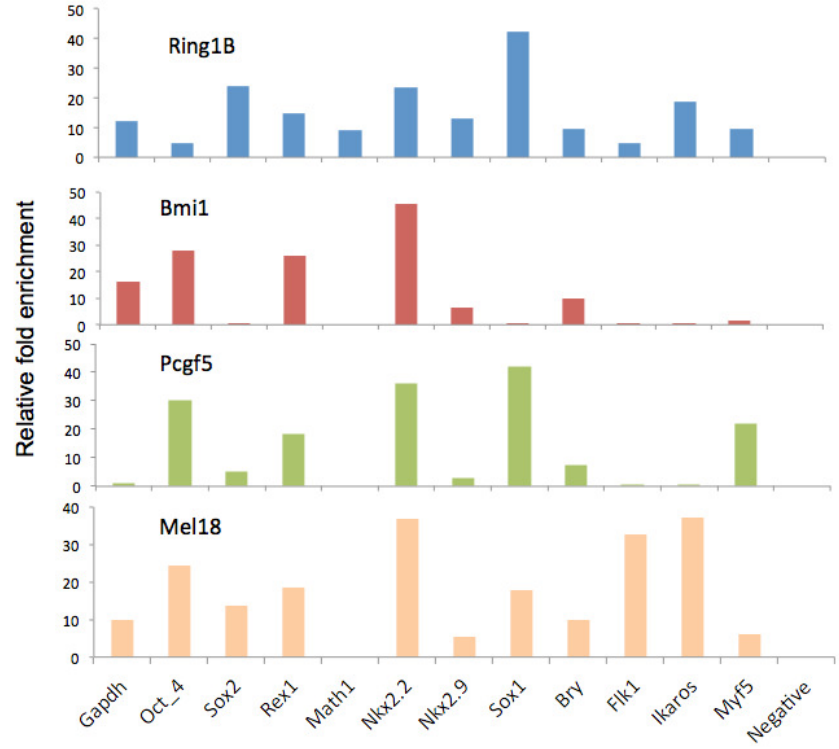

(B)

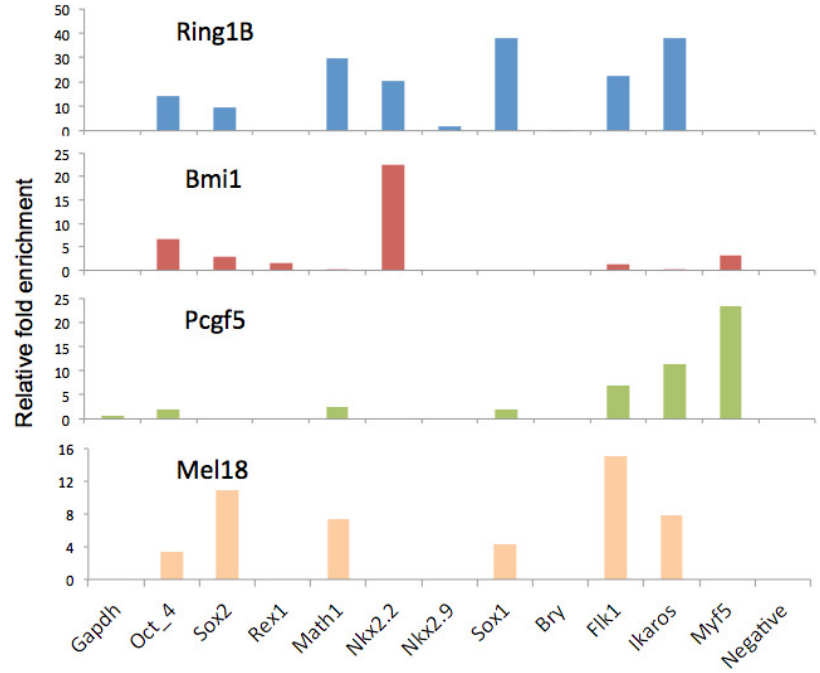

Figure 29. PRC1 components bind to shared and unique targets in populations recapitulating YS and P-Sp hematopoiesis.
ChIP-qPCR of RING1B and PCGF homologues in (A) d3.5 EB Bry^{+}Flk1^{+} cells and (B) reaggregated d5.5 Flk1^{+} cells. Enrichment levels are expressed relative to 10% input. Results calculated from average results of 3 technical replicates.

4.3 SUMMARY & DISCUSSION

In summary, we performed a DNA microarray comparison of populations derived from E8.5 primitive streak, in order to identify differentially expressed genes that may be involved in definitive hematopoietic fate determination. *Pcgf5* was more highly expressed in the derived hematopoietic population along with essential hematopoietic genes *Runx1* and *Gata2*, suggesting its involvement in hematopoietic development. Knockdown of *Pcgf5* resulted in increased expression of neuro-ectodermal genes and downregulation of hematopoietic genes, pointing to novel *Pcgf5* involvement in PRC1-regulated hemangioblasts. ChIP-qPCR of RING1B and PCGF homologues BMI1, PCGF5 and MEL18 in *in vitro* populations that recapitulate YS and P-Sp hematopoiesis, also showed PCGF5 binding to known PRC1-regulated hemangioblast targets, as well as simultaneous activity of PRC1 variants as identified by RING1B-PCGF binding. These results highlight the involvement of *Pcgf5* in hematopoietic development, as well as the complexity of epigenetic regulation involved.

PCGF is involved in chromatin compaction as part of the Polycomb Repressive Complex 1 (PRC1). PRC1 is involved in epigenetic regulation in partnership with PRC2, whereby PRC1 monoubiquitylation of H2Ak119 (H2AK119ub) stabilizes PRC2-mediated H3K27me3, resulting in chromatin compaction and inhibition of Pol II transcription initiation and elongation and subsequent silencing of the target gene. The main components of PRC1 are the E3 ubiquitin ligase RING1A/B, and a member from each of the PCGF and CBX families, the latter being involved in recognition of H3K27me3 to facilitate PRC1 recruitment. PRC1 is known to be involved in early development- *Bmi1* and *Mel18* knockout in mice result in hematopoietic

defects, while *Ring1B* knockout is embryonic lethal following gastrulation arrest[259-261]. No knockout data is currently available for *Pcgf5*, but its close homology to *Bmi1* (80% sequence similarity) suggests that *Pcgf5* could be similarly involved in hematopoiesis. Composition of PRC1 is dynamic and may comprise of different PCGF and CBX family subunits, allowing various PRC1 to differentially repress genes according to the cell's developmental state. For example, during the proliferating ESC stage, activity of PRC1 containing CBX7 and MEL18 inhibits CBX2, CBX4, CBX7 and CBX8, as well as BMI1. However, in differentiated ESC, the active PRC1 containing CBX2/4 and BMI1 inhibits CBX7 and other genes associated with pluripotency[173, 175]. Hence the non-redundancy of PRC1 components contributes to PRC1 ability to form variants with different functions.

Most *Pcgf* studies focus on the more prominent homologue *Bmi1*, which is known to be part of PRC1 and has been characterized in various roles ranging from hematopoiesis, skeletal patterning, cancer, as well as neural and liver development[262-266]. However, the role of *Pcgf5* has yet to be well characterized, particularly in hematopoiesis; thus far it has only been described to regulate lymphoid cell size by modifying cell cycle progression[267]. As *Bmi1* and *Pcgf5* share high sequence similarity, we hypothesized that PCGF5 might similarly play an important, novel role in PRC1 regulation during hematopoietic development. ChIP-qPCR of RING1B as well as PCGF homologues revealed not only that PCGF5 and RING1B have shared targets, thus suggesting the activity of PCGF5-PRC1; but also that PCGF homologues are simultaneously active and do not have identical targets. This potentially allows for the formation of distinct PRC1 variants that target different lineages or targets. While this is only hinted at from ChIP-

qPCR data in this section, we further provide evidence as such in subsequent ChIP-seq data. Such diversity gained from distinct PRC1 variants can allow for greater complexity in transcriptional regulation, as various combinations of active PRC1 variants can differentially regulate the system, thus resulting in a finely-tuned epigenetic environment than can better respond to changes.

CHAPTER 5:

CHIP-SEQUENCING OF PRC1 IN *IN VITRO*-DERIVED HEMATOPOIETIC POPULATIONS

5.1 INTRODUCTION

PRC1 complexes are involved in epigenetic regulation during development, and canonically monoubiquitinate H2AK119 in response to H3K27me3 at a target locus by PRC2. This inhibits the progression of RNA Pol II or prevents Pol II from forming the initiation complex[169-170]. Together with PCGF-mediated chromatin compaction[171], the target gene is thus repressed.

As previously described in section 4.2.3, ChIP-qPCR of PRC1 components in d3.5 $Bry^{+}Flk1^{+}$ and d5.5 $Flk1^{+}$ EBs, which recapitulate YS and P-Sp hematopoiesis respectively[193], identified that PRC1 variants are simultaneously involved in regulation of hematopoietic development. In particular, PCGF5 was found to bind to known PRC1-regulated hemangioblast targets, highlighting the involvement of *Pcgf5* in hematopoietic development.

Based on the hypothesis that PRC1 variants are involved in early mouse hematopoietic development by binding to and subsequently repressing targets, we sought to identify these targets to elucidate how and when PRC1 variants regulate these genes, thus contributing to hematopoietic development. By comparing targets identified from chromatin immunoprecipitation followed by high-throughput sequencing (ChIP-seq) of PRC1 components, we identify and characterize the role of PRC1, in particular Pcgf5-PRC1, as hematopoietic development progresses.

5.2 RESULTS

5.2.1 ChIP-seq of PRC1 in *in vitro*- derived hematopoietic populations

Small-scale ChIP-seq[215] against PRC1 and associated histone marks H3K27me3 and H2AK119ub was carried out on *in vitro*-derived populations that are generated in the recapitulation of YS and P-Sp hematopoiesis (Table 5), namely d3.5 Bry^+Flk1^- (thereafter d3.5 Bry^+) EBs, d3.5 Bry^+Flk1^+ EBs, and reaggregated d5.5 $Flk1^+$ EBs. To identify targets bound by each of the PRC1 components, reads were mapped to the mouse genome using DFilter, a detection algorithm for next-gen massively-parallel sequencing data that more accurately identifies regulatory features compared to assay-specific algorithms[216]. The top 3 targets by peak strength, as well as another 3 randomly- selected targets, were validated using ChIP-qPCR (fig. 30-32). UCSC Genome Browser visualization also verified binding of PRC1 components to Sox1, Sox2 and Nkx2.2 genes in d3.5 Bry^+Flk1^+ and d5.5 $Flk1^+$ populations (fig. 33A-C). This corresponded with earlier ChIP-qPCR data that identified these binding targets (fig. 29), and together with low microarray signal of Sox1, Sox2 and Nkx2.2 in all 3 cell populations (fig. 33D), these results suggest that PRC1 targeting indeed mediates transcriptional repression of these genes. There was high correlation of H3K27me3 and H2AK119ub peaks in all 3 samples as expected (fig. 34A). Together with the high number of reads for each library (>$40x10^6$ reads) (Table 5) and subsequently- observed high peak values of targeted genes, these results indicate that the ChIP-seq went well.

To further verify the ChIP-seq results, we hypothesized that in order to provide a permissive environment for hematopoiesis to occur in hematopoietic populations, fewer genes associated with hematopoiesis would be epigenetically silenced in d3.5 Bry^+Flk1^+ and d5.5 $Flk1^+$ populations, compared to the non-hematopoietic d3.5 Bry^+ population. Using Ingenuity Pathway Analysis' (IPA) Gene Ontology (GO) terms to identify the numbers of hematopoietic genes targeted in each ChIP-seq, we identified that the largest fraction of hematopoietic genes targeted by H3K27me3 and H2AK119ub were in the d3.5 Bry^+ population (fig. 34B, C) as expected, compared to the remaining 2 hematopoietic populations.

We also hypothesized that genes associated with particular hematopoietic fates would be differentially targeted by PRC1 across the 3 ChIP-seq populations. To test this, Model-based Analysis for Chip-Seq (MACs) was used to identify shared H3K27me3 and H2AK119ub ChIP-seq targets that overlap by >1 bp. Overlapping targets were then compared using a Venn diagram across the 3 ChIP-seq populations (fig. 35A). H3K27me3/H2AK119ub targets unique to the d3.5 Bry^+ population are expected to include genes important for hematopoiesis. Indeed, we identified targets such as Bmp4, Runx1 and Lmo2, which are required for normal hematopoiesis[218, 220, 268] in the sector of 3057 targets. H3K27me3/H2AK119ub targets found in both d3.5 Bry^+ and d5.5 $Flk1^+$ but not the hemangioblast-containing d3.5 Bry^+Flk1^+ populations are expected to include genes associated with primitive hematopoietic lineages, but the only known hematopoietic factor identified is Gata2, which is essential for normal hematopoiesis and generation of primitive hematopoietic cells from mesoderm[269-270]. This may be due to the heterogeneity of the d3.5 Bry^+

population, which contains mesoderm as well as pre-hemangioblast cells[192], thus introducing noise into the Venn comparison and obscuring the identification of more genes associated with primitive hematopoiesis. Finally, H3K27me3/H2AK119ub targets found in both d3.5 EB populations but not the d5.5 Flk1$^+$ population are expected to include genes associated with definitive hematopoietic lineages, and this is supported by the identification of targets such as Fli1, Gata 3 and Scl/Tal1, which are known to be indispensable for normal HSC development[271-275], in the sector comprising 865 targets. Using microarray of the 3 cell populations, we identified 13 candidate genes that are upregulated in d5.5 Flk1$^+$ compared to the other two d3.5 populations (Fig. 35B), which can be studied in future for their potential role in hematopoietic development. Hence, PRC1/2-mediated repression is involved in regulating hematopoietic factors to facilitate hematopoietic development.

Hox genes are highly conserved homeodomain-containing transcription factors that are important in early development, including hematopoiesis[276-277]. In addition, Hox genes are well-characterized targets of PRC1; polycomb genes were first discovered in *D. melanogaster* as key regulators of Hox gene expression[279-280]. Indeed, we identified a number of Hox genes differentially targeted by H3K27me3/H2AK119ub across the three ChIP-seq populations. Several targeted Hox genes were selected for validation by qPCR to identify if their gene expression matched the state of PRC1 targeting in that population (fig. 36). *Hoxb8*, which is targeted by H3K27me3/H2AK119ub across all 3 ChIP-seq populations, was shown to have inhibited gene expression as expected. *Hoxc13*, which is targeted by H3K27me3/H2AK119ub only in d3.5 Bry$^+$ and d3.5 Bry$^+$Flk1$^+$ population, has significantly upregulated expression in d5.5 Flk1$^+$. Similarly, Hoxa7 and Hoxb1, which are not targeted by

H3K27me3/H2AK119ub in any of the 3 ChIP-seq populations, show highly upregulated gene expression in all 3 populations. Hence, the gene expression of targeted Hox genes matches the state of PRC1 targeting in that ChIP-seq population.

Hox genes are spatially regulated, in that anterior 3' Hox genes (Hox 1-6) are highly expressed in primitive HSPCs, but are downregulated together with upregulation of 5' Hox genes (Hox 7-13) upon cell differentiation and maturation[280-281]. Comparison of RING1B-BMI1 overlapping targets between d3.5 $Bry^{+}Flk1^{+}$ hemangioblast-containing population and d5.5 $Flk1^{+}$, which is believed to give rise to the HSC, identified a number of 5' Hox genes uniquely targeted in the latter population. DNA microarray verified that 3' Hox genes are upregulated and 5' Hox genes downregulated in d5.5 $Flk1^{+}$ (fig. 37), suggesting that the BMI1-PRC1 complex is involved in Hox gene regulation during P-Sp hematopoiesis. Hence, BMI1-PRC1 is involved in the temporal regulation of Hox genes during hematopoietic development.

In summary, we performed ChIP-seq of PRC1 components in ESC-derived populations that recapitulate YS and P-Sp hematopoiesis. We identify that hematopoietic genes are more frequently regulated by H3K27me3/ H2AK119ub in non-hematopoietic d3.5 Bry^{+}, compared to hematopoietic d3.5 $Bry^{+}Flk1^{+}$ and d5.5 $Flk1^{+}$. Comparisons of targets bound by H3K27me3/H2AK119ub in the 3 ChIP-seq populations identify hematopoietic genes associated with the expected hematopoietic fate of particular Venn comparison sectors. In addition, selected Hox genes targeted by H3K27me3/H2AK119ub across all 3 ChIP-seq populations display gene expression patterns that match their regulation by PRC1/2, and BMI1-PRC1

is found to be involved in the temporal regulation of Hox genes. Together, these results support the conclusion that the ChIP-seq went well, and that results obtained from the analyses are biologically relevant.

Cell Population	ChIP-seq	# of reads ($x10^6$)	#of peaks called ($x10^{3)}$
D3.5 Bry^+	H3K27me3	42.06	38.63
	H2AK119ub	48.71	42.67
D3.5 Bry^+Flk1^+	H3K27me3	58.05	13.10
	H2AK119ub	50.03	23.79
	RING1B	90.42	41.72
	BMI1	84.06	42.45
	PCGF5	90.17	27.34
	MEL18	83.11	43.71
D5.5 $Flk1^+$	H3K27me3	55.97	17.16
	H2AK119ub	54.11	27.12
	RING1B	88.14	42.06
	BMI1	88.74	38.52

Table 5. List of ChIP-seq samples.

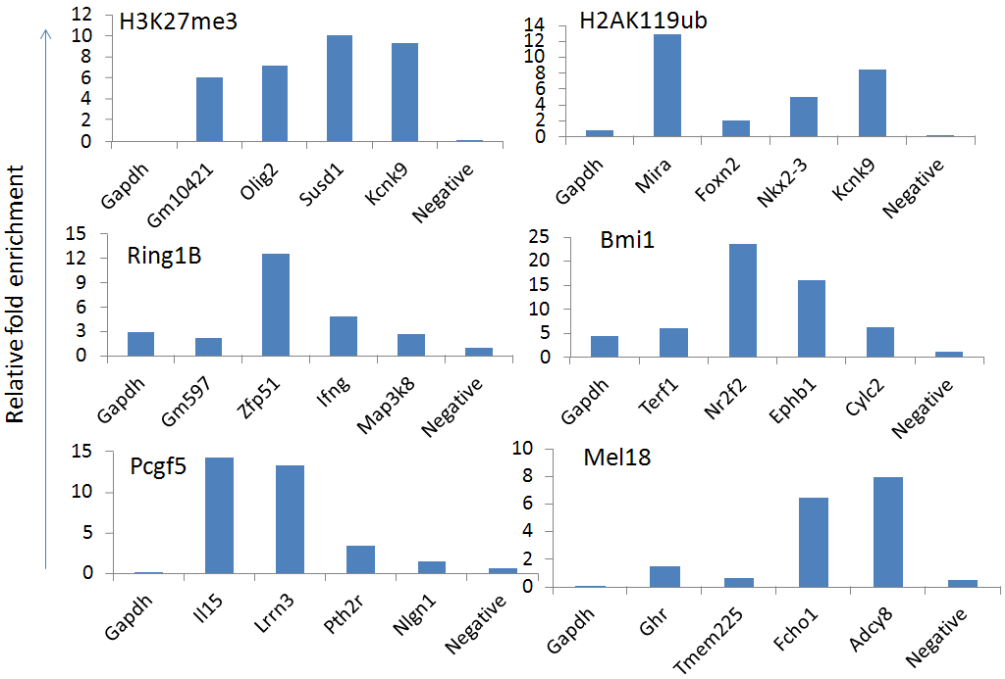

Figure 30. Target validation of d3.5 Bry^{+}Flk1^{+} ChIP-seq.
ChIP-qPCR of selected targets from d3.5 Bry^{+}Flk1^{+} ChIP-seq. Fold enrichment relative to 10% input. Results calculated from average results of 3 technical replicates.

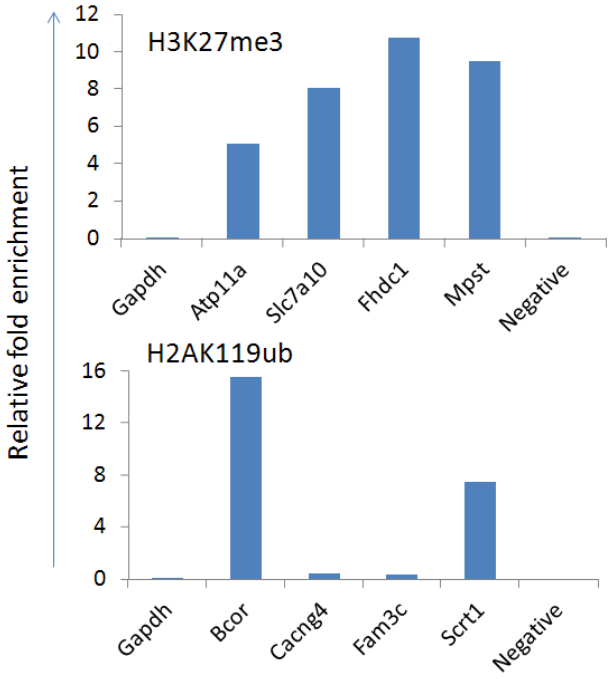

Figure 31. Target validation of d3.5 Bry^{+}Flk1^{-} ChIP-seq.
ChIP-qPCR of selected targets from d3.5 Bry^{+}Flk1^{-} ChIP-seq. Fold enrichment relative to 10% input. Results calculated from average results of 3 technical replicates.

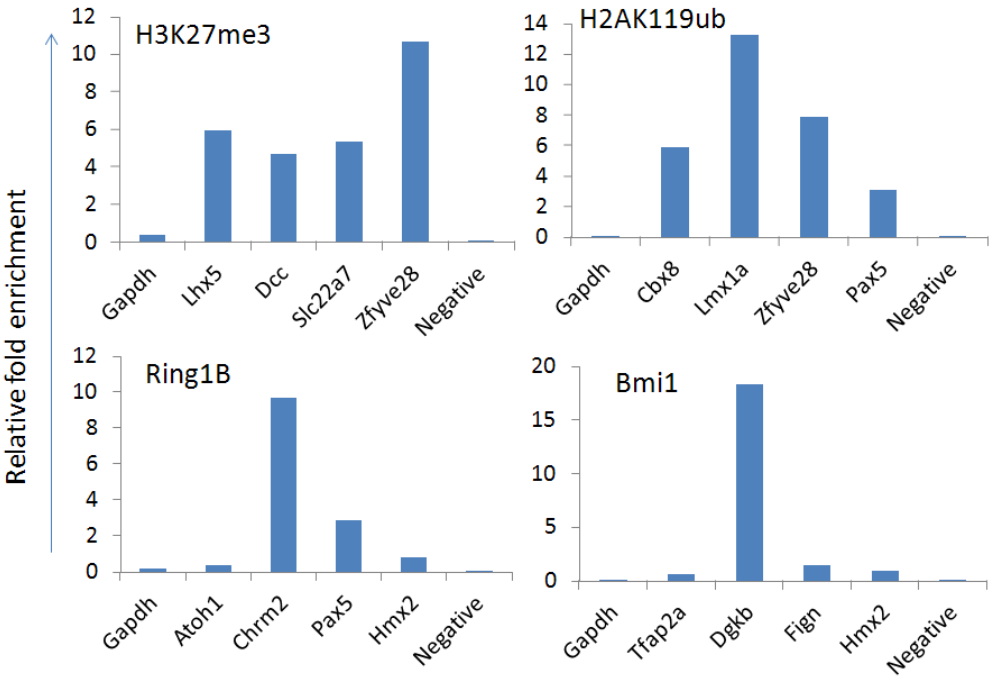

Figure 32. Target validation of d5.5 Flk1^{+} ChIP-seq.
ChIP-qPCR of selected targets from d5.5 Flk1^{+} ChIP-seq. Fold enrichment relative to 10% input. Results calculated from average results of 3 technical replicates.

(A)

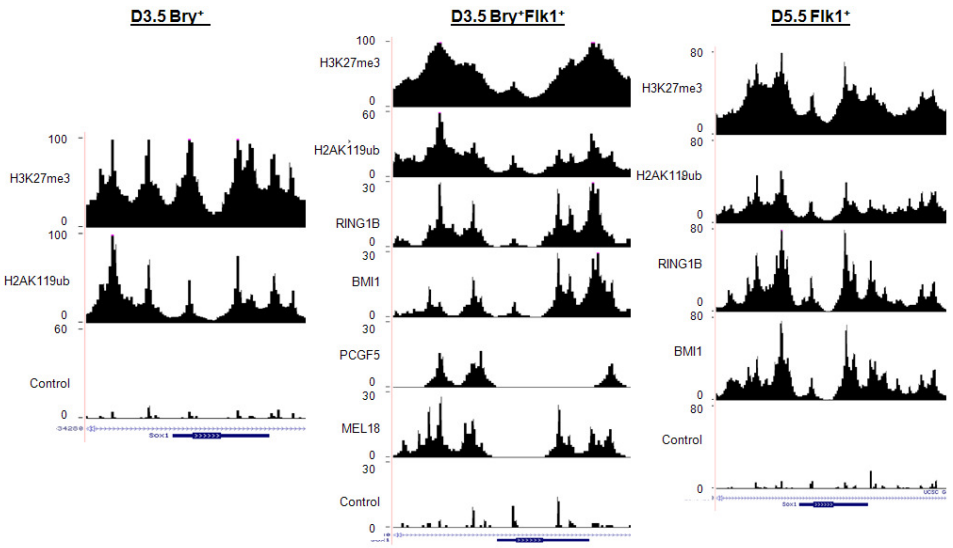
D3.5 Bry+
D3.5 Bry+Flk1+
D5.5 Flk1+
H3K27me3
H2AK119ub
RING1B
BMI1
PCGF5
MEL18
Control
Sox1

(B)

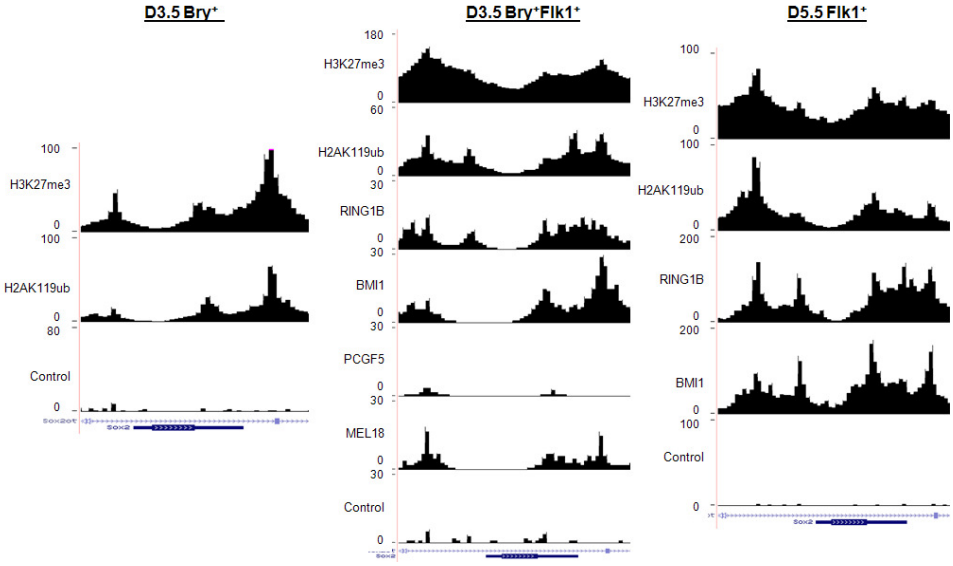
D3.5 Bry+
D3.5 Bry+Flk1+
D5.5 Flk1+
H3K27me3
H2AK119ub
RING1B
BMI1
PCGF5
MEL18
Control
Sox2

(C)

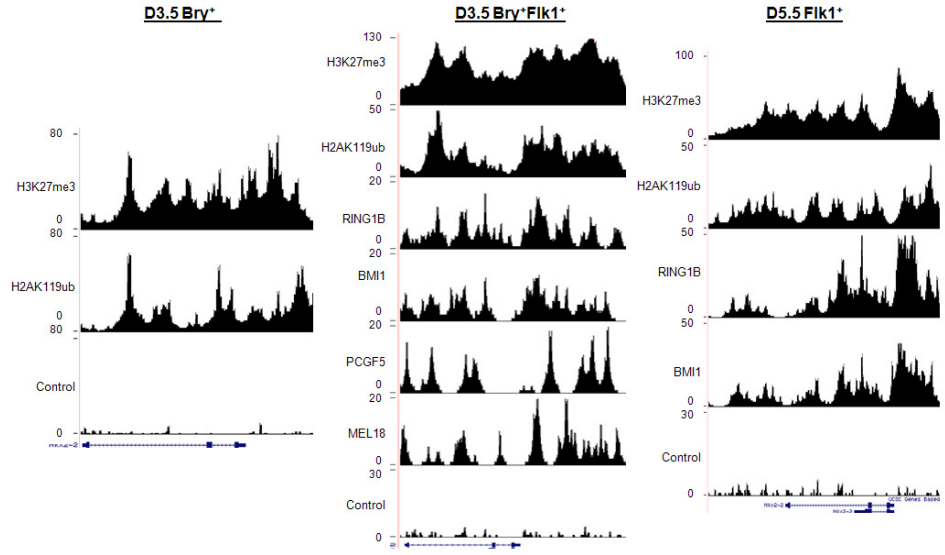

(D)

	Average microarray signal		
	D3.5 Bry$^+$	D3.5 Bry$^+$Flk1$^+$	D5.5 Flk1$^+$
Sox1	5.8	7.4	8.4
Sox2	16.4	5.8	6.3
Nkx2.2	3.6	2.3	5.6

Figure 33. PRC1 component binding at selected genes.
Binding of PRC1 components to (A) Sox1, (B) Sox2 and (C) Nkx2.2 in (left) d3.5 Bry$^+$, (middle) d3.5 Bry$^+$Flk1$^+$ and (right) d5.5 Flk1$^+$ populations. The input library is included as a control for background signal. Numbers indicate peak height. (D) Average microarray signal of Sox1, Sox2 and Nkx2.2 in respective cell populations.

(A)

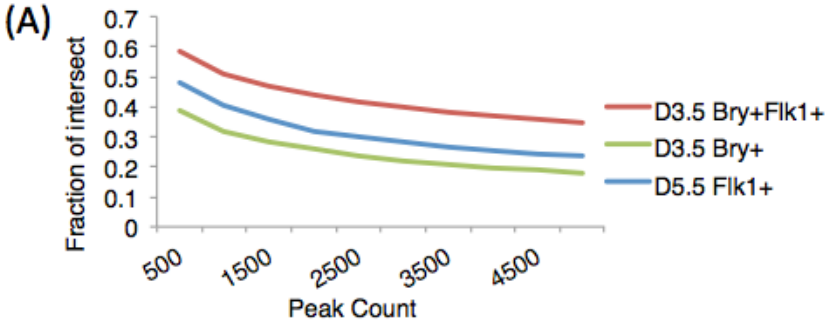

(B)

GO Terms
Hematopoietic or lymphoid organ development
Hematopoietic progenitor cell differentiation
Hematopoietic stem cell proliferation
Hematopoietic stem cell differentiation
Hemangioblast cell differentiation
Regulation of hematopoietic progenitor cell differentiation
Regulation of hematopoietic stem cell migration

(C)

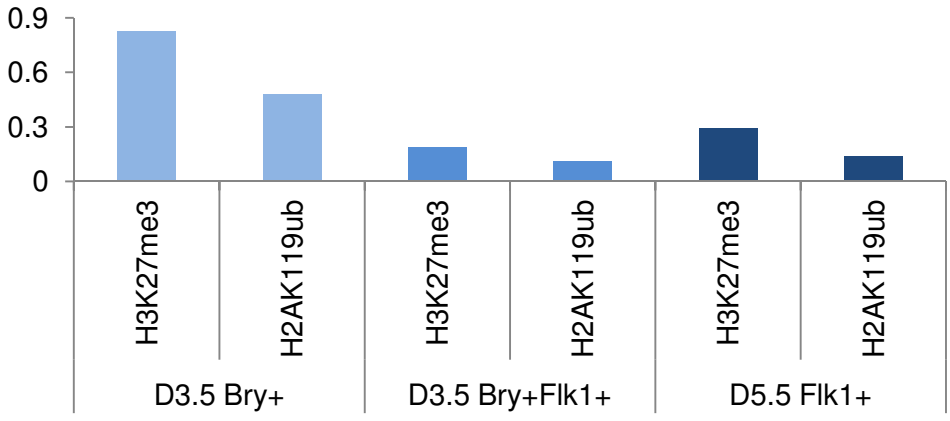

Figure 34. ChIP-seq analysis of H3K27me3 and H2AK119ub targets. (A) Correlation of peak intersections between H3K27me3 and H2AK119ub targets in ChIP-seq samples. (B) List of hematopoietic GO terms used. (C) Number of hematopoietic genes targeted in ChIP-seq populations, as a fraction of total number of peaks called.

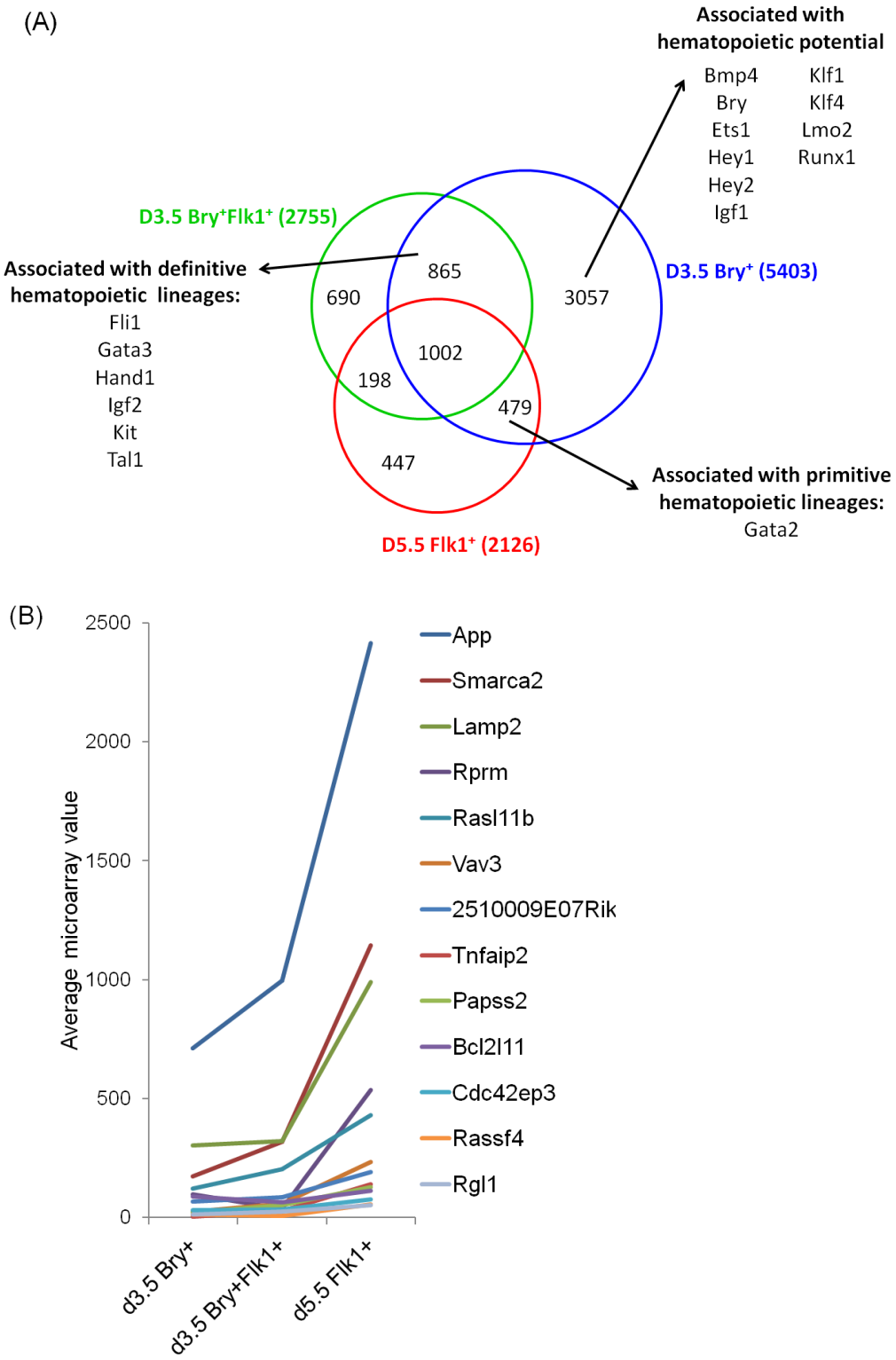

Figure 35. H3K27me3/H2Ak119ub shared targets in the 3 ChIP-seq populations.

(A) List of targets identified by Venn comparison of H3K27me3/H2AK119ub shared targets supporting expected hematopoietic association. (B) H3K27me3/H2AK119ub targets located in sector shared by d3.5 Bry$^+$ and d3.5 Bry$^+$Flk1$^+$ ChIP-seq, that have increased expression in d5.5 Flk1+ population according to microarray of the 3 cell populations.

(A)

	D3.5 Bry$^+$	D3.5 Bry$^+$Flk1$^+$	D5.5 Flk1$^+$
Hoxb8	Y	Y	Y
Hoxc13	Y	Y	-
Hoxa9	Y	-	-
Hoxa5	Y	-	-
Hoxb4	Y	-	-
Hoxa7	-	-	-
Hoxb1	-	-	-

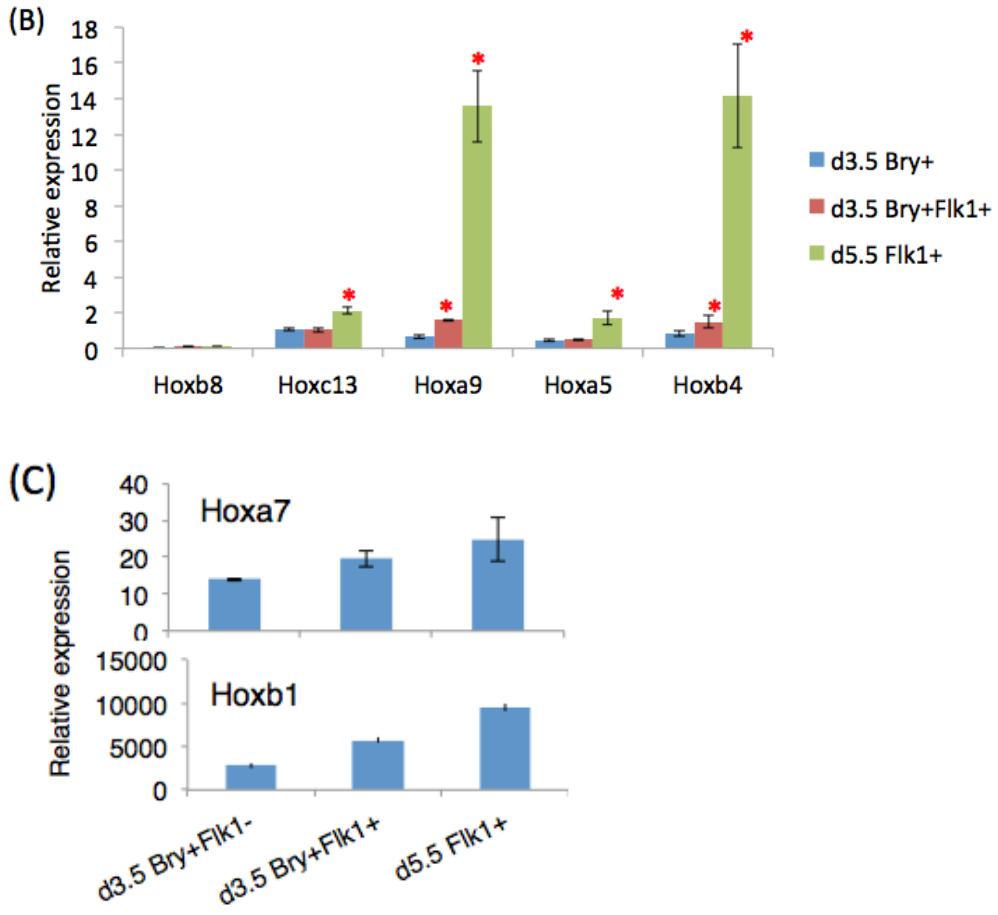

Figure 36. Validation of selected H3K27me3/H2AK119ub Hox targets.
(A) List of selected H3K27me3/H2AK119ub Hox targets, listed by presence of histone mark. (Y): targeted by H3K27me3/ H2AK119ub in sample population; (-): not targeted. (B) QPCR of repressed Hox genes. (C) Non-targeted *Hoxa7* and *Hoxb1* have high expression levels in all 3 ChIP populations. Expression levels relative to *β-actin*.

(A)

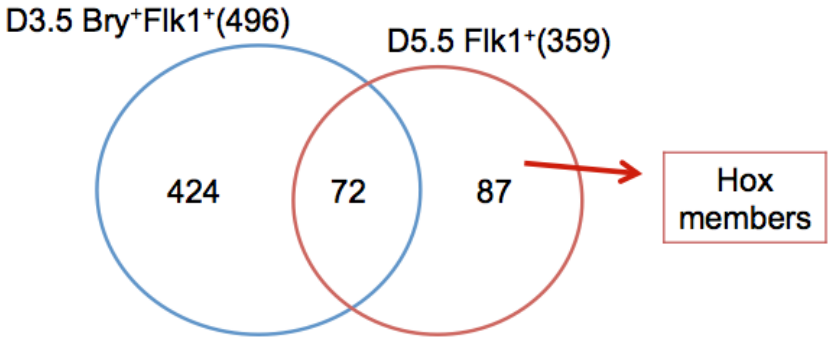

(B)

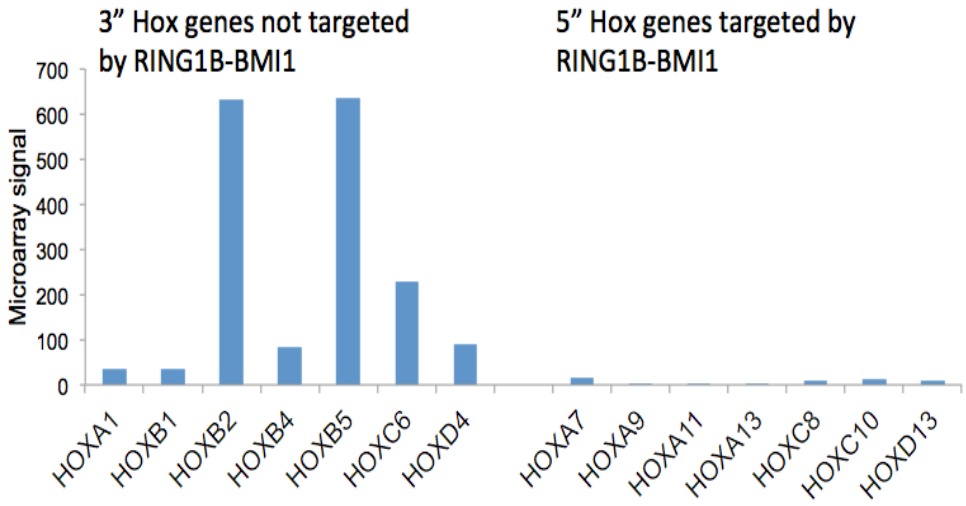

Figure 37. Validation of 5' Hox genes targeted by RING1B-BMI1.
(A) Venn comparison of RING1B-BMI1 targets in d3.5 Bry$^+$Flk1$^+$ and d5.5 Flk1$^+$ ChIP-seq. (B) Average DNA microarray signal of selected 3' vs. 5' Hox genes in d5.5 Flk1$^+$ population.

5.2.2 RING1B-PCGF complexes are functionally distinct, yet operate jointly

The composition of PRC1 is dynamic and displays non-redundancy between paralogous members of the CBX and PCGF families, leading to the formation of PRC1 variants that are functionally distinct, with activity and binding targets depending on the cell state and environment[172,174]. Hence, following validation of the ChIP-seq data, we sought to determine whether RING1B-PCGF pairs regulate specific lineages and targets during hematopoietic specification.

MACs analysis identified shared targets of RING1B and PCGF homologues in d3.5 Bry^+Flk1^+ ChIP-seq that overlap by > 1 bp. Gene Ontology (GO) analysis of these targets (tables 6-9) suggests that RING1B-BMI1 regulates neuronal lineages, while RING1B-PCGF5 is involved in regulating a number of mesodermal lineages. RING1B-MEL18 does not appear to regulate any particular lineage, suggesting that MEL18 may not be a major PRC1 member during this period.

Comparison of genes targeted by RING1B-PCGF in d3.5 Bry^+Flk1^+ cells showed that target overlaps between RING1B-PCGF pairs ranged from 27% (RING1B-BMI1) to 61% (RING1B-MEL18), indicating varying levels of redundancy between PCGF homologues, with BMI1 displaying the least redundancy (fig. 38A). Further analysis identified a subset that is targeted only by RING1B-PCGF5, but not RING1B-BMI1 or RING1B-MEL18. Dkk1, a Wnt antagonist, and p63, which suppresses Notch signaling in mouse keratinocytes[282], are uniquely targeted by RING1B-PCGF5 in d3.5 Bry^+Flk1^+ ChIP-seq (fig. 38A). DNA microarray of the 2 $Flk1^+$ populations showed that both *Dkk1* and *p63* are repressed in the d3.5 Bry^+Flk1^+ population (fig. 38B),

albeit only slightly for *Dkk1*, which was more highly expressed in the d3.5 Bry^+ population (data not shown). As the Wnt/ Notch signaling pathway is an essential system in hematopoiesis, we were keen to identify if PCGF5 uniquely mediated PRC1 regulation of Dkk1 and p63. ChIP-qPCR of Dkk1 and p63 in d3.5 Bry^+Flk1^+ and d5.5 $Flk1^+$ populations validated the binding of PCGF5 to the 2 targets in the former population. P63 was released from repression by PCGF5 in the later d5.5 $Flk1^+$ population (fig. 38C), corresponding to the increase in *p63* expression (fig 38B). However, Dkk1 was instead targeted by BMI1 (fig. 38C), resulting in a strong repression of its gene expression as shown by microarray (fig. 38B). This suggests that PCGF homologues may regulate targets either independently or in a coordinated manner.

Hence we provide evidence that PRC1 variants are functionally distinct, by identifying that RING1B-BMI1 targets neural lineages, while RING1B-PCGF5 targets mesodermal lineages in d3.5 Bry^+Flk1^+ cells. MEL18 binding has greater redundancy, suggesting a minor role in PRC1 activity. We also identify the joint regulation of Dkk1 by BMI1 and PCGF5 in a temporal manner, suggesting that PRC1 variants are coordinately involved in epigenetic regulation.

Overlap pairs	GO term	# genes	P-value
RING1B/BMI1	behavior	46	1.06E-06
	learning	24	1.06E-06
	development of body axis	34	9.85E-06
	contextual conditioning	10	1.11E-05
	conditioning	15	1.19E-05
	concentration of norepinephrine	8	2.88E-05
	proliferation of cells	78	3.11E-05
	development of sensory organ	28	3.32E-05
	clonal expansion of fibroblast cell lines	3	3.73E-05
	pathfinding of axons	3	3.73E-05
RING1B/PCGF5	hematologic cancer	5	1.88E-04
	growth of connective tissue	2	2.49E-04
	abnormal morphology of diencephalon	3	4.12E-04
	abnormal morphology of limb bud	3	4.12E-04
	lymphohematopoietic cancer	7	4.82E-04
	hematological neoplasia	7	5.25E-04
	morphogenesis of embryonic limb	4	7.45E-04
	development of female reproductive tract	5	9.07E-04
	proliferation of bone marrow cell lines	4	1.06E-03
	tumorigenesis of melanoma	3	1.07E-03
RING1B/MEL18	release of lipid	6	2.69E-05
	behavioral flexibility	2	4.75E-05
	neurotransmission	10	4.76E-05
	apoptosis of enterocytes	3	6.79E-05
	behavior	19	6.94E-05
	synaptic transmission of cells	6	1.39E-04
	volume of lung tumor	2	1.42E-04
	cell death of intestinal cells	4	1.48E-04
	translocation of vesicles	2	2.83E-04
	replication of Vaccinia virus WR	2	4.69E-04

Table 6. GO analysis of RING1B/ PCGF targets from d3.5 Bry+Flk1+ ChIP-seq.

Associated Network Functions	Network Score
Cardiovascular System Development and Function, Cellular Development, Cellular Growth and Proliferation	45
Cellular Movement, Cancer, Cell Death and Survival	41
Organ Morphology, Skeletal and Muscular System Development and Function, Connective Tissue Development and Function	22
Nervous System Development and Function, Organ Morphology, Embryonic Development	16
Cancer, Cell Death and Survival, Connective Tissue Disorders	16

Diseases and Disorders	p-value	#molecules
Cardiovascular Disease	1.02E-03	25
Organismal Injury and Abnormalities	1.02E-03	21
Developmental Disorder	1.23E-03	40
Hereditary Disorder	1.33E-03	3
Ophthalmic Disease	1.33E-03	3

Physiological System Development and Function	p-value	#molecules
Behavior	1.06E-06	53
Embryonic Development	9.85E-06	67
Organismal Development	9.85E-06	86
Organ Development	3.32E-05	59
Tissue Development	3.32E-05	86

Table 7. Top biological networks and pathways associated with RING1B-BMI1 target genes.
RING1B ChIP-seq peaks were identified with DFilter and overlapped with BMI1 ChIP-seq in D3.5 $Bry^{+}Flk1^{+}$ cells, and IPA was used to generate the list of networks associated with its biological, molecular and cellular functions. The network score is used to rank networks according to their degree of relevance to the network-eligible molecules in the dataset.

Associated Network Functions	Network Score
Cellular Development, Connective Tissue Development and Function, Cell Cycle	24
Cellular Development, Cellular Growth and Proliferation, Hematological System Development and Function	17
Cellular Compromise, Organ Morphology, Skeletal and Muscular System Development and Function	17
Embryonic Development, Organ Development, Organismal Development	2
Cellular Movement, Cell Signaling, Post-Translational Modification	2

Diseases and Disorders	p-value	#molecules
Cancer	1.88E-04	12
Hematological Disease	1.88E-04	9
Infectious Disease	2.20E-03	3
Neurological Disease	3.65E-03	8
Organismal Injury and Abnormalities	3.95E-03	8

Physiological System Development and Function	p-value	#molecules
Tissue Development	2.94E-04	22
Nervous System Development and Function	4.12E-04	16
Organ Morphology	4.12E-04	20
Tissue Morphology	4.12E-04	22
Embryonic Development	7.45E-04	22

Table 8. Top biological networks and pathways associated with RING1B-PCGF5 target genes.
RING1B ChIP-seq peaks were identified with DFilter and overlapped with PCGF5 ChIP-seq in D3.5 $Bry^{+}Flk1^{+}$ cells, and IPA was used to generate the list of networks associated with its biological, molecular and cellular functions. The network score is used to rank networks according to their degree of relevance to the network-eligible molecules in the dataset.

Associated Network Functions	Network Score
Tissue Morphology, Cellular Development, Cellular Growth and Proliferation	30
Cellular Function and Maintenance, Cellular Growth and Proliferation, Digestive System Development and Function	14
Gastrointestinal Disease, Hepatic System Disease, Liver Fibrosis	12
Hematological System Development and Function, Inflammatory Response, Tissue Morphology	12
Cell-To-Cell Signaling and Interaction, Nervous System Development and Function, Drug Metabolism	10

Diseases and Disorders	p-value	#molecules
Cancer	1.42E-04	12
Respiratory Disease	1.42E-04	22
Infectious Disease	4.69E-04	2
Inflammatory Response	5.64E-04	6
Neurological Disease	4.10E-03	6

Physiological System Development and Function	p-value	#molecules
Behavior	4.75E-05	20
Nervous System Development and Function	4.76E-05	27
Tumor Morphology	1.42E-04	9
Cardiovascular System Development and Function	4.69E-04	18
Tissue Development	7.00E-04	30

Table 9. Top biological networks and pathways associated with RING1B-MEL18 target genes.
RING1B ChIP-seq peaks were identified with DFilter and overlapped with MEL18 ChIP-seq in D3.5 $Bry^{+}Flk1^{+}$ cells, and IPA was used to generate the list of networks associated with its biological, molecular and cellular functions. The network score is used to rank networks according to their degree of relevance to the network-eligible molecules in the dataset.

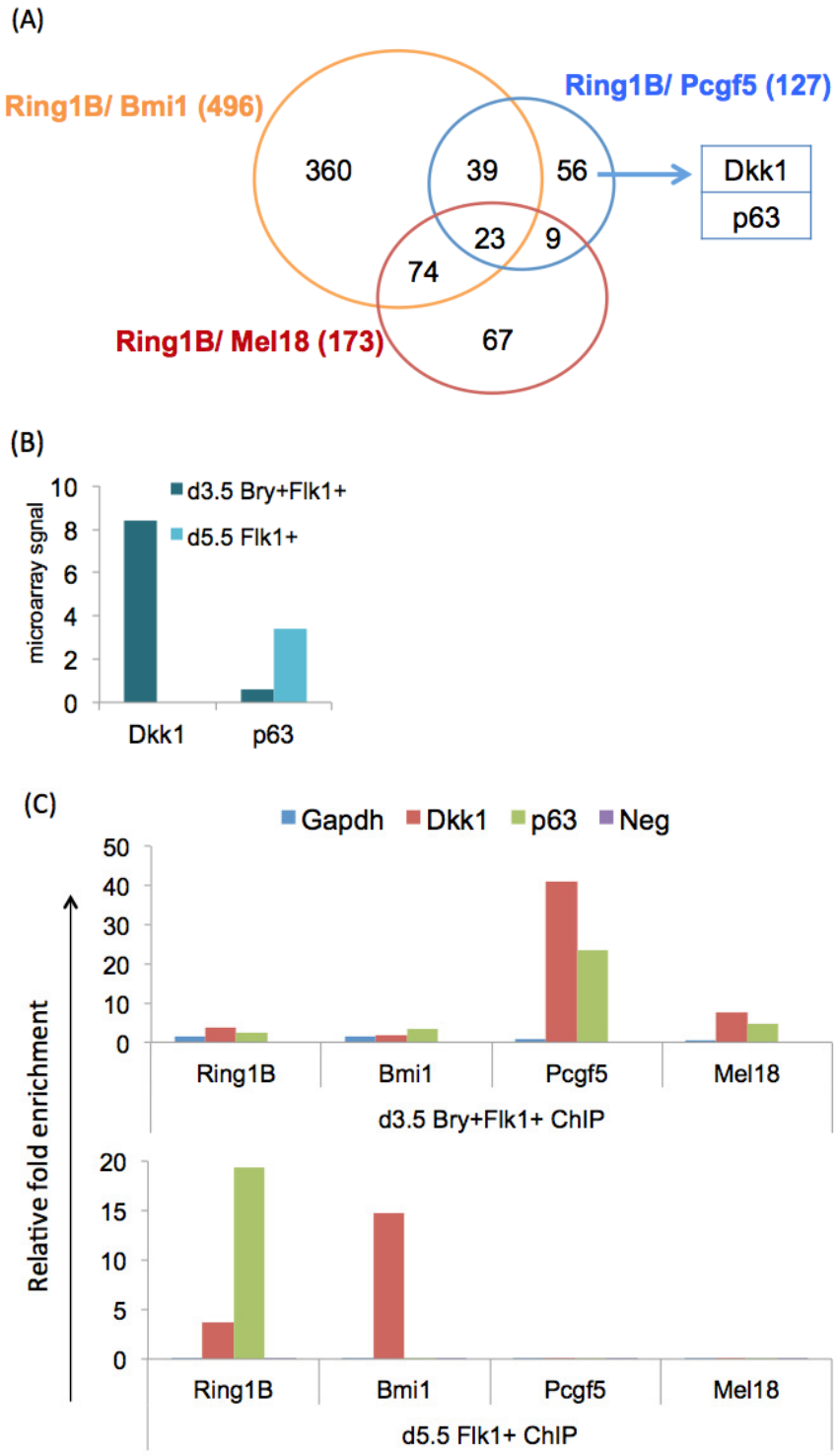

Figure 38. Dynamic regulation of Dkk1 and p63 by PRC1 variants.
(A) Venn comparisons of RING1B/ PCGF targets from d3.5 Bry^{+}Flk1^{+} ChIP-seq. (B) DNA microarray signal of Dkk1 and p63 in d3.5 Bry^{+}Flk1^{+} and reaggregated d5.5 Flk1^{+} populations. (C) ChIP-qPCR of Dkk1 and p63 in d3.5 Bry^{+}Flk1^{+} and d5.5 Flk1^{+} populations. Results calculated from average results of 3 technical replicates.

5.2.3 Ring1B-independent function of Pcgf5

Analysis of the level of peak association between RING1B and PCGF homologues indicate that while many targets of BMI1 and MEL8 overlap with that of RING1B, the same is not so for PCGF5 targets (fig. 39A). This supports the lack of PCGF5 binding to RING1B observed in previous co-IP experiments (fig. 28B). Analysis of targets bound to both PCGF and H2AK119ub but not RING1B showed that while the majority of BMI1-H2AK119ub targets co-bound to RING1B, only about half of PCGF5- and MEL18-H2AK119ub targets did the same (fig. 39B), suggesting that while BMI1 preferentially binds to RING1B, PCGF5 and MEL18 may bind equally to either RING1A or RING1B to form PRC1.

To identify if there is a RING1B-independent function of PCGF5, we performed GO analysis which showed that whilst RING1B-PCGF5 shared targets are associated with mesodermal development such as hematopoietic and skeletal-muscular development; RING1B-independent PCGF5 targets, whilst still associated with mesoderm in the form of cardiovascular development, are additionally associated with metabolic processes such as protein synthesis and lipid metabolism (Table 10). The top 10 RING1B-independent PCGF5 targets (Table 11) span a variety of lineages and processes. Microarray signal of these targets in d3.5 $Bry^{+}Flk1^{+}$ cells are mostly low, while non-targeted Bry displays a high microarray signal. This validates the hypothesis that PCGF5 is involved in repression. However, cross-reference of these 10 targets with H3K27me3 and H2AK119ub ChIP-seq data in the same d3.5 $Bry^{+}Flk1^{+}$ population identified that only Cdh8 and Tbc1d30 are targeted by H3K27me3, and Lrrn3 and Dbpht2 are targeted by

H2AK119ub (Table 11), indicating that other gene regulatory mechanisms are likely to be involved in the control of these targets.

To further identify PRC1-independent roles of PCGF, we identified PCGF targets that were not bound to H3K27me3, H2AK119ub or RING1B (Fig. 40A). Although we cannot currently exclude the contribution of RING1A to this set of targets, we identified 1159 PRC1-independent targets of PCGF5, 48 of which were identified by GO to be hematopoiesis-associated. Comparing the microarray data for each of the three cell populations (d3.5 Bry^+, d3.5 Bry^+Flk1^+ and d5.5 $Flk1^+$), we further shortlisted 13 candidate genes that are more highly expressed in the two hematopoietic populations, compared to the non-hematopoietic d3.5 Bry^+ population (fig. 40B). Future functional characterization of these candidate targets will reveal if they are involved in HSC generation and development.

(A)

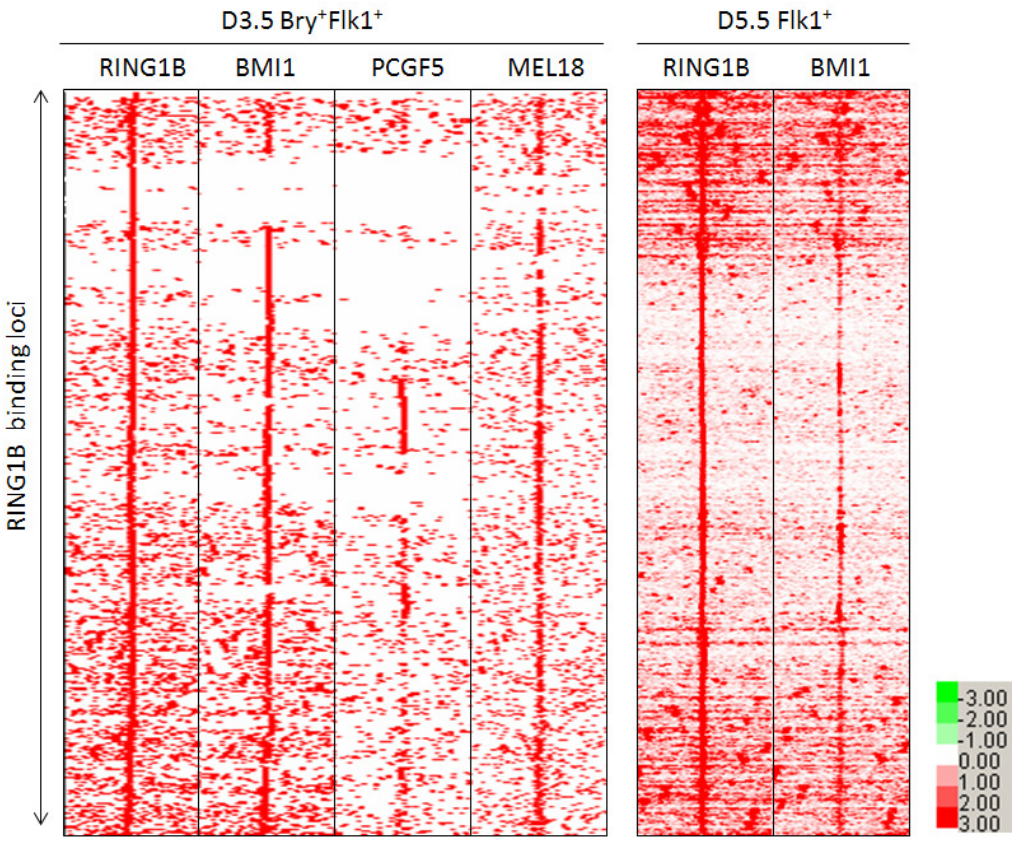

(B)

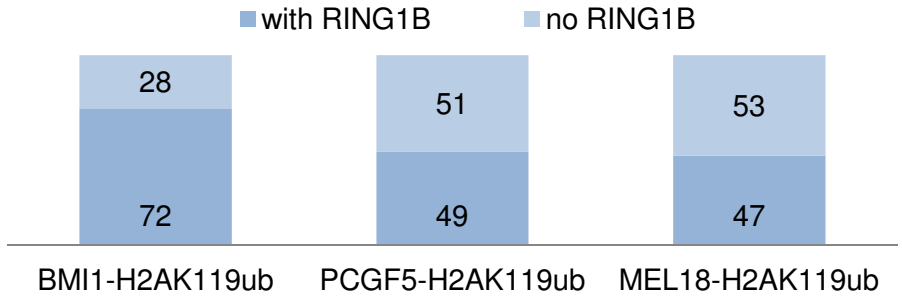

Figure 39. PCGF5 peaks are not strongly associated with RING1B peaks.
(A) Heat map of clustered density matrix showing binding densities of RING1B, BMI1, PCGF5 and MEL18 in the 2 Flk1$^+$ ChIP-seq datasets, clustered according to RING1B binding sites. Each line represents a genomic location of a binding site ± 5-kb. (B) % of PCGF-H2AK119ub targets that co-bind to RING1B.

Associated Network Functions	Network Score
Digestive System Development and Function, Tissue Morphology, Cardiovascular Disease	33
Cellular Development, Gene Expression, Cardiovascular System Development and Function	31
Connective Tissue Disorders, Dermatological Diseases and Conditions, Gastrointestinal Disease	29
Protein Synthesis, Amino Acid Metabolism, Molecular Transport	29
Drug Metabolism, Endocrine System Development and Function, Lipid Metabolism	27

Diseases and Disorders	p-value	#molecules
Connective Tissue Disorders	7.94E-05	57
Metabolic Disease	7.94E-05	25
Developmental Disorder	1.12E-04	69
Skeletal and Muscular Disorders	1.12E-04	51
Cardiovascular Disease	2.41E-04	66

Physiological System Development and Function	p-value	#molecules
Nervous System Development and Function	4.91E-09	268
Behaviour	6.53E-08	147
Cardiovascular System Development and Function	4.73E-07	151
Embryonic Development	4.73E-07	254
Organismal Development	4.73E-07	298

Table 10. Top biological networks and pathways associated with RING1B-independent PCGF5 target genes.
PCGF5 ChIP-seq peaks were identified with DFilter and overlapped with RING1B ChIP-seq in D3.5 $Bry^{+}Flk1^{+}$ cells. IPA was used to generate the list of networks associated with the biological, molecular and cellular functions of targets that do not overlap with RING1B. The network score is used to rank networks according to their degree of relevance to the network-eligible molecules in the dataset.

Gene	Average microarray signal	Function	Targeted by
Il15	10.37	Regulates NKC, T-cell proliferation and activity	-
Fam98a	N.A.	Potential amplification of MAPK activation by EGF	-
Lrrn3	3.3	neuron-related	H2AK119ub
Ndufa4	5097.55	NADH dehydrogenase	-
Gm1140	4.95	No known function	-
Uty	5,1	Histone demethylase	-
Cdh8	3.9	Mediates cell-cell adhesion; strongly expressed in dorsal claustrum	H3K27me3
Tbc1d30	N.A.	GTPase-activating protein	H3K27me3
Nap1l3	9.45	Modulate nucleosome structure & gene expression during brain development	-
Dbpht2	0.3	Exclusively expressed in pituitary from E13.5-15 Downstream of Lhx3, which is critical for early pituitary development.	H2AK119ub
Bry	1338.75	Mesoderm marker	-

Table 11. List of top 10 RING1B-independent PCGF5 target genes.

(A)

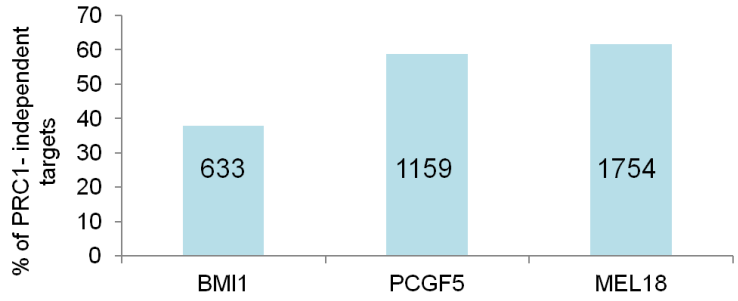

(B)

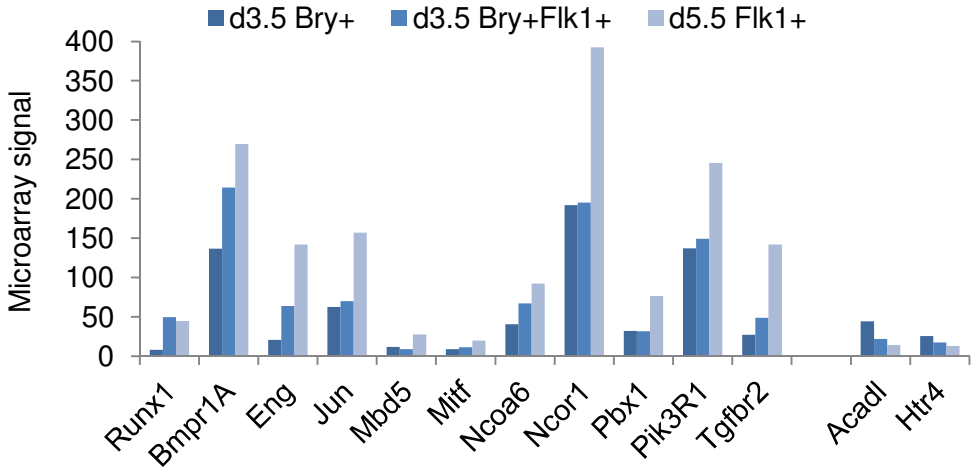

Figure 40. Potential PRC1-independent PCGF targets.
(A) % of PCGF targets that do not simultaneously bind H3K27me3, H2AK119ub or RING1B. Numerals on each bar indicate numbers of PRC1-independent targets in that group. (B) List of PRC1-independent PCGF5 targets that are more highly expressed in hematopoietic populations d3.5 Bry^+Flk1^+ and/or d5.5 $Flk1^+$ compared to d3.5 Bry^+, according to microarray of all three populations.

5.2.4 Potential novel method of RING1B-PCGF recruitment

In *D. melanogaster*, PRC1 is recruited via Polycomb response elements (PREs). PRC1 is also believed to interact with H3K27me3 to recruit PRE-bound complexes to the target gene via intralocus looping. However, equivalent PREs have yet to be identified in mammals[283]. Hence, the mechanism of PRC1 recruitment to target genes has yet to be fully solved.

Analysis of the genomic annotation (fig. 41) and distance of peaks to transcriptional start site (TSS) (fig. 42) from d3.5 $Bry^{+}Flk1^{+}$ ChIP-seq samples indicates that whilst H3K27me3 and H2AK119ub peaks are located proximal to the TSS, the peaks of RING1B and PCGF homologues are spread out across the gene. The distal location of bound RING1B and PCGF suggests that DNA looping is also required to catalyze the H2AK119ub mark near the TSS during this stage. This is further supported by an increase in prevalence of the location of RING1B (71%) and PCGF (64-72%) peaks in intergenic regions, which are known to harbor enhancers[284-285], compared to H3K27me3 (39%) and H2AK119ub (49%) peaks (fig. 41). Enhancers also employ three-dimensional DNA looping to facilitate proximal clustering of the locus control region, which may be located ten of kbs away, to the target promoter[286-287].

Regulatory Sequence Analysis Tools (RSAT) oligo-analysis programme was used to perform *de novo* motif finding based on peaks obtained from each ChIP-seq sample. Shortlisting the top 3 motifs by p-value, we identified a motif (TCCAGA) that was common to RING1B, BMI1 and PCGF5, but not MEL18 (Fig. 43) from d3.5 $Bry^{+}Flk1^{+}$ ChIP-seq data, as well as RING1B and BMI1 from d5.5 $Flk1^{+}$ ChIP-seq data. This motif was found to contribute to 10-20% of ChIP-seq target sequences (Table 12), and has low sequence

similarity to known motifs according to STAMP analysis[288], which performs alignment, similarity and database matching for DNA motifs, suggesting that it is a novel motif that may be involved in PRC1 recruitment (fig. 44). In addition, another motif (CTTTCA) was identified as shared between RING1B, BMI1 and PCGF5 in only d3.5 $Bry^{+}Flk1^{+}$ ChIP-seq. This motif contributed to 8-15% of ChIP-seq target sequences (Table 13), and also does not have high similarity to known motifs (fig. 45).

Hence we identify a potential mode of recruitment of RING1B-PCGF variants to target promoters, involving DNA looping previously observed only in *D. melanogaster* but not yet in mammals.

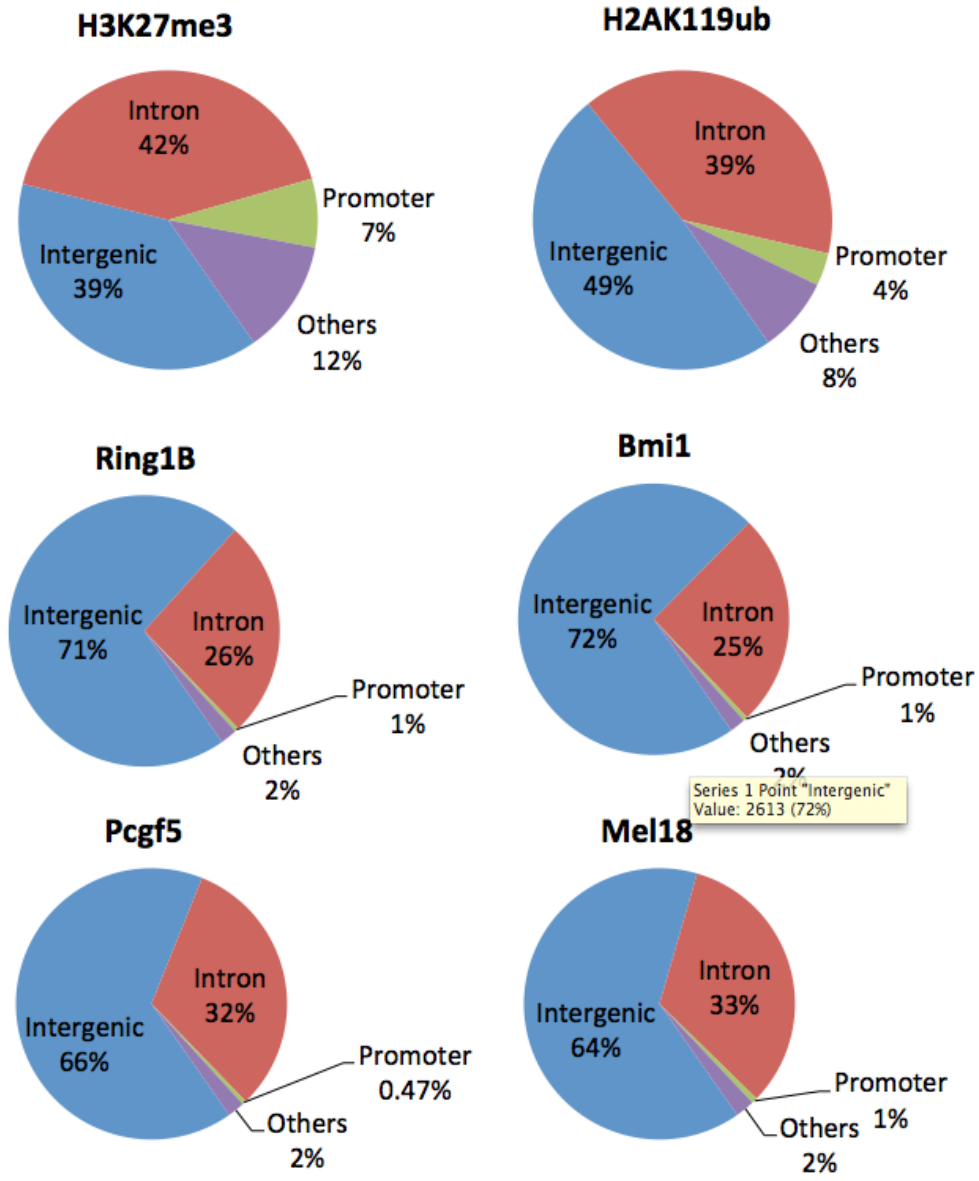

Figure 41. Genomic annotation of d3.5 Bry+Flk1+ ChIP-seq targets. ChIP-seq peaks were annotated based on genomic location using Hypergeometric Optimization of Motif Enrichment (HOMER) software.

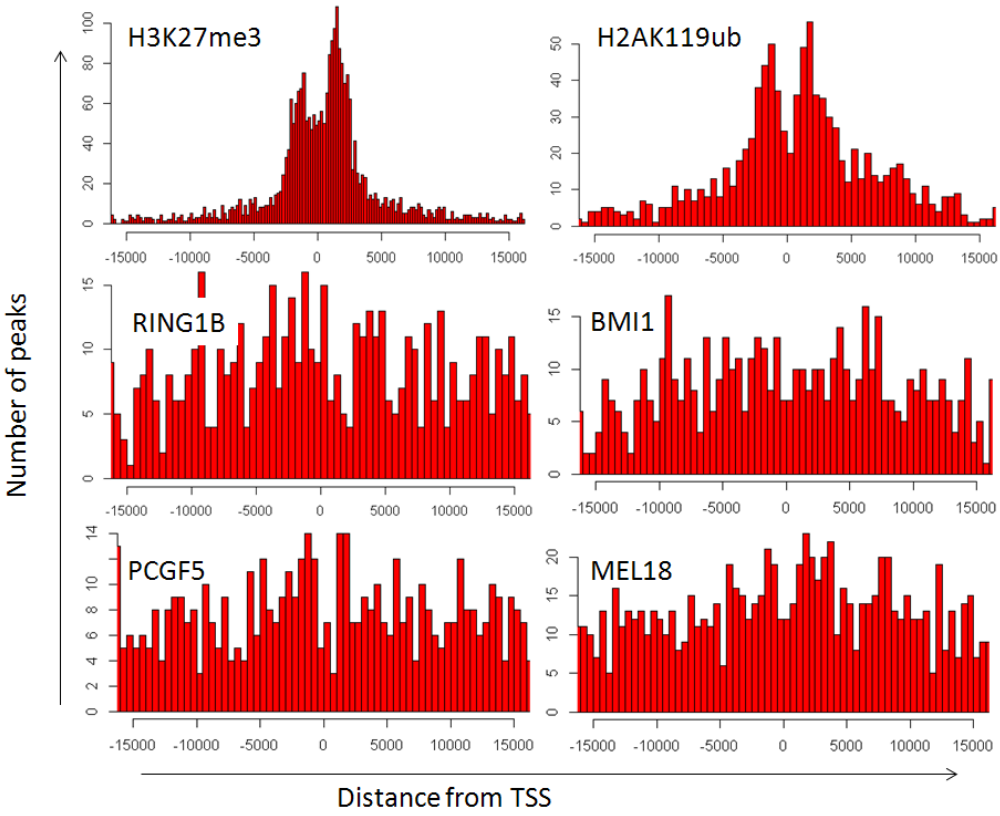

Figure 42. Distance of d3.5 Bry^{+}Flk1^{+} ChIP-seq peaks to TSS.

Sample	ChIP-seq target	Top 3 *de novo* motifs (RSAT)
D3.5 Bry^{+}Flk1^{+}	RING1B	
	BMI1	
	PCGF5	
	MEL18	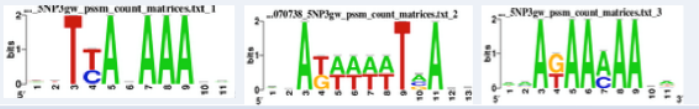
D5.5 Flk1^{+}	RING1B	
	BMI1	

Figure 43. Top 3 de novo motifs identified from RING1B and PCGF homologue ChIP-seq peaks.
RSAT oligo-analysis software was used to perform de novo motif analysis on ChIP-seq data. Motifs are not listed in order.

Population	Target	#sequences	#occurrences	%occurrences
D3.5 Bry^{+}Flk1^{+}	Ring1B	3253	558	17.15%
	Bmi1	3624	409	11.29%
	Pcgf5	2743	283	10.32%
D5.5 Flk1^{+}	Ring1B	4401	892	20.27%
	Bmi1	3700	552	14.92%

Table 12. Rate of occurrence of TCCAGA motif in ChIP-seq samples. Number of times motif TCCAGA appears in ChIP-seq binding sequence identified by HOMER software. %occurrences calculated as a fraction of the total number of binding sequences.

Name	*E value*	*Alignment*	*Motif*
MA0092.1_Hand1_T	1.6690e-05	--TCCAGA-- NWNCCAGAYN	
MA0266.1_ABF2	6.9732e-05	TCCAGA- TCTAGAN	
MA0292.1_ECM22	8.5250e-05	TCCAGA- TCCGGAN	
MA0144.1_Stat3	1.7043e-04	---TCTGGA- CTTCCNGGAA	
MA0380.1_SIP4	3.0006e-04	TCCAGA- YCCGGAN	

Figure 44. STAMP analysis of TCCAGA de novo motif. Identified motif TCCAGA was annotated with JASPAR and TRANSFAC 11.3 databases, using information content trimming >0.4.

Population	Target	#sequences	#occurrences	%occurrences
D3.5 Bry^{+}Flk1^{+}	Ring1B	3253	488	15.00%
	Bmi1	3624	298	8.22%
	Pcgf5	2743	345	12.58%

Table 13. Rate of occurrence of CTTTCA motif in ChIP-seq samples.
Number of times motif CTTTCA appears in ChIP-seq binding sequence identified by HOMER software. %occurrences calculated as a fraction of the total number of binding sequences.

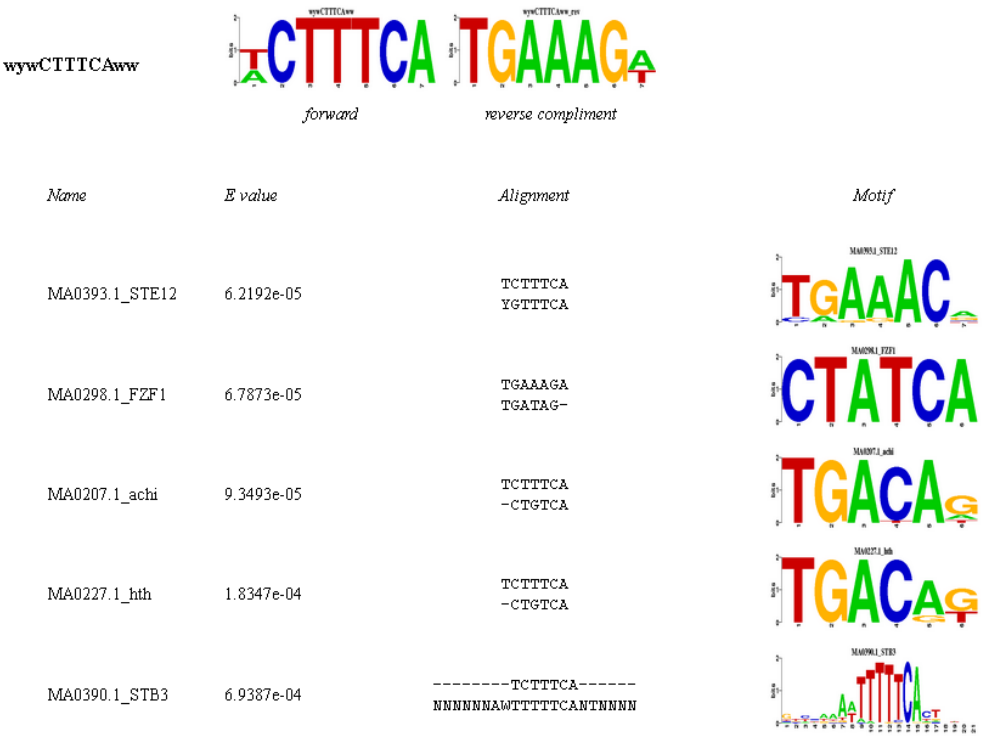

Figure 45. STAMP analysis of CTTTCA de novo motif.
Identified motif CTTTCA was annotated with JASPAR and TRANSFAC 11.3 databases, using information content trimming >0.4.

5.3 SUMMARY & DISCUSSION

In summary, we performed ChIP-sequencing of PRC1 components RING1B, BMI, PCGF5 and MEL18, as well as PRC1 and PRC2 histone marks H2AK119ub and H3K27me3 respectively, in ESC-derived differentiated cell populations that recapitulate YS and P-Sp hematopoiesis. Selected targets for each ChIP-seq were validated by ChIP-qPCR. We identified that a greater number of hematopoietic genes as determined by GO terms were repressed by PRC1 and PRC2, as identified by H3K27me3 and H2AK119ub binding respectively, in populations with less hematopoietic potential. Comparison of RING1B-BMI1 targets across all 3 ChIP-seq populations identified shared as well as unique targets for each population. Notably, several genes uniquely targeted in particular sectors were found to be associated with the expected hematopoietic program of that sector. RING1B-BMI1 was found to target several Hox genes, which are well-known targets of PRC1. The gene expression profiles of several PRC1-targeted Hox genes corresponded to the presence or absence of binding by gene-silencing histone marks H3K27me3 or H2AK119ub. Together, these results provide evidence to support that the ChIP-seq went well, and that functionally accurate data can be derived from it.

DNA microarray further verified the high expression of 3' Hox genes not targeted by RING1B-BMI1, and low expression of 5' Hox genes targeted by RING1B-BMI1 in the reaggregated d5.5 $Flk1^{+}$ population, indicating the likely involvement of the Bmi1-PRC1 complex in Hox gene regulation during P-Sp hematopoiesis. GO analysis of PCGF-RING1B overlapping targets revealed that while BMI-RING1B appears to target neural lineages, PCGF5-RING1B targets mostly mesodermal lineages, while MEL18-RING1B does not appear

to target any particular lineages, indicating that the different PRC1 variants, as differentiated by their partner PCGF subunit, may function simultaneously to regulate various targets or lineages during different stages of development. This was further supported by evidence that while PCGF5 targeting alone regulates *p63* gene expression, both PCGF5 and BMI1 appear to be required to regulate *Dkk1* across YS and P-Sp hematopoietic populations. In addition, the relatively large proportion of PCGF5 targets that do not overlap with RING1B targets suggests that a potential PRC1-independent role of PCGF5 remains to be explored. PRC1-independent binding of BMI1 was previously suggested be involved in induction of DNA damage sites[289], indicating that PRC1-independent functions may be common to PCGF homologues. Finally, evidence that PRC1 components and H2AK119ub/ H3K27me3 bind at different sites, as well as identification of a novel *de novo* motif common to RING1B, BMI1 and PCGF5, suggests that DNA looping may be required to recruit PRC1 for monoubiquitination at targets sites.

Despite canonical knowledge that PRC1 is recruited in response to H327me3, the mechanism of PRC1 recruitment remains a mystery, particularly in mammals. In *D. melanogaster*, the DNA-binding proteins Pleiohomeotic (PHO) and PHO-like (PHOL) recruit PRC1 to the PRE [283,290-291]. Mutation of PHO or PHOL leads to Hox gene silencing defects, while mutation of PHO-binding sites inhibits silencing and dislodges PRC1 from the PRE[292-293], reflecting the requirement of PHO or PHOL for PRE-mediated silencing. However, PHO-binding sites are not sufficient for Polycomb silencing; additional DNA-binding factors such as GAGA factor, Pipsqueak, Zeste, Protein dorsal switch 1 (DSP1), Specificity protein 1 (SP1), Luna and Grainyhead have also been identified, although their involvement *in vivo* has

yet to be verified[167,294,]. On the other hand, in the mammalian system only several recruiters have been proposed. Yin and yang 1 (YY1), a PHO homologue, has been identified as a potential recruiter[295]. However, the limited overlap of YY1 and PRC2 in mouse ESCs suggests that YY1 is not a major recruiter[180]. PRC1 interaction with H3K27me3 has also been proposed to facilitate interlocus looping, allowing the PRE-bound complex to further silence the target locus[283]. Hence, the variety of mechanisms proposed suggests that PRC1 recruitment may be cell- and gene- specific, to allow for greater variation in regulating the more complex mammalian system.

Our identification here of two novel DNA binding motifs shared between RING1B, BMI1 and PCGF5 is a step towards identifying a PRE-like unit in the mammalian system. The shared motif also highlights the potential competition between BMI1 and PCGF5 in PRC1-mediated repression. PCGF homologues are known to have non-redundant functions, with different family members pairing with RING1B exclusively to form distinct PRC1 variants with different targets. Our results suggest an added facet in the form of competition for target binding between PRC1 variants, further substantiating the non-redundancy of PCGF homologues. Validation of the identified motifs and hypothesized method of PRC1 recruitment may be tested in future using methods including Chromosome Conformation Capture (3C), in which chromosomal interactions can be observed and quantified using PCR in cross-linked interacting DNA segments[296-297]; or Chromatin Interaction Analysis by Paired-End Tag Sequencing (ChIA-PET), which incorporates ChIP on top of 3C-type analysis, allowing it to analyze chromatin interactions between specific DNA- or chromatin-interacting proteins[298-299]. However, a major obstacle is the fact that standard protocols for these methods involve

large numbers of cells, which are not feasibly obtained with our current differentiation protocols. Hence, small-scale protocols of these methods will first have to be developed and optimized before we can further elucidate how PRC1 is recruited for epigenetic regulation during hematopoietic development.

The PCGF family is involved in chromatin compaction, similar to the homologous *Psc* family found in *Drosophila.* While PCGFs are almost exclusively studied as part of PRC1, *Psc* is known to function in a PRC1-independent manner, promoting follicle stem cell differentiation by inhibiting self-renewal[300]. From our experiments, we find that a large number of PCGF5 targets do not overlap with RING1B targets. This may be due to several reasons:

1. PCGF5 preferentially interacts with RING1A instead of RING1B
2. PCGF5 has PRC1-independent function

The canonical PRC1 complex contains RING1A/B, which are closely related and have overlapping functions in development[301-302]. However, Gao *et al* suggest that despite this widespread assumption, MEL18 appears to associate preferentially with RING1B, while BMI1 and PCGF5 associate preferentially with RING1A[172]. Despite this finding, numerous previous studies have successfully characterized and validated PRC1 function based on RING1B data alone[173-175]. In line with evidence that PRC1 function may be cell- and tissue- specific, future work including co-IP experiments can further verify if PCGF5 indeed preferentially binds to RING1A during hematopoietic development.

The second hypothesis presents an exciting, novel scenario: that PCGF5, like *Psc*, may have similar PRC1-independent functions. Bmi1 is known to be expressed in intestinal stem cells[303], but similar non-PRC1 associated functions of PRC1 components have yet to be well characterized. Such a study would bring new insight into the role of PCGF homologues, for example whether repression previously attributed to PRC1 may in fact be mediated by RING1B-independent PCGF activity, and if so, how repression is executed. This may involve PCGF-mediated chromatin compaction that is sufficient for gene silencing, or recruitment of other repressors induced by PCGF binding. Alternatively, RING1B-independent PCGF may also be involved in entirely different functions aside from epigenetic regulation.

CHAPTER 6:

CONCLUSION

6.1 Summary & concluding remarks

This thesis focuses on the developmental processes involved in early embryonic hematopoiesis, using both *in vivo* and *in vitro* derived populations. The main conclusions derived from our study are that only a small number of genes distinguish the transcriptome profiles of YS and P-Sp hemangioblast derived colonies, despite their distinct hematopoietic potentials. We also characterized the simultaneous roles of PRC1 variants, including that of novel PCGF5-PRC1, in epigenetic regulation during the transition from YS to P-Sp hematopoiesis. We also identify a potential mechanism for PRC1 recruitment in mammals, previously found only in *D. melanogaster*.

To provide a comprehensive view on the thesis, future work may include studying whether the PRC1 functions and mechanisms identified are similarly active during the developmental period described in part 1 of the thesis, i.e. during development of the YS and P-Sp hemangioblast-derived colonies. Preliminary data indicates that PRC1 components do indeed target Bex6 and selected prolactins in both d3.5 $Bry^{+}Flk1^{+}$ and d5.5 $Flk1^{+}$ populations (Fig. 46A, B). *Bex6* is silenced in both populations according to microarray data (Fig. 46C), which may be explained by the ChIP-seq data that identifies strong PCGF5 binding to Bex6 in the earlier population, and slightly increased binding by BMI1 in the later population. Whether PCGF homologues similarly regulate *Bex6* and other prolactin targets in the same coordinated manner identified in *Dkk1* regulation remains to be identified.

Our results have also thus far identified a correlation between PRC1 targets and transcriptional repression; however, further experiments are required to

validate this relationship. Knockdown of PRC1 components, particularly of PCGF homologues BMI1, PCGF5 and MEL18, in d3.5 $Bry^{+}Flk1^{+}$ and d5.5 $Flk1^{+}$ populations followed by ChIP-seq would verify PRC1 targets identified in our current screen, while that followed by ChIP-qPCR would validate the causal relationship between PRC1 component binding and transcriptional repression of the target.

Whilst the initial goal of my project was to identify key factors important for HSC generation and development, my thesis has turned out to contribute more towards the understanding of PRC1 and its variants, particularly during hematopoietic development. The work described further supports published evidence of the redundancy of PRC1 components, particularly that of PCGF homologues; and further identifies the role of simultaneously active PRC1 variants in regulating targets either independently or in a coordinated manner. While previous work by Tavares *et al*[180] and Gao *et a*[172] raises the question of how PRC1 is recruited, my results provide a potential answer in the form of two *de novo* motifs that may be involved in facilitating a looping mechanism that recruits PRC1 at a location distant from the epigenetically-targeted promoter. Identification of potential chromatin structures using 3C or ChIA-PET, and site-specific mutation of the *de novo* motifs to determine if target binding is affected, are some experiments that can be carried out in future to validate this hypothesis. These results would thus provide long-awaited insight to PRC1 recruitment in the mammalian system.

With newfound insight derived from our results that hematopoietic fate specification may occur much earlier than at day 4 of hemangioblast-derived colony development, we now understand that transcriptome comparison of

earlier embryo-derived colonies (i.e. < day 4) might have yielded a greater number of differentially-expressed genes with greater potency in influencing hematopoietic fate. Indeed, with recent advancements in microfluidics, technologies such as Fluidigm's powerful C1 Single-Cell Auto Prep system[304] can not only track single-colony gene expression profiles from day 0 to day 4 of colony development, but also potentially enable ChIP-seq of PRC1 components in single colonies, providing detailed snapshots of the transcriptome as well as epigenome previously unavailable at the time.

We originally aimed to perform ChIP-seq on all the PCGF homologues, i.e. BMI1, PCGF5 and MEL18, across all three cell populations (d3.5 Bry^+, d3.5 Bry^+Flk1^+ and d5.5 $Flk1^+$). Unfortunately, due to various reasons, including the limiting number of d5.5 $Flk1^+$ cells that could be generated, we were unable to perform PCGF5 and MEL18 ChIP-seq on d3.5 Bry^+ and d5.5 $Flk1^+$ populations, comparisons of which would have yielded great insight into the roles of PCGF5 and its homologues in hematopoietic development. Nonetheless, the current dataset has proven to be biologically relevant and has generated several interesting questions regarding the role of PRC1 and its components in hematopoietic development. Future work aimed at further elucidating the function of PRC1 variants will benefit by building upon the current dataset with PCGF5 and MEL18 ChIP-seq in d5.5 $Flk1^+$ cells, which would allow us to compare RING1B-PCGF targets across the 2 hematopoietic populations recapitulating YS and P-Sp hematopoiesis; as well as RING1A ChIP-seq to fully exclude PRC1 involvement, to better identify and characterize PRC1-independent PCGF function in epigenetic regulation, as well as any potential non-epigenetic roles in hematopoietic development.

The goal of research is ultimately for the benefit of society, whether directly via translation into clinical applications, or indirectly by increasing the pool of knowledge that others may build on. While current results do not yet provide a direct link between *Pcgf5* activity and hematopoietic diseases, it is known that deregulation of BMI1 can affect PRC1-mediated repression, and overexpression of BMI1 is associated with a range of solid tumours including lung, breast, colon and prostate, as well as in malignant hematopoietic cancers[305-307]. Given that PCGF5 is closely related to BMI1 and has high sequence similarity, it is possible that defects in PCGF5 are similarly involved in disease progression. If so, we hope that the insight gained from this work, as well as the novel finding of PCGF5-mediated regulation in hematopoietic development, will eventually benefit patients by improving the diagnosis and treatment of hematopoietic diseases.

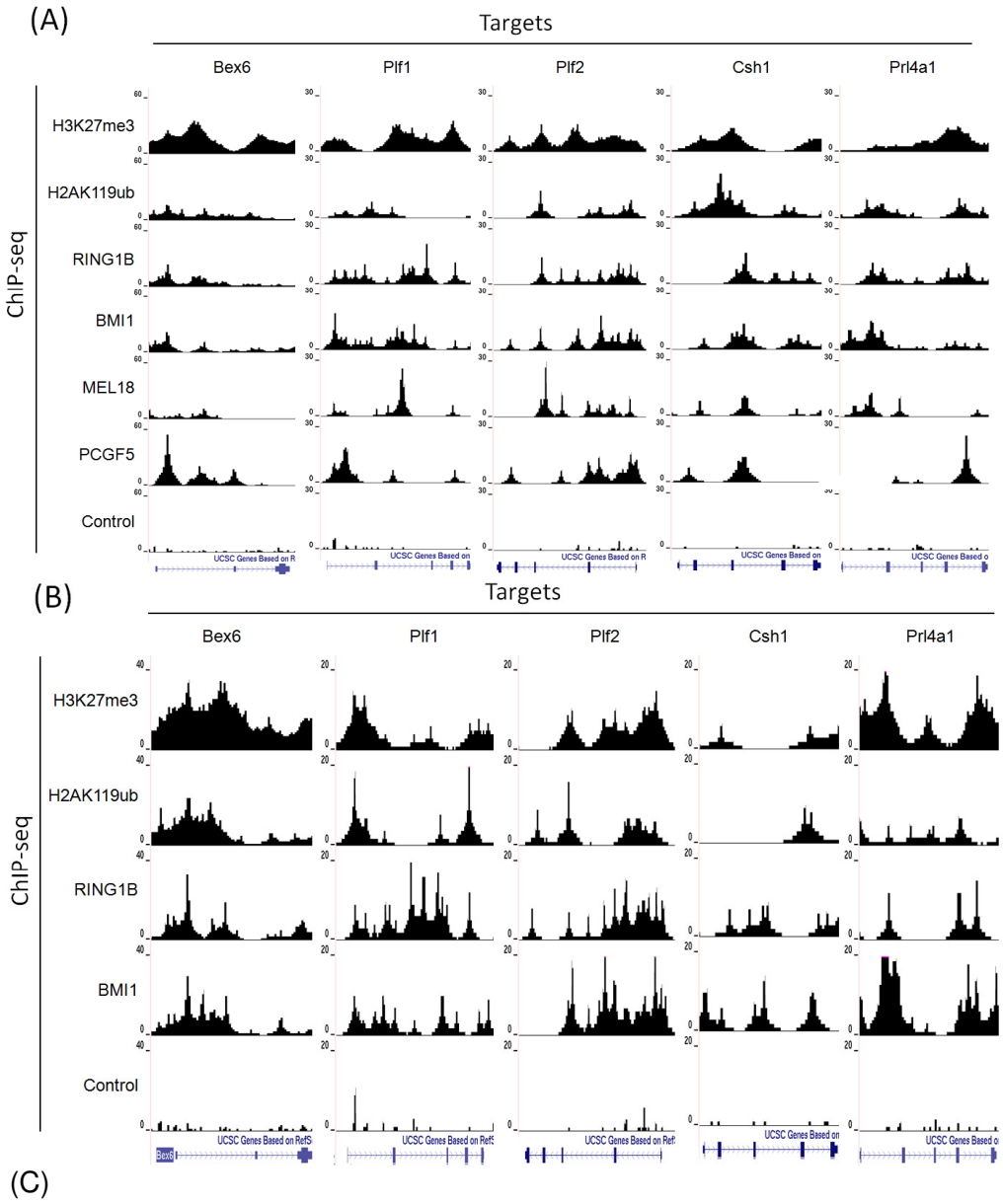

	d3.5 Bry^+Flk1^+	d5.5 $Flk1^+$
Bex6	-	-
Plf1	8.5	6.5
Plf2	19.2	12.15
Csh1	-	-
Prl4A1	6.8	3.1

Figure 46. PRC1 regulation of Bex6 and prolactin targets.
UCSC Genome Browser peak values of Bex6 and selected prolactin targets in (A) d3.5 Bry^+Flk1^+ ChIP-seq and (B) d5.5 $Flk1^+$ ChIP-seq. (C) Average microarray values of Bex6 and selected prolactins in d3.5 Bry^+Flk1^+ and d5.5 $Flk1^+$ populations. (-) indicates no expression value obtained for that gene.

Bibliography

1. Till, J.E. and McCulloch, E.A. A direct measurement of the radiation sensitivity of normal mouse bone marrow cells. *Radiat. Res.* **14**, 213-222 (1961)
2. Harrison, D.E. Competitive repopulation: a new assay for long-term stem cell functional capacity. *Blood* **55**,77-81 (1980)
3. Harrison, D.E., Jordan, C.T., Zhong, R.K., Astle C.M. Primitive hematopoietic stem cells: direct assay of most productive populations by competitive repopulation with simple binomial, correlation and covariance calculations. *Exp. Hematology* **21**, 206-219 (1993)
4. Szilvassy, S.J., Humphries, R.K., Lansdorp, P.M., Eaves, A.C., Eaves, C.J. Quantitative assay for totipotent reconstituting hematopoietic stem cells by a competitive repopulation strategy. *Proc. Natl. Acad. Sci. U.S.A.* **87**, 8736-8740 (1990)
5. Osawa, M.. Hanada, K-I., Hamada, H., Nakauchi, H. Long term lymphohematopoietic reconstitution by a single CD34-low/negative hematopoietic stem cell. *Science* **273**(5272), 242-245 (1996)
6. Spangrude, G.J., Heimfeld, S., and Weissman, I.L. Purification and characterization of mouse hematopoietic stem cells. *Science* **241***,* 58–62 (1988)
7. Baum, C.M., Weissman, I.L., Tsukamoto, A.S., Buckle, A.M., and Peault, B. Isolation of a candidate human hematopoietic stem-cell population. *Proc. Natl. Acad. Sci. U.S.A.* **89(7)**, 2804–2808 (1992)
8. Baron, M.H, Isern, J. and Fraser, S.T. The embryonic origins of erythropoiesis in mammals. *Blood* **119**(21), 4828-4837 (2012)
9. Rosenbauer, F. and Tenen, D.G. Transcription factors in myeloid development: balancing differentiation with transformation. *Nature Reviews Immunology* **7**, 105-117 (2007)
10. Shochat, C. *et al*. Gain-of-function mutations in interleukin-7 receptor-α (IL7R) in childhood acute lymphoblastic leukemias. *J. Exp. Med.* **208**(5), 901-908 (2011)
11. Kondo, M. Lymphoid and myeloid lineage commitment in multipotent hematopoietic progenitors. *Immunol. Rev.* **238**(1), 37-46 (2010)
12. Zhang, C.C., Lodish, H.F. Cytokines regulating hematopoietic stem cell function. *Curr. Opin. Hematol.* **15**(4), 307-311 (2008)
13. Hassan, H.T., Zander, A. Stem cell factor as a survival and growth factor in human normal and malignant hematopoiesis. *Acta. Haematol.* **95**, 257–262 (1996)
14. Kollet, O., Dar, A., Shivtiel, S. *et al*. Osteoclasts degrade endosteal components and promote mobilization of hematopoietic progenitor cells. *Nat. Med.* **12,** 657–664 (2006)
15. Bowie, M.B., Kent, D.G., Copley, M.R., Eaves, C.J. Steel factor responsiveness regulates the high self-renewal phenotype of fetal hematopoietic stem cells. *Blood* **109,** 5043–5048 (2007)
16. Petit-Cocault, L., Volle-Challier, C., Fleury, M. *et al*. Dual role of Mpl receptor during the establishment of definitive hematopoiesis. *Development* **134,** 3031–3040 (2007)
17. Solar, G.P., Kerr, W.G., Zeigler, F.C. *et al*. Role of c-mpl in early hematopoiesis. *Blood* **92**, 4–10 (1998)
18. de Haan, G., Weersig, E., Dontje, B. *et al*. In vitro generation of long-term repopulating hematopoietic stem cells by fibroblast growth factor-1. *Dev. Cell* **4,** 241–251 (2003)

19. Yeoh, J.S., van Os, R., Weersing, E, *et al*. Fibroblast growth factor-1 and 2 preserve long-term repopulating ability of hematopoietic stem cells in serum-free cultures. *Stem Cells* **24,**1564–1572 (2006)
20. Crcareva, A., Saito, T., Kunisato, A. *et al*. Hematopoietic stem cells expanded by fibroblast growth factor-1 are excellent targets for retrovirus-mediated gene delivery. *Exp. Hematol*. **33,** 1459–1469 (2005)
21. Zhang, C.C., Lodish, H.F. Insulin-like growth factor 2 expressed in a novel fetal liver cell population is a growth factor for hematopoietic stem cells. *Blood* **103,** 2513–2521 (2004)
22. Chiba, S. Notch signaling in stem cell systems. **Stem Cells 24,** 2437–2447 (2006)
23. Mancini, S.J., Mantei, N., Dumortier, A. *et al.* Jagged1-dependent Notch signaling is dispensable for hematopoietic stem cell self-renewal and differentiation. *Blood* **105,** 2340–2342 (2005)
24. Bhardwaj, G., Murdoch, B., Wu, D. *et al*. Sonic hedgehog induces the proliferation of primitive human hematopoietic cells via BMP regulation. *Nat. Immunol.* **2**, 172–180 (2002)
25. Pimanda, J.E., Donaldson, I.J., de Bruijn, M.F. *et al*. The SCL transcriptional network and BMP signaling pathway interact to regulate RUNX1 activity. *Proc. Natl. Acad. Sci. USA* **104,** 840–845. (2007)
26. Hogan, B.L. Bone morphogenetic proteins: multifunctional regulators of vertebrate development. *Genes Dev.* **10**, 1580-1594 (1996)
27. Walmsley, M., Ciasu-Uitz, A., Patient, R. Adult and embryonic blood and endothelium derive from distinct precursor populations which are differentially programmed by BMP in Xenopus. *Development* **129**, 5682-5695 (2002)
28. Winnier, G., Blessing, M., Labosky, P.A., Hogan, B.L. Bone morphogenetic protein-4 is required for mesoderm formation and patterning in mouse. *Genes Dev.* **9**, 2105-2116 (1995)
29. Huelsken, J., Vogel, R., Brinkmann, V., Erdmann, B., Birchmeier, C., Birchmeier, W. Requirement for beta-catenin in anterior-posterior axis formation in mice. *J. Cell Biol.* **148**, 567-578 (2000)
30. Kelly, O.G., Pinson, K.I., Skarnes, W.C. The Wnt co-receptors Lrp5 and Lrp6 are essential for gastrulation in mice. *Development* **131**, 2803-2815 (2004)
31. Liu, P., Wakamiya, M., Shea, M.J., Albrecht, U., Behringer, R.R., Bradley, A. Requirement for Wnt3 in vertebrate axis formation. *Nat. Genet.* **22**, 361-365 (1999)
32. Lengerke, C., Schmitt, S., Bowman, T.V., Jang, I.H., Maouche-Chretien, L., McKinney-Freeman, S., Davidson A.J., Hammerschmidt, M., Rentzsch, F., Green, J.B.A., Zon, L.I., Daley, G.Q. BMP and Wnt specify hematopoietic fate by activation of the *Cdx-Hox* pathway. *Cell Stem Cell* **2(1)**, 72-82 (2008)
33. Moore, M.A., Metcalf, D. Ontogeny of the haematopoietic system: yolk sac origin of *in vitro* and *in vivo* colony forming cells in the developing mouse embryo. *Br. J. Haematol.* **18**, 279-296 (1970)
34. Kispert, A. and Hermann, B.G. The Bracyhury gene encodes a novel DNA binding protein. *EMBO J.* **12**, 4898-4899 (1993)
35. Kispert, A. and Hermann, B.G. Immunohistochemical analysis of the Brachury protein in wild-type and mutant mouse embryos. *Dev. Biol*. **161**, 179-193 (1994)
36. Yamaguchi, T.P. *et al.* Flk1, a flt-related receptor tyrosine kinase is an early marker for endothelial cell precursors. *Development* **118**, 489-498 (1993)

37. Palis, J., McGrath, K.E. and Kingsley, P.D. Initiation of hematopoiesis and vasculogenesis in murine yolk sac explants. *Blood* **86**, 156-163 (1995)
38. Kabrun, N., Bühring H, Choi K, Ullrich A, Risau W, Keller G. Flk-1 expression defines a population of early embryonic hematopoietic precursors. *Development* **124**, 2039-2048 (1997)
39. Lugus, J.J., Parc, C., Ma, Y.D., Choi, K. Both primitive and definitive blood cells are derived from Flk1^{+} mesoderm. *Blood* **113**, 563-566 (2009)
40. Shalaby, F. *et al*. Failure of blood-island formation and vasculogenesis in Flk1-deficient mice. *Nature* **376**, 62-66 (1995)
41. Martin, B.L. and Kimelman, D. Regulation of canonical Wnt signaling by Brachyury is essential for posterior mesoderm formation. *Developmental Cell* **15**, 121-133 (2008)
42. Murray, P.D.F. The development in vitro of the blood of the early chick embryo. *Proc. R. Soc. Lond. B Biol. Sci.* **111**, 497–521 (1932)
43. Haar, J.L., and Ackerman, G.A. A phase and electron microscopic study of vasculogenesis and erythropoiesis in the yolk sac of the mouse. *Anat. Rec.* **170**, 199–223 (1971)
44. Cumano, A., Dieterlen-Lievre, F., Godin, I. Lymphoid potential, probed before circulation in mouse, is restricted to caudal intraembryonic splanchnopleura. *Cell* **86**, 907-916 (1996)
45. Palis J, Kennedy M, Robertson S, Wall C, Keller G. Development of erythroid and myeloid progenitors in the yolk sac and embryo proper of the mouse embryo. Development **126**, 5073-5084 (1999)
46. Young, P.E., Baumhueter, S., Lasky, L.A. The sialomucin CD34 is expressed on hematopoietic cells and blood vessels during murine development. *Blood* **85**, 96-105 (1995)
47. Takakura, N., Huang X., Naruse, T., Hamaguchi, I., Dumont, D.J., Yancopoulos, G.D., Suda, T. Critical role of the TIE2 endothelial cell receptor in the development of definitive hematopoiesis. *Immunity* **9**, 677-686 (1998)
48. Kallianpur, A.R., Jorda, J.E., Brandt, S.J. The SCL gene is expressed in progenitors of both the hematopoietic and vascular systems during embryogenesis. *Blood* **83**, 1200-1208 (1994)
49. Robertson, S.M., Kennedy, M. Shannon, J.M., Keller, G. A transitional stage in the commitment of mesoderm to hematopoiesis requiring the transcription factor SCL/tal-1. *Development* **127**, 2447-2459 (2000)
50. Orkin, S. GATA-binding transcription factors in hematopoietic stem cells. *Blood* **80**, 575-581 (1992)
51. Huber, T., Kouskoff, V., Fehling, H.J., Palis, J., Keller, G. Haemangioblast commitment is initiated in the primitive streak of the mouse embryo. *Nature* **432**, 625-630 (2004)
52. Dzierzak, E. and Speck, N.A. Of lineage and legacy: the development of mammalian hematopoietic stem cells. *Nature Immunology* **9**(2), 129-136 (2008)
53. Robin, C. *et al.* Human placenta is a potent hematopoietic niche containing hematopoietic stem and progenitor cells throughout development. *Cell Stem Cell* **5**, 385-395 (2009)
54. McGann, J.K., Silver, L., Liesveld, J., Palis, J. Erythropoietin-receptor expression and function during the initiation of murine yolk sac erythropoiesis. *Exp. Hematology* **25**, 1149-1157 (1997)
55. Leder, A., Kuo, N., Shen, M.M., Leder, P. *In situ* hybridization reveals co-expression of embryonic and adult α globin genes in the earliest murine erythrocyte progenitors. *Development* **116**, 1041–1049 (1992)

56. Choi, K., Kennedy, M., Kazarov, A., Papdimitriou, J.C., Keller, G. A common precursor for hematopoietic and endothelial cells. *Development* **125**, 725-732 (1998)
57. McGrath, K.E. and Palis, J. Hematopoiesis in the yolk sac: more than meets the eye. *Exp. Hematology* **33**, 1021-1028 (2005)
58. Wong, P.M.C., Chung, S-H., Reicheld, S.M., Chui, D.H.K. Hemoglobin switching during murine embryonic development: evidence for two populations of embryonic erythropoietic progenitor cells. *Blood* **67**, 716–721 (1986)
59. Takahashi, K., Yamamura, F., Naito, M. Differentiation, maturation, and proliferation of macrophages in the mouse yolk sac**.** *Journal of Leukocyte Biology* **45**, 87 (1989)
60. Gory-Faure, S., Prandini, M.H., Pointu, H. et al. Role of vascular endothelial-cadherin in vascular morphogenesis. *Development* **126**, 2093–2102 (1999)
61. Rampon, C., Huber, P. Multilineage hematopoietic progenitor activity generated autonomously in the mouse yolk sac: analysis using angiogenesis-defective embryos. *Int. J. Dev. Biol.* **47**, 273–280 (2003)
62. Yoder, M.C., Hiatt, K. Engraftment of embryonic hematopoietic cells in conditioned newborn recipients. *Blood* **86**(6), 2176-2183 (1997)
63. Godin, I., Garcia-Porrero, J.A., Dierterlen-Lievre, F., Cumano, A. Stem cell emergence and hematopoietic activity are incompatible in mouse intraembryonic sites. *J. Exp. Med.* **190**(1), 43-52 (1999)
64. Godin, I., Dierterlen-Lievre, F., Cumano, A. Emergence of multipotent hematopoietic cells in the yolk sac and paraaortic splanchnopleura in mouse embryos, beginning at 8.5 days postcoitus. *Proc. Natl. Acad. Sci. U.S.A.* **92**(3), 773-777 (1995)
65. Lancrin, C., Sroczynska, P., Stephenson, C., Allen, T., Kouskoff, V., Lacaud, G. The haemangioblast generates haematopoietic cells through a haemogenic endothelium stage. *Nature* **457**(7231), 892-895 (2009)
66. Eilken, H.M., Nishikawa, S., Schroeder, T. Continuous single-cell imaging of blood generation from haemogenic endothelium. *Nature* **457**(7231), 896-900 (2009)
67. Soriano, R. Generalized *lacZ* expression with the ROSA26 Cre reporter strain. *Nature Genetics* **21**, 70-71 (1999)
68. Chen, M.J., Yokomizo, T., Zeigler, B.M., Dzierzak, E., Speck, N.A. Runx1 is required for the endothelial to hematopoietic cell transition but not thereafter. *Nature* **457**, 887-891 (2009)
69. Ema, H., Nakauchi, H. Expansion of hematopoietic stem cells in the developing liver of a mouse embryo. *Blood* **95**, 2284-2288 (2000)
70. Gekas, C., Dieterlen-Lievre, F., Orkin, S. H., Mikkola, H. K. The placenta is a niche for hematopoietic stem cells. *Dev. Cell* **8**, 365-375 (2005)
71. Morrison, S. J., Hemmati, H. D., Wandycz, A. M., Weissman, I. L. The purification and characterization of fetal liver hematopoietic stem cells. *Proc. Natl. Acad. Sci. U.S.A.* **92**, 10302-10306 (1995)
72. Cumano, A., Godin, I. Ontogeny of the hematopoietic system. *Ann. Rev. Immunol.* **25**, 745-785 (2007)
73. Harrison, D. E., Zhong, R. K., Jordan, C. T., Lemischka, I. R., Astle, C. M. Relative to adult marrow, fetal liver repopulates nearly five times more effectively long-term than short-term. *Exp. Hematology* **25**, 293-297 (1997)
74. Rebel, V. I., Miller, C. L., Eaves, C. J., Lansdorp, P. M. The repopulation potential of fetal liver hematopoietic stem cells in mice exceeds that of their liver adult bone marrow counterparts. *Blood* **87**, 3500-3507 (1996)

75. McGrath, K.E. *et al*. A transient definitive erythroid lineage with unique regulation of the β-globin locus in the mammalian embryo. *Blood* **117**(17), 4600-4608 (2011)
76. Martin, M.A. & Bhatia, M. Analysis of the human fetal liver hematopoietic microenvironment. *Stem Cells & Dev.* **14**, 493-504 (2005)
77. Chou, S., Lodish, H.F. Fetal liver hepatic progenitors are supportive stromal cells for hematopoietic stem cells. *Proc. Natl. Acad. Sci. U.S.A.* **107**(17), 7799-7804 (2010)
78. Kim, I., Saunders, T.L., Morrison, S.J. Sox17 dependence distinguishes the transcriptionial regulation of fetal from adult hematopoietic stem cells. *Cell* **130**, 470-483 (2007)
79. He, S., Kim, I., Lim, M.S., Morrison, S.J. Sox17 expression confers self-renewal potential and fetal stem cell characteristics upon adult hematopoietic progenitors. *Genes and Dev.* **25**, 1613-1627 (2011)
80. Alvarez-Silva, M., Belo-Diabangouaya, P., Salaun, J. and Dieterlen-Lievre, F. Mouse placenta is a major hematopoietic organ. *Development* **130**, 5437-5444 (2003)
81. Ottersbach, K., Dzierzak, E. The murine placenta contains hematopoietic stem cells within the vascular labyrinth region. *Developmental Cell* **8**, 377-387 (2005)
82. Kallianpur, A.R., Jordan, J.E., Brandt, S.J. The SCL/TAL-1 gene is expressed in progenitors of both the hematopoietic and vascular systems during embryogenesis. *Blood* **83**, 1200-1208 (1994)
83. Muroyama, Y., Fujiwara, Y., Orkin, S.H., Rowitch, D.H. Specification of astrocytes by bHLH protein SCL in a restricted region of the neural tube. *Nature* **438**, 360-363 (2005)
84. Visvader, J.E., Fujiwara, Y., Orkin, S.H. Unsuspected role for the T-cell leukemia protein SCL/tal-1 in vascular development**.** *Genes Dev*. **12,** 473-479 (1998)
85. Robb, L., Lyons, I., Li, R., Hartley, L., Kontgen, F,, Harvey, R.P., Metcalf, D., Begley, C.G. Absence of yolk sac hematopoiesis from mice with a targeted disruption of the scl gene. *Proc. Natl. Acad. Sci. USA* **92,** 7075-7079 (1995)
86. Shivdasani, R.A., Mayer, E.L., Orkin, S.H. Absence of blood formation in mice lacking the T-cell leukaemia oncoprotein tal-1/SCL. *Nature* **373,** 432-434 (1995)
87. Shivdasani, R.A., Mayer, E.L., Orkin, S.H. Absence of blood formation in mice lacking the T-cell leukaemia oncoprotein tal-1/SCL. *Nature* **373,** 432-434 (1995)
88. Wilson, N.K., Calero-Nieto, F.J., Ferreira, R., Gottgens, B. Transcriptional regulation of haematopoietic transcription factors. *Stem Cell Research & Therapy* **2**(6), (2011)
89. Porcher, C. *et al*. The T cell leukemia oncoprotein SCL/tal-1 is essential for development of all hematopoietic lineages. *Cell* **86**(1), 47-57 (1996)
90. Wilson, N.K., Calero-Nieto, F.J., Ferreira, R., Gottgens, B. Transcriptional regulation of haematopoietic transcription factors. *Stem Cell Research & Therapy* **2**(6), (2011)
91. Gottgens, B., Broccardo, C., Sanchez, M.J., Deveaux, S., Murphy, G., Gothert, J.R., Kotsopoulou, E., Kinston, S., Delaney, L., Piltz, S., Barton, L.M., Knezevic, K., Erber, W.N., Begley, C.G., Frampton, J., Green, A.R. The scl +18/19 stem cell enhancer is not required for hematopoiesis: identification of a 5'bifunctional hematopoietic-endothelial enhancer bound by Fli-1 and Elf-1. *Mol. Cell Biol.* **24,** 1870-1883 (2004)
92. Sanchez, M.J., Bockamp, E.O., Miller, J., Gambardella, L., Green, A.R.

Selective rescue of early haematopoietic progenitors in Scl(-/-) mice by expressing Scl under the control of a stem cell enhancer**.** *Development* **128,** 4815-4827 (2001)
93. Sanchez, M., Gottgens, B., Sinclair, A.M., Stanley, M., Begley, C.G., Hunter, S., Green, A.R. An SCL 3'enhancer targets developing endothelium together with embryonic and adult haematopoietic progenitors. *Development* **126,** 3891-3904 (1999)
94. Silberstein, L., Sanchez, M.J., Socolovsky, M., Liu, Y., Hoffman, G., Kinston, S., Piltz, S., Bowen, M., Gambardella, L., Green, A.R., Gottgens, B. Transgenic analysis of the stem cell leukemia +19 stem cell enhancer in adult and embryonic hematopoietic and endothelial cells. *Stem Cells* **23:**1378-1388 (2005)
95. Begley, C.G., Green, A.R. The SCL gene: from case report to critical hematopoietic regulator. *Blood* **93**, 2760-2770 (1999)
96. O'Neil, J., Billa, M., Oikemus, S., Kelliher, M. The DNA binding activity of TAL-1 is not required to induce leukemia/lymphoma in mice. *Oncogene* **20,** 3897-3905 (2001)
97. Warren, A.J., Colledge, W.H., Carlton, M.B., Evans, M.J., Smith, A.J., Rabbitts, T.H. The oncogenic cysteine-rich LIM domain protein rbtn2 is essential for erythroid development. *Cell* **78**, 45–57 (1994)
98. Royer-Pokora, B., Rogers, M., Zhu, T.H., Schneider, S., Loos, U., Bolitz, U. The TTG-2/RBTN2 T cell oncogene encodes two alternative transcripts from two promoters: the distal promoter is removed by most 11p13 translocations in acute T cell leukaemia's (T-ALL) *Oncogene* **10,** 1353–1360 (1995)
99. Osada, H., Grutz, G., Axelson, H., Forster, A., Rabbitts, T.H. Association of erythroid transcription factors: complexes involving the LIM protein RBTN2 and the zinc-finger protein GATA1. *Proc Natl Acad Sci USA* **92:**9585-9589 (1995)
100. Wadman, I.A., Osada, H., Grutz, G.G., Agulnick, A.D., Westphal, H., Forster, A., Rabbitts, T.H. The LIM-only protein Lmo2 is a bridging molecule assembling an erythroid, DNA-binding complex which includes the TAL1, E47, GATA-1 and Ldb1/NLI proteins. *EMBO J* **16**, 3145-3157 (1997)
101. Speck, N.A., Gilliland, D.G. Core-binding factors in haematopoiesis and leukaemia. *Nat. Rev. Cancer* **2,** 502-513 (2002)
102. Melnikova, I.N.*,* Crute, B.E.*,* Wang, S.*,* Speck, N.A. Sequence specificity of the core-binding factor*. J. Virol.* **67,** 2408–2411 1993)
103. Wang, S., Wang, Q., Crute, B.E., Melnikova, I.N., Keller, S.R., Speck, N.A. Cloning and characterization of subunits of the T-cell receptor and murine leukemia virus enhancer core-binding factor. *Mol. Cell Biol.* **13**, 3324-3339 (1993)
104. Redondo, J.M., Pfohl, J.L., Hernandez-Munain, C., Wang, S., Speck, N.A., Krangel, M.S. Indistinguishable nuclear factor binding to functional core sites of the T-cell receptor delta and murine leukemia virus enhancers. *Mol. Cell Biol.* **12,** 4817-4823 (1992)
105. Zhang, D.E., Hetherington, C.J., Meyers, S. *et al*. CCAAT enhancer-binding protein (C/EBP) and AML1 (CBF alpha2) synergistically activate the macrophage colony-stimulating factor receptor promoter. *Mol. Cell Biol.* **16,** 1231-1240 (1996)
106. Zhang, D.E., Fujioka, K., Hetherington, C.J. *et al*. Identification of a region which directs the monocytic activity of the colony-stimulating factor 1 (macrophage colony-stimulating factor) receptor promoter and binds PEBP2/CBF (AML1). *Mol. Cell Biol.* **14,** 8085-8095 (1994)

107. de Bruijn, M.F., Speck, N.A. Core-binding factors in hematopoiesis and immune function. *Oncogene* **23,** 4238–4248 (2004)
108. Okuda, T., van Deursen, J., Hiebert, S.W., Grosveld, G., Downing, J.R. AML1, the target of multiple chromosomal translocations in human leukemia, is essential for normal fetal liver hematopoiesis. *Cell* **84**, 321-330 (1996)
109. Wang, Q., Stacy, T., Miller, J.D. *et al*. The CBFbeta subunit is essential for CBFalpha2 (AML1) function in vivo. Cell. **87,** 697-708 (1996)
110. North, T. *et al*. Runx1 is expressed in adult mouse hematopoietic stem cells and differentiating myeloid and lymphoid cells, but not in maturing erythroid cells. *Stem Cells* **22**(2), 158-168 (2004)
111. Lacaud, G. *et al*. Runx1 is essential for hematopoietic commitment at the hemangioblast stage of development in vitro. *Blood* **100**(2), 458-466 (2002)
112. Miyoshi, H., Shimizu, K., Kozu, T., Maseki, N., Kaneko, Y., Ohki, M. The t(8;21) breakpoints on chromosome 21 in acute myeloid leukemia clustered within a limited region of a novel gene, *AML1. Proc. Natl. Acad. Sci. USA.* **88**, 10431–10434 (1991)
113. Romana, S.P., Mauchauffe, M., Le Coniat, M. *et al.* The t(12;21) of acute lymphoblastic leukemia results in a tel-AML1 gene fusion. *Blood* **85,** 3662–3670 (1995)
114. Asou, N. The role of a Runt domain transcription factor AML1/RUNX1 in leukemogenesis and its clinical implications. *Critical Reviews in Oncology/Hematology* **45**(2), 129-150 (2003)
115. Bloomfield, C.D., Lawrence, D., Byrd, J.C. *et al.* Frequency of prolonged remission duration after high-dose cytarabine intensification in acute myeloid leukemia varies by cytogenetic subtype. *Cancer Res.* **58,** 4173–4179 (1998)
116. Ko, L.J., Engel, J.D. DNA-binding specificities of the GATA transcription factor family. *Mol. Cell Biol.* **13**, 4011–4022 (1993)
117. Weiss, M.J., Orkin, S.H. GATA transcription factors: key regulators of hematopoiesis. *Exp. Hematol.* **23**, 99–107 (1995)
118. Pevny, L., Simon, M.C., Robertson E. *et al.* Erythroid differentiation in chimaeric mice blocked by a targeted mutation in the gene for transcription factor GATA-1. *Nature* **349**, 257–260 (1991)
119. Shivdasani, R.A., Fujiwara, Y. , McDevitt, M.A., Orkin, S.H. A lineage-selective knockout establishes the critical role of transcription factor GATA-1 in megakaryocyte growth and platelet development. *EMBO J.* **16**, 3965–3973 (1997)
120. Vincente, C., Conchillo, A., Garcia-Sanchez, M.A., Odero, M.D. The role of the GATA2 transcription factor in normal malignant hematopoiesis. *Critical Reviews in Oncology/Hematology* **82**(1), 1-17 (2012)
121. Grass, J.A., Boyer, M.E., Pal, S., Wu, J., Weiss, M.J., Bresnick, E. GATA-1-dependent transcriptional repression of GATA-2 via disruption of positive autoregulation and domain-wide chromatin remodeling. Proc. Natl. Acad. Sci. USA **100**, 8811–8816 (2003)
122. Ikonomi, P., Noguchi, C.T., Miller, W., Kassahun, H., Hardison, R., Schechter, A.N. Levels of GATA-1/GATA-2 transcription factors modulate expression of embryonic and fetal hemoglobins. *Gene* **261**, 277–287 (2000)
123. Ling, K.W., Ottersbach, K., van Hamburg J.P. *et al.* GATA-2 plays two functionally distinct roles during the ontogeny of hematopoietic stem cells. *J. Exp. Med.* **200**, 871–882 (2004)
124. Tsai, F.Y. and Orkin, S.H. Transcription factor GATA-2 is required for

proliferation/survival of early hematopoietic cells and mast cell formation, but not for erythroid and myeloid terminal differentiation. *Blood* **89**(10), 3636-43 (1997)
125. Takahashi, S., Shimizu, R., Suwabe N. *et al.* GATA factor transgenes under GATA-1 locus control rescue germline GATA-1 mutant deficiencies. *Blood* **96**, 910–916 (2000)
126. Davidson, E.H. Emerging properties of animal gene regulatory networks. *Nature* **468**, 911-920 (2010)
127. modENCODE Consortium, Roy, S., Ernst, J., Alekseyenko, A.A., Artieri, C. *et al*. *Science* **330**, 1787-1797 (2010) Wilson, N.K. *et al*. Combinatorial transcriptional control in blood stem/ progenitor cells: genome-wide analysis of ten major transcriptional regulators. *Cell Stem Cell* **7**(4), 532-544 (2010)
128. Berger, S.L., Kouzarides, T., Shiekhattar, R., Shilatifard, A. An operational definition of epigenetics. *Genes Dev.* **23**, 781-783 (2009)
129. Bird, A. Perceptions of epigenetics. *Nature* **447,** 396-398 (2007)
130. Fazzari, M.J., Greally, J.M. Introduction to epigenomics and epigenomewide analysis. *Methods Mol. Biol.* **620,** 243-265 (2010)
131. Cedar, H., Bergman, Y. Epigenetics of haematopoietic cell development. *Nat. Rev. Immunol.* **11,** 478-488 (2011)
132. Zhu, J., Park, C.W., Sjeklocha, L., Kren, B.T., Steer, C.J. High-level genomic integration, epigenetic changes, and expression of sleeping beauty transgene. B*iochemistry* **49**, 1507-1521 (2010)
133. Wang, Y., Moore, B.T., Peng, X., Xiao, P. Epigenetics and hematopoietic stem or progenitor cells. *Human Genet. Embryol.* **S2**:004. doi:10.4172/2161-0436.S2-004 (2012)
134. Luger, K., Mader, A.W., Richmond, R.K., Sargent, D.F., Richmond, T.J. Crystal structure of the nucleosome core particle at 2.8A˚ resolution. *Nature* **389,** 251–260 (1997)
135. Jenuwein, T., Allis, C.D. Translating the histone code. *Science* **293**, 1074–1080 (2001)
136. Rice, K.L., Hormaeche, I., Licht, J.D. Epigenetic regulation of normal and malignant hematopoiesis. *Oncogene* **26**, 6697-6714 (2007)
137. Verdone, L., Agricola, E., Caserta, M., Di Mauro, E. Histone acetylation in gene regulation. *Bried Funct. Genomic Proteomic* **5**, 209-221 (2006)
138. Huo, X., Zhang, J. Important roles of reversible acetylation in the function of hematopoietic transcription factors. *J. Cell Mol. Med.* **9**, 103–11 (2005)
139. Huang, S., Qiu, Y., Stein, R.W., Brandt, S.J. p300 functions as a transcriptional coactivator for the TAL1/SCL oncoprotein. *Oncogene* **18,** 4958–4967 (1999
140. Huang, Y., Greene, E., Murray Stewart, T., Goodwin, A.C., Baylin, S.B., Woster, P.M. *et al*. Inhibition of lysine-specific demethylase 1 by polyamine analogues results in reexpression of aberrantly silenced genes. *Proc. Natl. Acad. Sci. USA* **104,** 8023–8028 (2007)
141. Ambros, V., Chen, X. The regulation of genes and genomes by small RNAs. *Development* **134,** 1635–1641 (2007)
142. Lewis, B.P., Burge, C.B., Bartel, D.P. Conserved seed pairing, often flanked by adenosines, indicates that thousands of human genes are microRNA targets. *Cell* **120,** 15-20 (2005)
143. Lewis, B.P., Shih, I.H., Jones-Rhoades, M.W., Bartel, D.P., Burge, C.B. Prediction of mammalian microRNA targets. *Cell* **115,** 787-798 (2003)

144. Ooi, A.G., Sahoo, D., Adorno, M., Wang, Y., Weissman, I.L. *et al*. (2010) MicroRNA-125b expands hematopoietic stem cells and enriches for the lymphoid-balanced and lymphoid-biased subsets. *Proc. Natl. Acad. Sci. USA* **107,** 21505-21510 (2003)
145. O'Connell, R.M., Chaudhuri, A.A., Rao, D.S., Gibson, W.S., Balazs, A.B. et al. MicroRNAs enriched in hematopoietic stem cells differentially regulate longterm hematopoietic output. *Proc. Natl. Acad. Sci. USA* **107,** 14235-14240 (2010)
146. Surdziel, E., Cabanski, M., Dallmann, I., Lyszkiewicz, M., Krueger, A. et al. Enforced expression of miR-125b affects myelopoiesis by targeting multiple signaling pathways. *Blood* **117,** 4338-4348 (2011)
147. Fu, Y.F., Du, T.T., Dong, M., Zhu, K.Y., Jing, C.B. *et al*. Mir-144 selectively regulates embryonic alpha-hemoglobin synthesis during primitive erythropoiesis. *Blood* **113,** 1340-1349 (2009)
148. Pase, L., Layton, J.E., Kloosterman, W.P., Carradice, D., Waterhouse, P.M. MiR-451 regulates zebrafish erythroid maturation in vivo via its target gata2. *Blood* **113,** 1794-1804 (2009)
149. Dore, L.C., Amigo, J.D., Dos Santos, C.O., Zhang, Z., Gai, X. *et al.* A GATA-1-regulated microRNA locus essential for erythropoiesis. *Proc. Natl. Acad. Sci. USA* **105,** 3333-3338 (2008)
150. Rasmussen, K.D., Simmini, S., Abreu-Goodger, C., Bartonicek, N., Di, G.M. *et al*. The miR-144/451 locus is required for erythroid homeostasis. *J. Exp. Med.* **207,** 1351-1358 (2010)
151. Papapetrou, E.P., Korkola, J.E., Sadelain, M. A genetic strategy for single and combinatorial analysis of miRNA function in mammalian hematopoietic stem cells. *Stem Cells* **28**: 287-296 (2010)
152. Okano, M., Xie, S., Li, E. Cloning and characterization of a family of novel mammalian DNA (cytosine-5) methyltransferases. *Nat. Genet.* **19,** 219-220 (1998)
153. Goto, T., Monk, M. Regulation of X-chromosome inactivation in development in mice and humans. *Microbiol. Mol. Biol. Rev.* **62**, 362–378 (1998)
154. Schaefer, C.B., Ooi, S.K., Bestor, T.H., Bourc'his, D. Epigenetic decisions in mammalian germ cells. *Science* **316**, 398–399 (2007)
155. Terranova, R., Agherbi, H., Boned, A., Meresse, S., Djabali, M. Histone and DNA methylation defects at Hox genes in mice expressing a SET domain-truncated form of Mll. *Proc. Natl. Acad. Sci. USA* **103**, 6629–6634 (2006)
156. Levings, P.P., Bungert, J. The human beta-globin locus control region. *Eur. J. Biochem.* **269**, 1589–1599 (2002)
157. Sashida, G., Iwama, A. Epigenetic regulation of hematopoiesis. *Int. J. Hematol.* DOI 10.1007/s12185-012-1183-x (2012)
158. Trowbridge, J.J., Snow, J.W., Kim, J., Orkin, S.H. DNA methyltransferase 1 is essential for and uniquely regulates hematopoietic stem and progenitor cells. *Cell Stem Cell* **5,** 442-449 (2009
159. Broske, A.M., Vockentanz, L., Kharazi, S., Huska, M.R., Mancini, E. *et al*. DNA methylation protects hematopoietic stem cell multipotency from myeloerythroid restriction. *Nat. Genet.* **41,** 1207-1215 (2009)
160. Calvanese, V., Fernandez, A.F., Urdinguio, R.G., Suarez-Alvarez, B., Mangas, C. *et al*. A promoter DNA demethylation landscape of human hematopoietic differentiation. *Nucleic Acids Res*. **40,** 116-131 (2011)
161. Hodges, E., Molaro, A., Dos Santos, C.O., Thekkat, P., Song, Q. *et al*. Directional DNA methylation changes and complex intermediate states accompany lineage specificity in the adult hematopoietic compartment.

Mol. Cell **44**, 17-28 (2011)
162. Figueroa, M.E., Abdel-Wahab, O., Lu, C., Ward, P.S., Patel, J. et al. Leukemic IDH1 and IDH2 mutations result in a hypermethylation phenotype, disrupt TET2 function, and impair hematopoietic differentiation. *Cancer Cell* **18**, 553-567 (2010)
163. Bracken, A.P., Helin, K. Polycomb group proteins: navigators of lineage pathways led astray in cancer. *Nat. Rev. Cancer* **9,** 773–84 (2009)
164. Jurgens, G. A group of genes controlling the spatial expression of the bithorax complex in *Drosophila. Nature* **31**: 153-155 (1985)
165. Gaytan de Ayala Alonso, A. *et al*. Genetic screen identifies novel Polycomb group genes in *Drosophila*. *Genetics* **176**: 2099-2108 (2007)
166. Schwartz, Y.B., Pirrotta, V. A new world of Polycombs: unexpected partnerships and emerging functions. *Nature Reviews* **14**: 853-864 (2013)
167. Schuettengruber, B., Chourrout, D., Vervoot, M., Leblanc, B. and Cavalli, G. Genome regulation by Polycomb and Trithorax proteins. *Cell* **128:**735-745 (2007)
168. Schwartz, Y.B. and Pirrotta, V. Polycomb silencing mechanisms and the management of genomic programmes. *Nature Rev. Genetics* **8**: 9-22 (2007)
169. Zhou, W. *et al*. Histone H2A monoubiquitination represses transcription by inhibiting RNA polymerase II transcriptional elongation. *Mol. Cell* **29**: 69-80 (2008)
170. Dellino, G.I. *et al*. Polycomb silencing blocks transcription initialtion. *Mol. Cell* **13**:887-893 (2004)
171. Grau, D.J. *et al.* Compaction of chromatin by diverse Polycomb group proteins requires localized regions of high charge. *Gene Dev*. **25**: 2210-2221 (2011)
172. Gao, Z. *et al*. PCGF homologues, CBX proteins and RYBP define functionally distinct PRC1 family complexes. *Molecular Cell* **45**, 344-356 (2012)
173. Morey, L. *et al*, Nonoverlapping functions of the polycomb group Cbx family of proteins in embryonic stem cells. *Cell Stem Cell* **10**, 47-62 (2012)
174. van den Boom, V. *et al*. Nonredundant and locus-specific gene repression functions of PRC1 paralog family members in human hematopoietic stem/ progenitor cells. *Blood* **121**(13), 2452-2461 (2013)
175. Klauke, K. *et al.* Polycomb Cbx family members mediate the balance between hematopoietic stem cell self-renewal and differentiation. *Nature Cell Biology* **15**(4), 353-362 (2013)
176. Park, I.K., Qian, D., Kiel, M. *et al.* Bmi-1 is required for maintenance of adult self-renewing haematopoietic stem cells. *Nature* **423,** 302–305 (2003)
177. Oguro, H., Yuan, J., Ichikawa, H. *et al*. Poised lineage specification in multipotential hematopoietic stem and progenitor cells by the polycomb protein Bmi1. *Cell Stem Cell* **6,** 279–286 (2010)
178. Nakamura, S., Oshima, M., Yuan, J. *et al*. Bmi1 confers resistance to oxidative stress on hematopoietic stem cells. *PLoS ONE* **7,** e36209 (2012)
179. Cales, C., Roman-Trufero, M., Pavon, L. *et al*. Inactivation of the polycomb group protein Ring1B unveils an antiproliferative role in hematopoietic cell expansion and cooperation with tumorigenesis associated with Ink4a deletion. *Mol. Cell Biol.* **28,** 1018–1028 (2008)
180. Tavares, L. *et al*. RYBP-PRC1 complexes mediate H2A ubiquitylation at Polycomb target sites independently of PRC2 and H3K27me3. *Cell* **148**, 664-678 (2012)

181. Keller, G. Embryonic stem cell differentiation: emergence of a new era in biology and medicine. *Genes and Dev. Review* **19**, 1129-1155 (2005)
182. Evans, M. and Kaufman, M. Establishment in culture of pluripotent cells from mouse embryos. *Nature* **22**, 154-156 (1981)
183. Martin, G. Isolation of a pluripotent cell line from early mouse embryos cultured in medium conditioned by terato-carcinoma stem cells. *Proc. Natl. Acad. Sci. U.S.A.* **78**, 7635 (1981)
184. Smith, A.G. *et al*. Inhibition of pluripotential embryonic stem cell differentiation by purified polypeptides. *Nature* **336**, 688-690 (1988)
185. Stewart, C.L. *et al*. Blastocyst implantation depends on maternal expression of leukemia inhibitory factor. *Nature* **359**, 76-79 (1992)
186. Porcher, C. *et al*. The T cell leukemia oncoprotein SCL/tal-1 is essential for development of all hematopoietic lineages. *Cell* **86**(1), 47-57 (1996)
187. Begley, C.G. and Green, A.R. The SCL gene: from case report to critical hematopoietic regulator. *Blood* **93**(9) 2760-2770 (1999)
188. Lacaud, G. *et al*. Runx1 is essential for hematopoietic commitment at the hemangioblast stage of development in vitro. *Blood* **100**(2), 458-466 (2002)
189. Lugus, J.J. *et al*. GATA2 functions at multiple steps in hemangioblast development and differentiation. *Development* **134**(2), 393-405 (2007)
190. Keller, G., Kennedy, M., Papayannopoulou, T., Wiles, M.V. Hematopoietic commitment during embryonic stem cell differentiation in culture. *Mol. and Cell. Biology* **13**(1), 473-486 (1993)
191. Fehling, H.J., Lacaud, G., Kubo, A. *et al*. Tracking mesoderm induction and its specification to the hemangioblast during embryonic stem cell differentiation. *Development* **130**, 4217-4227 (2003)
192. Kennedy, M., Firpo, M., Choi, K., Wall, C., Robertson, S., Kabrun, N., Keller, G. A common precursor for primitive erythropoiesis and definitive haematopoiesis. *Nature* **386**(6624), 488-493 (1997)
193. Irion, S. *et al*. Temporal specification of blood progenitors from mouse embryonic stem cells and induced pluripotent stem cells. *Development* **137**(1), 2829-2839 (2010)
194. Singapore Cancer Registry. Trends in cancer incidence in Singapore 2005-2009. Interim Annual Registry Report 2011
195. www.kkh.com.sg
196. Kuppers, R. and Hansmann, M.L. The Hodgkin and Reed/Sternberg cell. *Int. J. Biochem. Cell Bio*logy **37**(3), 511-517 (2005)
197. Gratwohl, A. *et al*. Quantitative and qualitative differences in use and trends of hematopoietic stem cell transplantation: a Global Observational Study. *Haematologica* **98**(8), 1282-1290 (2013)
198. Barker, J.N. *et al*. Determinants of survival after human leucocyte antigen-matched unrelated blood donor bone marrow transplantation in adults. *British Journal of Haematology* **118** (1), 257-260 (2002)
199. Laughlin, M.J. Umbilical cord blood for allogenic transplantation in children and adults. *Bone Marrow Transplant* **27**(1), 1-6 (2001)
200. Caldwell, J. *et al.* Culture perfusion schedules influence the metabolic activity and granulocyte–macrophage colony-stimulating factor production rates of human bone marrow stromal cells. *J. Cell. Physiol*ogy **147**, 344–353 (1991)
201. Shwartz, R.M. *et al. In vitro* myelopoiesis stimulated by rapid medium exchange and supplementation with hematopoietic growth factors. *Blood* **78**: 3155–3161 (1991)
202. Csaszar, E. *et al*. Rapid expansion of human hematopoietic stem cells

by automated control of inhibitory feedback signaling. *Cell Stem Cell* **10**(2), 218-229 (2012)
203. Zheng, Y. *et al*. Stem cell factor improves SCID-repopulating activity of human umbilical cord blood-derived hematopoietic stem/progenitor cells in xenotransplanted NOD/SCID mouse model. *Bone Marrow Transplant* **35**, 137–142 (2005)
204. De Felice, L. *et al*. Flt3LP3 induces the *ex-vivo* amplification of umbilical cord blood committed progenitors and early stem cells in short-term cultures. *British Journal of Haematology* **106**, 133–141 (1999)
205. Levac, K., Karanu, F., Bhatia, M. Identification of growth factor conditions that reduce *ex vivo* cord blood progenitor expansion but do not alter human repopulating cell function *in vivo*. *Haematologica* **90**, 166–172 (2005)
206. Murray, L.J. *et al.* Thrombopoietin, flt3, and kit ligands together suppress apoptosis of human mobilized $CD34^+$ cells and recruit primitive CD34+ Thy-1+ cells into rapid division. *Experimental Hematology* **27**, 1019–1028 (1999)
207. Robinson, S.N. *et al*. Superior *ex vivo* cord blood TNC and hematopoietic progenitor cell expansion following co-culture with bone marrow-derived mesenchymal stem cells. *Biol. of Blood Marrow Transplant* **12**(132) (2006)
208. Noort, W.A. *et al*. Mesenchymal stem cells promote engraftment of human umbilical cord blood-derived $CD34^+$ cells in NOD/SCID mice. *Experimental Hematology* **30**, 870–878 (2002)
209. Le Blanc, K. *et al*. Treatment of severe acute graft-versus-host disease with third party haploidentical mesenchymal stem cells. *Lancet* **363**, 1439–1441 (2004)
210. Jaroscak, J. *et al*. Augmentation of umbilical cord blood (UCB) transplantation with *ex vivo*-expanded UCB cells: results of a phase 1 trial using the AastromReplicell System. *Blood* **101**, 5061–5067 (2003)
211. Holyoake, T.L. *et al*. CD34 positive PBPC expanded *ex vivo* may not provide durable engraftment following myeloablative chemoradiotherapy regimens. *Bone Marrow Transplant* **19**, 1095–1101 (1997)
212. Lange, A., Raffoux, C. and Shaw, B. Biological and genetic aspects of donor-recipient matching in HSCT. *Bone Marrow Research* **2012,** article ID 212593 (2012)
213. Lohmann, F. and Bieker, J.J. Activation of Eklf expression during hematopoiesis by Gata2 and Smad5 prior to erythroid commitment. *Development* **135**, 2071-2082 (2008)
214. Kyba, M., Perlingeiro, R.C., Daley, G.Q. HoxB4 confers definitive lymphoid-myeloid engraftment potential on embryonic stem cell and yolk sac hematopoietic progenitors. *Cell* **109**(1), 29-37 (2008)
215. Ng, J.H. *et al*. In vivo epigenomic profiling of germ cells reveals germ cell molecular signatures. *Developmental Cell* **24**(3), 324-333 (2013)
216. Kumar, V. *et al*. Uniform, optimal signal processing of mapped deep-sequencing data. *Nature Biotech*. **31**, 615-622 (2013)
217. Porcher, C. *et al*. The T cell leukemia oncoprotein SCL/tal-1 is essential for development of all hematopoietic lineages. *Cell* **86**(1), 47-57 (1996)
218. Yamada, Y. *et al*. The T cell leukemia LIM protein Lmo2 is necessary for adult mouse hematopoiesis. *Proc. Natl. Acad. Sci. U.S.A*. **95**, 3890-3895 (1998)
219. North, T. *et al*. Runx1 is expressed in adult mouse hematopoietic stem cells and differentiating myeloid and lymphoid cells, but not in maturing

erythroid cells. *Stem Cells* **22**(2), 158-168 (2004)
220. Lacaud, G. *et al*. Runx1 is essential for hematopoietic commitment at the hemangioblast stage of development in vitro. *Blood* **100**(2), 458-466 (2002)
221. Costa, G., Mazan, A., Gandillet, A., Pearson, S., Lacaud, G., Kouskoff, V. SOX7 regulates the expression of VE-cadherin in the haemogenic endothelium at the onset of haematopoietic development. *Development* **139**, 1587-1598 (2012)
222. Weimers, D.O. *et al*. The mouse prolactin gene family locus. *Endocrinology* **144**(1), 313-325 (2003)
223. Cwikel, S. *et al*. Prolactin-induced expression of cytokine-inducible SH2 signaling inhibitors in human hematopoietic progenitors. *Experimental Hematology* **29**(8), 937-942 (2001)
224. Choong, M.L., Tan, A., Luo, B. and Lodish, H.F. A novel role for Proliferin 2 in the ex vivo expansion of hematopoietic stem cells. *FEBS Letters* **550**, 155-162 (2003)
225. Wang, X-Y., Yin, Y., Yuan, H., Sakamuri, T., Okano, H., Glazer, R.I. Musashi 1 modulates mammary progenitor cell expansion through Proliferin-mediated activation of the Wnt and Notch pathways. *Mol. Cell Biol.* **28**(11), 3589-3599 (2008)
226. Alvarez, E., Zhou, W., Witta, S.E. and Freed, C.R. Characterization of the Bex gene family in humans, mice and rats. *Gene* **357**(1), 18-28 (2005)
227. Mayani, H., Dragowska, W. and Lansdorp, P.M. Cytokine-induced selective expansion and maturation of erythroid versus myeloid progenitors from purified cord blood precursor cells. *Blood* **81**(12), 3252-3258 (1993)
228. Yang, Y. *et al*. MiR-17 partly promotes hematopoietic cell expansion through augmenting HIF-1α in osteoblasts. *PLoS ONE* **8**(7): e70232. doi:10.1371/journal.pone.0070232 (2013)
229. Ben-Jonathan, N., Arbogast, L.A., Hyde, J.F. Neuroendocrine (corrected) regulation of prolactin release. *Prog. Neurobiol*. **33**, 399-447 (1989)
230. Devost, D. and Boutin, J.M. Autoregulation of the rat prolactin gene in lactotrophs. *Mol. Cell. Endocrinology* **158**, 99-109 (1999)
231. Helmer, R.A. *et al.* Prolactin-induced Jak2 phosphorylation of RUSH: a key element in Jak/RUSH signaling. *Mol. Cell Endocrinol.* **325**(1-2): 143-9 (2010)
232. Trott, J.F. *et* al. Prolactin: The multifaceted potentiator of mammary growth and function. *Journal of Animal Science* **90**(5), 1674-1686 (2012)
233. Fujiwara, Y., Browne, C.P., Cunniff, K., Goff, S.C., Orkin, S.H. Arrested development of embryonic red cell precursors in mouse embryos lacking transcription factor GATA-1. *Proc. Natl. Acad. Sci. U.S.A.* **93**(22), 12355-12358 (1996)
234. McGrath, K.E., Koniski, A.D., Malik, J., Palis, J. Circulation is established in a step-wise pattern in the mammalian embryo. *Blood* **10**, *1669*-1676 (2003)
235. Li, W., Johnson, S.A., Shelly, W.C., Ferkowicz, M., Morrison, P., Li, Y. and Yoder, M.C. Primary endothelial cells isolated from the yolk sac and para-aortic splanchnopleura support the expansion of adult marrow stem cells in vitro. *Blood* **102**(13), 4345-4353 (2003)
236. Cheng, X., Huber, T.L., Chen, V.C., Gadue, P., Keller, G.M. Numb mediates the interaction between Wnt and Notch to modulate primitive erythropoietic specification from the hemangioblast. *Development* **135**(20), 3447-3458 (2008)

237. Kawano, Y., Kypta, R.. Secreted antagonists of the Wnt signaling pathway. *J. Cell Sci.* **116**, 2627-2634 2003)
238. Lee, H.M. *et al*. Downstream targets of HOXB4 in a cell line model of primitive hematopoietic progenitor cells. *Blood* **116**(5), 720-730 (2010)
239. Wilson, N.K. *et al*. Combinatorial transcriptional control in blood stem/ progenitor cells: genome-wide analysis of ten major transcriptional regulators. *Cell Stem Cell* **7**(4), 532-544 (2010)
240. Fleischman, R.A., Custer, R.P. and Mintz, B. Totipotent hematopoietic stem cells: normal self-renewal and differentiation after transplantation between mouse fetuses. *Cell* **30**, 351-359 (1982)
241. Mikkola, H. *et al*. Expression of CD41 marks the initiation of definitive hematopoiesis in the mouse embryo. *Blood* **101**, 508-516 (2003)
242. Faloon, P. *et al.* Basic fibroblast growth factor positively regulates hematopoietic development. *Development* **127**, 1931-1941 (2000)
243. Clarke, D.L., Linzer, D.I.H. Changes in prolactin receptor expression during pregnancy in the mouse ovary. *Endocrinology* **133**, 224-232 (1993)
244. Buck, K., Vanek, M., Groner, B., Ball, R.K. Multiple forms of prolactin receptor messenger ribonucleic acid are specifically expressed and regulated in murine tissues and the mammary cell line HC11. *Endocrinology* **130**, 1108-1114 (1992)

245. Kelly, P.A., Binart, N., Lucas, B., Bouchard, B., Goffin, V. Implications of multiple phenotypes observed in prolactin receptor knockout mice. *Front Neuroendocrinol.* **22**(2), 140-145 (2001)

246. Davis, J.A. *et al*. Expression of multiple forms of the prolactin receptor. *Mol. Endocrinol*. **3**, 674–680 (1989)
247. Trott, J.F. *et al*. Multiple new isoforms of the human prolactin receptor gene. *Adv. Exp. Med. Biol*. **554**, 495–499 (2004)
248. Lesueur, L. *et al*. Comparison of long and short forms of the prolactin receptor on prolactin induced milk protein gene transcription. *Proc. Natl. Acad. Sci. U.S.A.* **88**, 824–828 (1991)
249. Devi, Y.S. et al. Regulation of transcription factors and repression of Sp1 by prolactin signaling through the short isoform of its cognate receptor. *Endocrinology* **150**, 3327–3335 (2009)
250. Brooks, C.L. Molecular mechanisms of prolactin and its receptor. *Endocrine Reviews* **33**(4), 1-22 (2012)
251. Yang, X. *et al*. Angiogenesis is induced by signal transducer and activator of transcription 5 (STAT5A) is dependent on autocrine activity of Proliferin. *J. Biol. Chem.* **287**(9), 6390-6502 (2013)
252. Bengston, N.W. and Linzer, D. Inhibition of tumor growth by the antiangiogenic placental hormone, Proliferin-related protein. *Mol. Endocrin*. **14**(12), 1934-1943 (2000)
253. Wang, X.Y. *et al*. Mushashi1 modulates mammary progenitor cell expansion through Proliferin-mediated activation of the Wnt and Notch pathways. *Mol. Cell Biol*. **28**(11), 3589-3599 (2008)
254. Kinder, S.J., Tsang, T.E., Quinlan, G.A., Hadjantonakis, A-K., Nagy, A., Tam, P.P.L. The orderly allocation of mesodermal cells to the extraembryonic structures and the anteroposterior axis during gastrulation of the mouse embryo. *Development* **126**, 4691-4701 (1999)
255. Garcia-Martinez, V., Schoenwolf, G.C. Primitive-streak origin of the cardiovascular system in avian embryos. *Dev. Biol.* **159**(2), 706-719 (1993)
256. Vandamme, J. *et al*. Interaction proteomics analysis of Polycomb

proteins defines distinct PRC1 complexes in mammalian cells. *Mol. and Cell. Proteomics* **10.4**, 1-23 (2010)
257. Sanchez, C. *et al*. Proteomics analysis of Ring1B/Rnf2 interactors identifies a novel complex with the Fbxl10/Jdhm1B histone demethylase and the Bcl6 interacting corepressor. *Mol. and Cell. Proteomics* **6.5**, 820-834 (2007)
258. Mazzarella, L. *et al*. Embryonic stem cell-derived hemangioblasts remain epigenetically plastic and require PRC1 to prevent neural gene expression. *Blood* **117**(1), 83-87 (2011)
259. van der Lugt, N.M. *et al*. Posterior transformation, neurological abnormalities, and severe hematopoietic defects in mice with a targeted deletion of the bmi-1 proto-oncogene. *Genes Dev*. **8**(7), 757-769 (1994)
260. Akasak, T. *et al*. A role for mel-18, a Polycomb group-related vertebrate gene, during anteroposterior specification of the axial skeleton. *Development* **122**, 1513-1522 (1996)
261. Voncken, J.W. *et al*. Rnf2 (Ring1b) deficiency causes gastrulation arrest and cell cycle inhibition. *Proc. Natl. Acad. Sci. U.S.A.* **100**(5), 2468-2473 (2003)
262. Alkema, M.J., Wiegant, J., Raap, A.K., Berns, A., van Lohuizen, M. Characterization and chromosomal localization of the human proto-oncogene BMI-1. *Human Mol. Genet.* **2**(10), 1597–1603 (1993)
263. Siddique, H.R., Saleem, M. Role of BMI1, a stem cell factor, in cancer recurrence and chemoresistance: preclinical and clinical evidences. *Stem Cells* **30**(3), 372–378 (2012)
264. Lessard, J., Sauvageau, G. Bmi-1 determines the proliferative capacity of normal and leukemic stem cells. *Nature* **423**(6937), 255–260 (2003)
265. Fan, L., Xu, C., Wang, C., Tao, J., Ho, C. et al. Bmi1 Is required for hepatic progenitor cell expansion and liver tumor development. *PLOS One* **7**(9), e46472 (2012)
266. Shakhova, O., Leung, C., Marino, S. Bmi1 in development and tumorigenesis of the central nervous system. *J. Mol. Med.* **83**(8), 596–600 (2005)
267. Cochrane, C.L., Medyouf, H., Weng, A.P. Polycomb group ring finger 5 (PCGF5) is a Notch transcriptional target and regulates cell size and cell cycle in hematopoietic progenitors. *ASH Annual Meeting poster abstract* **1325** (2008)
268. Sadlon, T.J., Lewis, I.D., D'Andrea, R.J. BMP4: its role in development of the hematopoietic system and potential as a hematopoietic growth factor. *Stem Cells* **22**(4):457-474 (2004)
269. Tsai, F.Y. and Orkin, S.H. Transcription factor GATA-2 is required for proliferation/survival of early hematopoietic cells and mast cell formation, but not for erythroid and myeloid terminal differentiation. *Blood* **89**(10), 3636-43 (1997)
270. Vicente, C., Conchillo, A., García-Sánchez, M.A., Odero, M.D. The role of the GATA2 transcription factor in normal and malignant hematopoiesis. *Crit. Rev. Oncol. Hematol.* **82**(1): 1-17 (2012)
271. Kruse, E.A. *et al*. Dual requirement for the ETS transcription factors Fli-1 and Erg in hematopoietic stem cells and the megakaryotic lineage. *Proc. Natl. Acad. Sci. U.S.A.* **106**(33), 13814-13819 (2009)
272. Pimanda, J.E. *et al*. Gata2, Fli1 and Scl form a recursively wired gene-regulatory circuit during early hematopoietic development. *Proc. Natl. Acad. Sci. U.S.A.* **104**(45), 17692-17697 (2007)
273. Endoh, M., Ogawa, M., Orkin, S. and Nishikawa, S. SCL/tal-1

dependent process determines a competence to select the definitive hematopoietic lineage prior to endothelial differentiation. *EMBO J.* **21**(24), 6700-6708 (2002)
274. D'Souza, S., Elefanty, A.G., Keller, G. SCL/Tal-1 is essential for hematopoietic commitment of the hemangioblast but not for its development. *Blood* **105**(10), 3862-3870 (2005)
275. Ku, C-J., Hosoya, T., Maillard, I. and Engel, J.D. GATA-3 regulated hematopoietic stem cell maintenance and cell-cycle entry. *Blood* **119**(10), 2242-2251 (2012)
276. Argiropoulos, B. and Humpries, R.K. *Hox* genes in hematopoiesis and leukemogenesis. *Nature Oncogene* **26**, 6766-6776 (2007)
277. Alharbi, R.A., Pettengell, R., Pandha, H.S. and Morgan, R. The role of Hox genes in normal hematopoiesis and acute leukemia. *Nature Leukemia* **27**, 1000-1008 (2013)
278. Lewis, E.B. A gene complex controlling segmentation in *Drosophila. Nature* **276**, 565–570 (1978)
279. Cao, R., Tsukada, Y., Zhang, Y. Role of Bmi-1 and Ring1A in H2A ubiquitylation and Hox gene silencing. *Mol. Cell.* **20**, 845–854 (2005)
280. Magli, M.C. *et* al. Coordinate regulation of HOX genes in human hematopoietic cells. *Proc. Natl. Acad. Sci. U.S.A.* **88**, 6348-6352 (1991)
281. Sauvageau, G. *et al*. Differential expression of homeobox genes in functionally distinct $CD34^+$ subpopulations of human bone marrow cells. *Proc. Natl. Acad. Sci. U.S.A.* **91**, 12223-12227 (1994)
282. Nguyen, B-C. *et al*. Cross-regulation between Notch and p63 in keratinocyte commitment to differentiation. *Genes & Dev*. **20**, 1028-1042 (2006)
283. Simon, J., Kingston, R.E. Mechanisms of polycomb silencing: knowns and unknowns. *Nature Reviews* **10**, 697-708 (2009)
284. The ENCODE Project Consortium. Identification and analysis of functional elements in 1% of the human genome by the ENCODE pilot project. Nature **447**, 799-816 (2007)
285. Heintzman, N.D. *et al*. Distinct and predictive chromatin signatures of transcriptional promoters and enhancers in the human genome. *Nature Genetics* **39**, 311-318 (2007)
286. Su, W. *et al*. DNA looping and enhancer activity: Association between DNA-bound NtrC activator and RNA polymerase at the bacterial *glnA* promoter. *Proc. Natl. Acad. Sci. U.S.A.* **87**, 5504-5508 (1990)
287. Kolovos, P. *et al*. Enhancers and silencers: an integrated and simple model for their function. *Epigenetics and Chromatin* **5**(1) (2012)
288. Mahony, S., Benos, P.V. STAMP: a web tool for exploring DNA-binding motif similarities. *Nucleic Acids Research* **35**(Web Server issue):W253-W258 (2007)
289. Ginjala, V. *et al*. BMI1 is recruited to DNA breaks and contributes to DNA damage-induced H2A ubiquination and repair. *Mol. Cell Biol.* **31**(10), 1972-1982 (2011)
290. Brown, J.L., Mucci, D., Whiteley, M., Dirksen, M.L., Kassis, J.A. The *Drosophila* Polycomb group gene pleiohomeotic encodes a DNA binding protein with homology to the transcription factor YY1. *Mol. Cell* **1**, 1057-1064 (1998)
291. Brown, J.L., Fritsch, C., Muller, J., Kassis, J.A. The *Drosophila pho-like* gene encodes a YY1-related DNA binding protein that is redundant with *pleiohomeotic* in homeotic gene silencing. *Development* **130**, 285-294 (2003)
292. Klymenko, T., Papp, B., Muller, J. *et al*. A Polycomb group protein

complex with sequence-specific DNA-binding and selective methyl-lysine-binding activities. *Genes Dev.* **20**(9), 1110-1122 (2006)
293. Wang, L., Brown, J.L., Cao, R., Zhang, Y., Kassis, J.A. *et al*. Hierarchical recruitment of polycomb group silencing complexes. *Molecular Cell* **14**, 637-646 (2004)
294. Schuettengruber, B., Gatapathi, M., Leblanc, B., Portoso, M., Jaschek, R., Tolhuis, B., van Lohuizen, M., Tanay, A., Cavalli, G. Functional anatomy of Polycomb and Trithorax chromatin landscapes in *Drosophila* embryos. *PLoS Biol.* **7**(1): e1000013. doi:10.1371/journal.phbio.1000013 (2009)
295. Wilkinson, F.H., Park, K., Atchison, M.L. Polycomb recruitment to DNA *in vivo* by the YY1 REPO domain. *Proc. Natl. Acad. Sci. U.S.A.* **103**(51), 19296-19301 (2006)
296. Dekker, J., Rippe, K., Dekker, M., Kleckner, N. Capturing chromosome conformation. *Science* **295**, 1306–1311 (2002)
297. Dekker, J. The three 'C' s of chromosome conformation capture: Controls, controls, controls. *Nat. Methods* **3**, 17–21 (2006)
298. Fullwood, M.J. *et al.* An oestrogen-receptor-α-bound human chromatin interactome. *Nature* **462**, 58–64 (2009)
299. de Wit, E. and de Laat, W. A decade of 3C technologies: insights into nuclear organization. *Genes and Development* **26**, 11-24 (2012)
300. Li, X., Han, Y., Xi, R. Polycomb group genes *Psc* and *Su(z)2* restrict follicle stem cell self-renewal and extrusion by controlling canonical and noncanonical Wnt signaling. *Genes Dev.* **24**, 933-946 (2010)
301. de Napoles, M., Mermoud, J.E., Wakao, R., Tang, Y.A., Endoh, M., Appanah, R., Nesterova, T.B., Silva, J., Otte, A.P., Vidal, M., Koseki, H., Brockdorff, N. Polycomb group proteins Ring1A/B link ubiquitylation of histone H2A to heritable gene silencing and X inactivation. *Developmental Cell* **7**(5), 663-676 (2004)
302. Endoh, M., Endoh, T.A., Endoh, T., Fujimura, Y., Ohara, O., Toyoda, T., Otte, A.P., Okano, M., Brockdorff, N., Vidal, M., Koseki, H. Polycomb group proteins Ring1A/B are functionally linked to the core transcriptional regulatory circuitry to maintain ES cell identity. *Development* **135**, 1513-1524 (2008)
303. Sangiori, E., Capecchi, M.R. *Bmi1* is expressed *in vivo* in intestinal stem cells. *Nature Genetics* **40**, 915-920 (2008)
304. http://www.fluidigm.com/c1-single-cell-auto-prep-system.html
305. Breuer, R.H., Snijders, P.J., Smit, E.F., Sutedja, T.G., Sewalt, R.G., Otte, A.P. *et al*. Increased expression of the EZH2 polycomb group gene in BMI-1-positive neoplastic cells during bronchial carcinogenesis. *Neoplasia* **6,** 736–743 (2004)
306. Glinsky, G.V., Berezovska, O., Glinskii, A.B. Microarray analysis identifies a death-from-cancer signature predicting therapy failure in patients with multiple types of cancer. *J. Clin. Invest*. **115,** 1503–1521 (2005)
307. Steele, J.C., Torr, E.E., Noakes, K.L., Kalk, E., Moss, P.A., Reynolds, G.M. *et al*. The polycomb group proteins, BMI-1 and EZH2, are tumour-associated antigens. *Br. J. Cancer* **95,** 1202–1211 (2006)